Angewandte Chemie
Eine Zeitschrift der Gesellschaft Deutscher Chemiker

Supporting Information

Display Selection of a Hybrid Foldamer–Peptide Macrocycle

S. Dengler, R. T. Howard, V. Morozov, C. Tsiamantas, W.-E. Huang, Z. Liu, C. Dobrzanski, V. Pophristic, S. Brameyer, C. Douat, H. Suga, I. Huc**

Table of Contents

1. Supporting figures

1.1. Figure S1

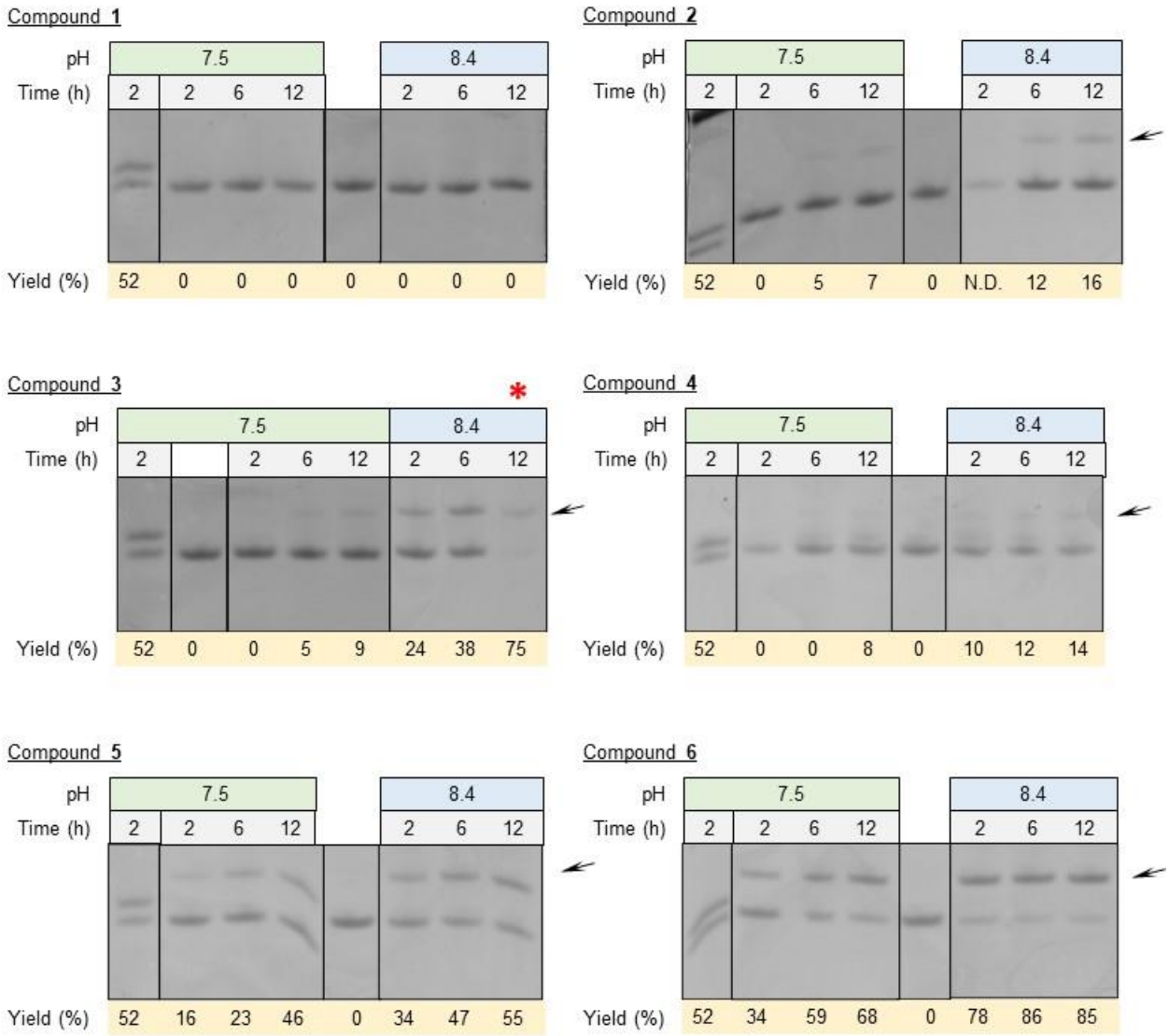

Figure S1 part 1. Assessment of tRNA acylation was carried out using mhRNA (microhelix RNA, a tRNA mimic) over the course of 24 hours, at two different pH values, 7.5 and 8.4, in green and blue, respectively. mhRNA acylated with the foldamer substrate is shown with an arrow while the lower band corresponds to "free" mhRNA. Acid-PAGE gels corresponding to the N-acetylated compounds **1–6** are shown. In all cases the first band corresponds to the acylation of ClAc-Trp-CME which is used as a control. The band which is not labelled is a reaction in which DMSO has been added instead of the activated substrate. In the case of compound **3**, improper loading of one of the gel wells led to a fading effect (indicated by a red asterisk). However, since both charged and uncharged microhelix tRNA are visible the technical issue did not hinder the accurate quantification of the aminoacylation reaction.

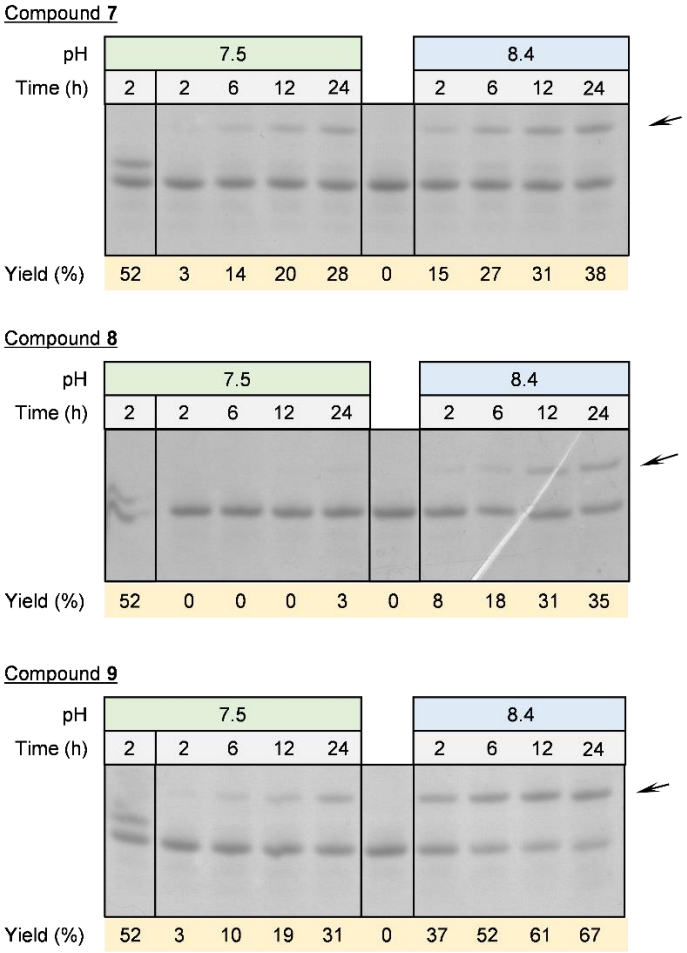

Figure S1 part 2. Assessment of tRNA acylation was carried out using mhRNA (microhelix RNA, a tRNA mimic) over the course of 24 hours, at two different pH values, 7.5 and 8.4, in green and blue, respectively. mhRNA acylated with the foldamer substrate is shown with an arrow while the lower band corresponds to "free" mhRNA. Acid-PAGE gels corresponding to the N-chloroacetylated compounds **7–9** are shown. In all cases the first band corresponds to the acylation of ClAc-Trp-CME which is used as a control. The band which is not labelled is a reaction in which DMSO has been added instead of the activated substrate.

1.2. Figure S2

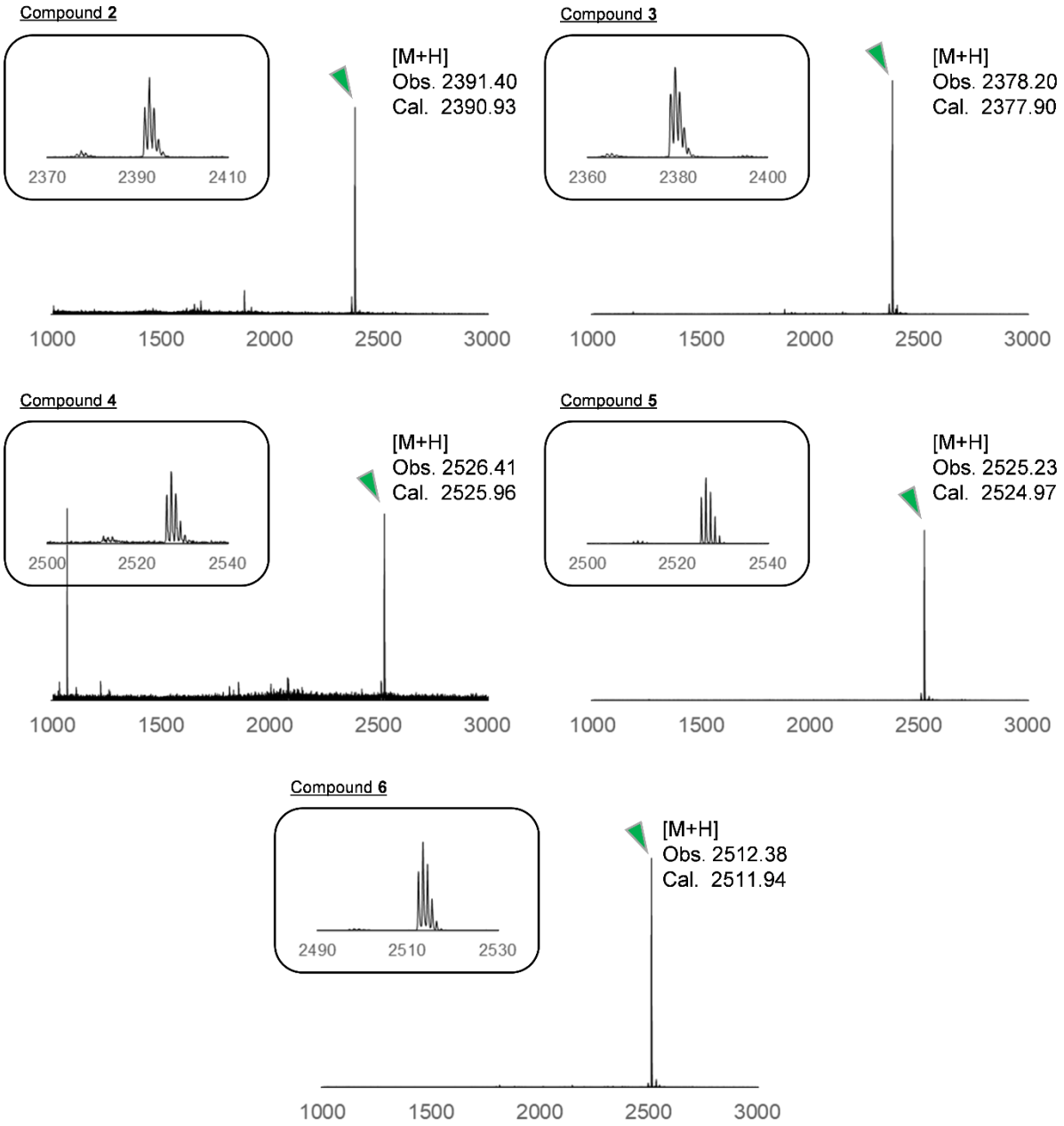

Figure S2 part 1. MALDI-TOF spectra of the translation reactions, demonstrating the successful incorporation of the foldamer substrates into peptide sequences. N-acetylated compounds **2**–**6** substituted the initiator Met residue in the MGGGTYY-flag sequence. The peaks ($[M+H]^+$) corresponding to the desired peptide sequences are shown with the green arrow. Flag stands for an octapeptide with the sequence DYKDDDDK.

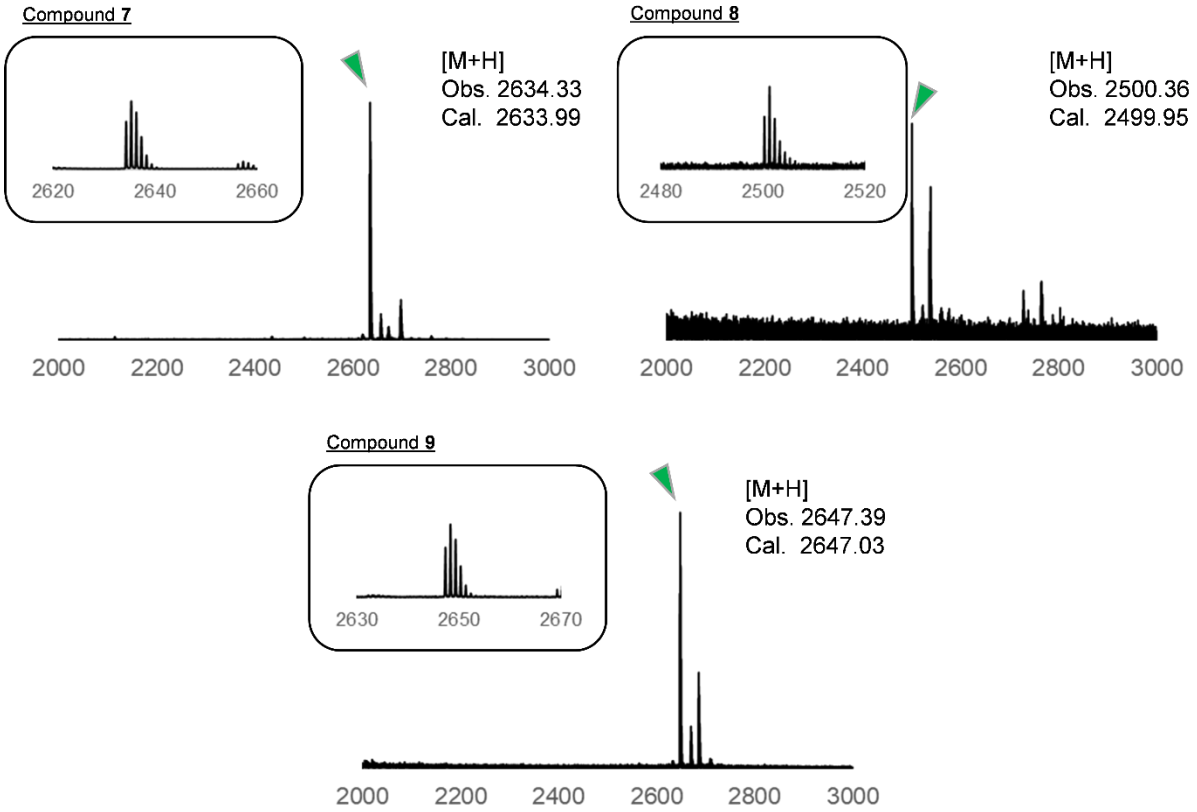

Figure S2 part 2. MALDI-TOF spectra of the translation reactions, demonstrating the successful incorporation of the foldamer substrates into peptide sequences. N-chloroacetylated compounds **7**–**9** substituted the initiator Met residue in MYAATAACA-flag with which the ClAc functionality of the downstream Cys residue readily cyclizes. The peaks corresponding to the desired peptide sequences are shown with the green arrow. Flag stands for an octapeptide with the sequence DYKDDDDK.

1.3. Figure S3

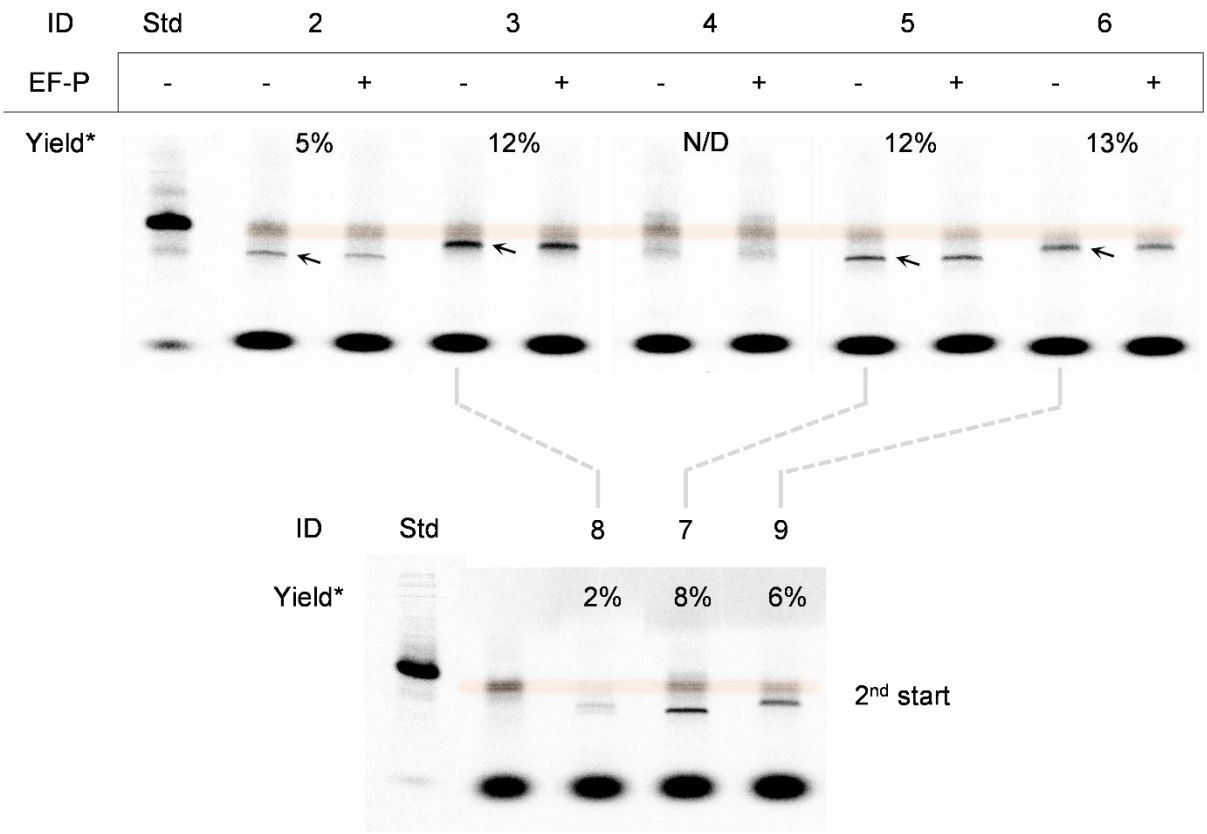

Figure S3. Quantification of the translation reactions by means of radioisotopes. Upper part: Substrates **2**–**6** were incorporated into the MGGGTYY-flag sequence, with and without elongation factor P (EF-P), a translation factor that was previously shown to facilitate the incorporation of "difficult" amino acids. In our case this factor had no effect on the incorporation efficiency. Lower part: Substrates **7**–**9** were incorporated in the MYAATAACA-flag sequence to yield macrocyclic foldamer-peptide hybrids. Lane 2 (unlabelled) corresponds to a translation reaction in which "uncharged" $tRNA^{fMet}_{CAU}$ (initiator tRNA) was added instead, demonstrating that the observed band corresponds to a peptide sequence lacking the initiating (foldamer) residue (highlighted in orange). Std stands for standard and it is a reaction in which Met has been added, allowing a direct comparison of the foldamer-initiated sequences with their "natural" counterparts. Yields are a comparison of the concentration of the foldamer-peptide hybrid and its "natural" counterpart. The intense band at the bottom of the gels corresponds to unreacted ^{14}C Asp.

1.4. Figure S4

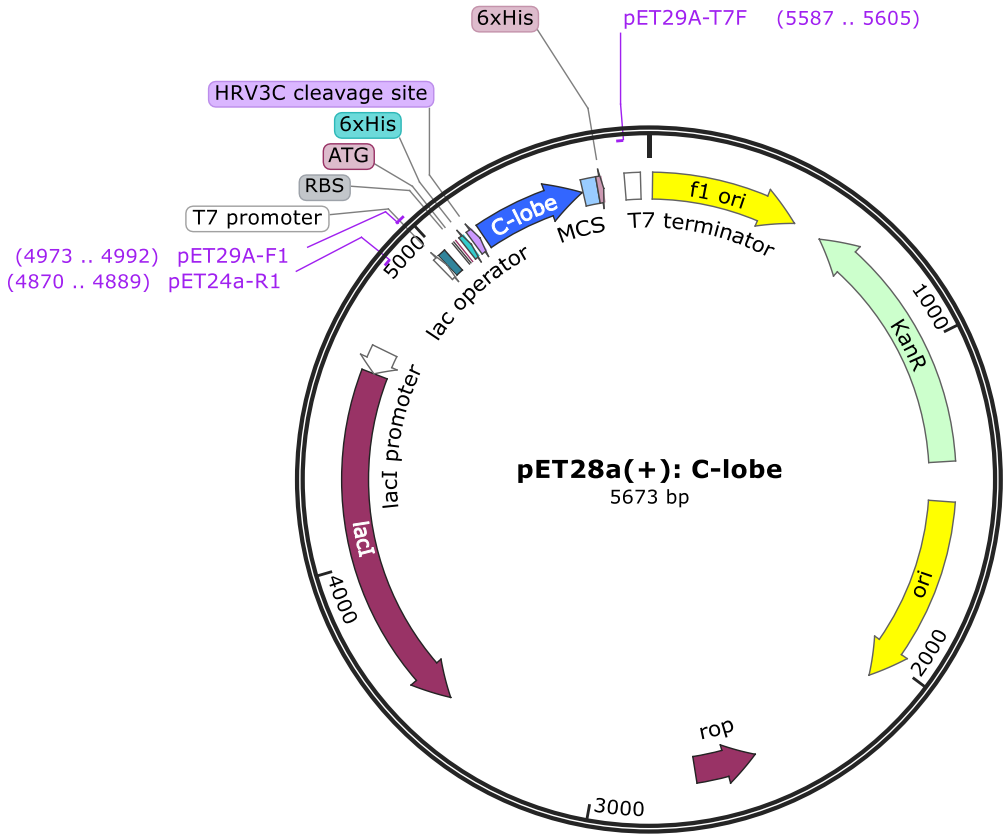

ATGGGCAGCAGCCATCATCATCATCATCACAGCAGCGGCCTGGAAGTTCTGTTCCAGGGGCCCCATATGGCTA
GCAATCTAGATTTCCAAGCACTAGAAGAAACTACAGAATATGACGGTGGCTATACCAGGGACTCTGTTCTGAT
TAGGGAGTTCTGGGAAATCGTTCATTCATTTACAGATGAACAGAAAAGACTCTTCTTGCAGTTTACAACGGGC
ACAGACAGAGCACCTGTGGGAGGACTAGGAAAATTAAAGATGATTATAGCCAAAAATGGCCCAGACACAGA
AAGGTTACCTACATCTCATACTTGCTTTAATGTGCTTTTACTTCCGGAATACTCAAGCAAAGAAAAACTTAAAG
AGAGATTGTTGAAGGCCATCACGTATGCCAAAGGATTTGGCATGCTGTAA

MGSSHHHHHHSSGLEVLFQ|GPHMASNLDFQALEETTEYDGGYTRDSVLIREFWEIVHSFTDEQKRLFLQFTTGTD
RAPVGGLGKLKMIIAKNGPDTERLPTSHTCFNVLLLPEYSSKEKLKERLLKAITYAKGFGML

Figure S4. pET28a(+) plasmid map (top), coding sequence (middle), and "C-lobe" protein expression product (bottom) used in this study; **|** indicates the HRV3C protease cleavage site.

1.5. Figure S5

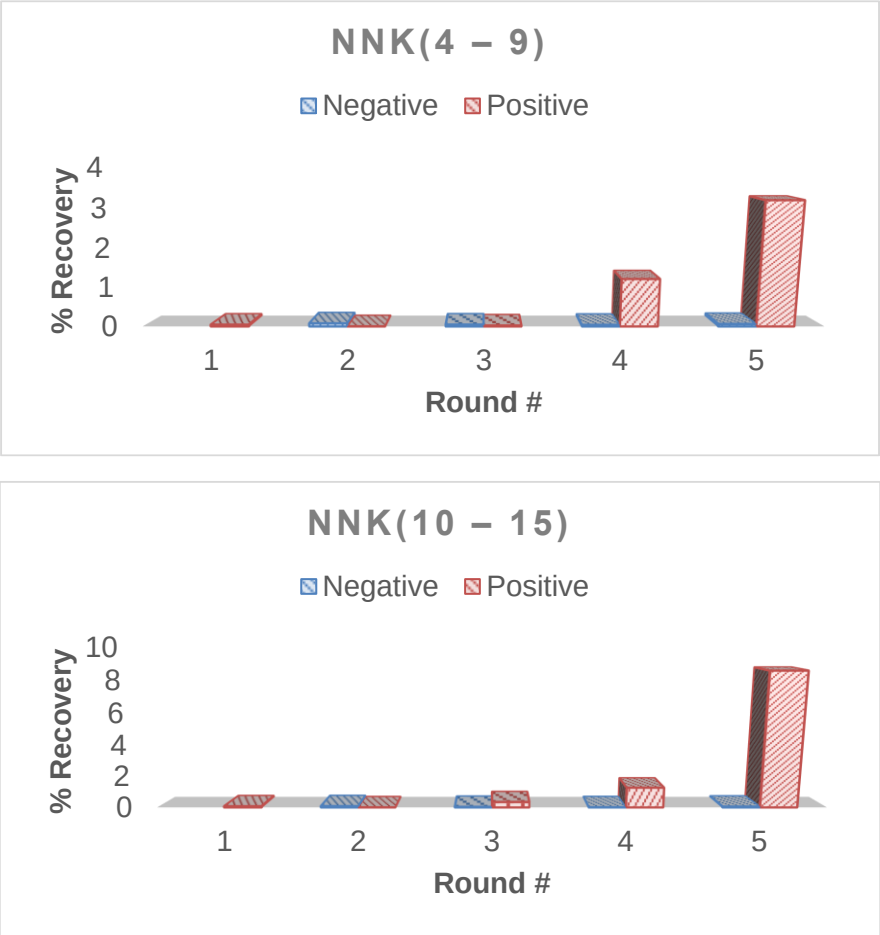

Figure S5. The recovery (%) for the 5 rounds of the selection experiment for the NNK4–9 (top) and NNK 10–15 (bottom) libraries as determined by qPCR for both positive (protein-modified beads, shown also in **Figure 2d**) and negative (non-modified beads).

1.6. Figure S6

```
                                                    Frequency
1  - - - - - - - xWR  YVYQKC*- - -  - - - -  11.49%
2  - - - - - - - xWR  YVYQRC*- - -  - - - -  11.39%
3  - - - - - - - xWR  RVYNRC*- - -  - - - -  7.86%
4  - - - - - - - xWR  YVYTKC*- - -  - - - -  7.84%
5  - - - - - - - xWR  YVYQPC*- - -  - - - -  6.12%
6  - - - - - - - xWR  YAYQKC*- - -  - - - -  4.54%
7  - - - - - - - xWR  YVYVKC*- - -  - - - -  2.99%
8  - - - - - - - xWR  RVYVRC*- - -  - - - -  2.46%
9  - - - - - - - xWR  YVYDKC*- - -  - - - -  2.39%
10 - - - - - - - xWR  YVYEKC*- - -  - - - -  2.22%
11 - - - - - - - xWR  YVY-KC*- - -  - - - -  1.65%
12 - - - - - - - xWR  YVYSRC*- - -  - - - -  1.49%
13 - - - - - - - xWR  YVYIKC*- - -  - - - -  1.26%
14 - - - - - - - xWR  YVYDRC*- - -  - - - -  1.24%
15 - - - - - - - xWR  RVYQRC*- - -  - - - -  1.12%
16 - - - - - - - xIR  VSYS-C*- - -  - - - -  1.05%
17 - - - - - - - xWR  YVYERC*- - -  - - - -  0.96%
18 - - - - - - - xWR  YVYAKC*- - -  - - - -  0.91%
19 - - - - - - - xC-  TNRSPC*- - -  - - - -  0.82%
20 - - - - - - - xWR  HILLTC*- - -  - - - -  0.80%

                                                    Frequency
1  - - - - - xKLSA  TNWILRRTC*  - - - -  8.65%
2  - - - xTNPLFT  YAKNWVLKRC  *- - -  2.06%
3  - - - xKQPGVN  AVLSYGLMSC  *- - -  1.93%
4  - - - - xKTMYK  NLLRRLAC*-  - - - -  1.76%
5  - - - - xSECPY  NDPRLVIVFC  *- - -  1.75%
6  - - - - xHDVRV  RAVLNVTAKC  *- - -  1.64%
7  - - - - xKPQYR  QLLTRLSC*-  - - - -  1.55%
8  - - - - - xVYQR  TWISRLRC*-  - - - -  1.45%
9  - - - xNPHAAR  FAVRAALRDC  *- - -  1.20%
10 - - - - - xSKPQ  VLAVVRASC*  - - - -  1.09%
11 - - - - xVWQLK  ETAWILRRSC  *- - -  1.06%
12 - - - - xTYTNP  LVLYALNYRC  *- - -  1.05%
13 - - - - xQWRKY  IVAAALRELC  *- - -  1.04%
14 - - - xANRYSG  QYRYTLQRLC  *- - -  1.01%
15 - - - xSVKYTD  MRVLTVTRVC  *- - -  1.00%
16 - - - - xSGTYK  NLLTKLSKC*  - - - -  0.99%
17 - - - - xNAHVL  AVVRTQDKSC  *- - -  0.97%
18 - - - xSLSETN  WILSRTLQC*  - - - -  0.95%
19 - - - xNGRYAQ  TLTRLTKLTC  *- - -  0.92%
20 - - - xSAYRIP  GVSAAVNWNC  *- - -  0.77%
```

Figure S6. A clustal alignment of the 20 most abundant sequences for both libraries, NNK4–9 (top) and 10–15 (bottom), in which: (x) stands for the Foldamer-G-F- segment, (*) for the G-S-G-S-G-S linker followed by the *amber* stop codon (TAG) and (-) in the middle of the sequence (sequences 11,16 & 19 in short library) indicates the appearance of the *amber* stop codon (TAG). The number on the right indicates the appearance frequency (number of reads/total number of reads x 100). Alignment of the top 50 sequences can be found in **Extended Data 1**.

1.7. Figure S7

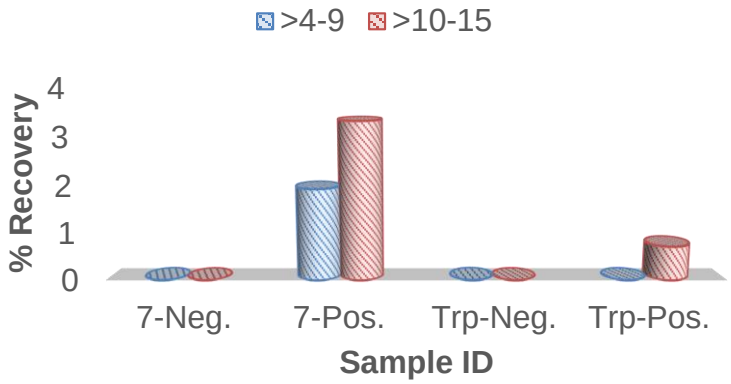

Figure S7. The top sequences of each library from the sequencing data, linked to their genotype, were exposed to protein-modified (Pos) and unmodified beads (Neg), and recovery determined by qPCR, highlighting the selectivity attributed to the scaffold from the abiotic residue (7-Neg vs 7-Pos). In a subsequent experiment, the abiotic initiator was substituted with Trp (capable of undergoing cyclization). While in the large peptide some binding could be retained, in the case of the shorter peptide was completely abolished, hinting on the significance of the peptide's foldamer-imposed orientation.

1.8. Figure S8

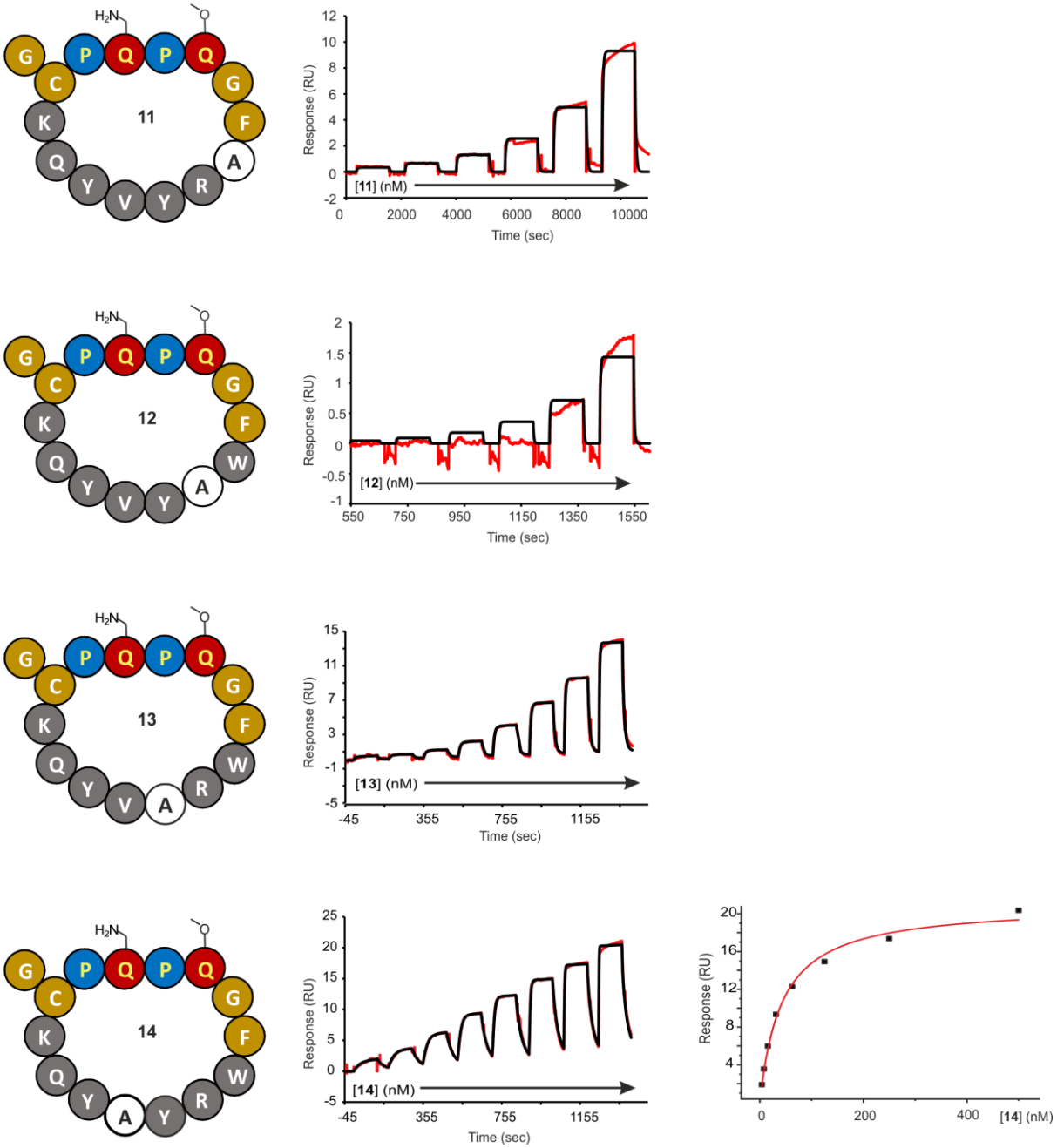

Figure S8 part 1 . SPR sensorgams of Ala-scan compounds **11**-**14** used as analytes, while C-lobe was immobilized on CM5-sensor chips via amine coupling with the use of NHS/EDC activation. Unreacted NHS esters on CM5 flow cells were further deactivated by injection of a 1M ethanolamine, HCl (pH 8) solution. In the case of macrocycle **14**, saturation was reached. This allowed to plot the Langmuir steady-state binding curve (at right), which confirmed the K_d value calculated from fitting the sensorgrams. The peptide chains belonging to variable windows are depicted as a grey pearl string and the foldamer segment is depicted with blue (P) and red (Q) balls. The constant α-amino acid residues are colored in gold. The glycine not involved in the macrocycle corresponds to the C-terminus of the sequence. The adjacent cysteine is involved in the thioether junction with the N-terminal foldamer P unit.

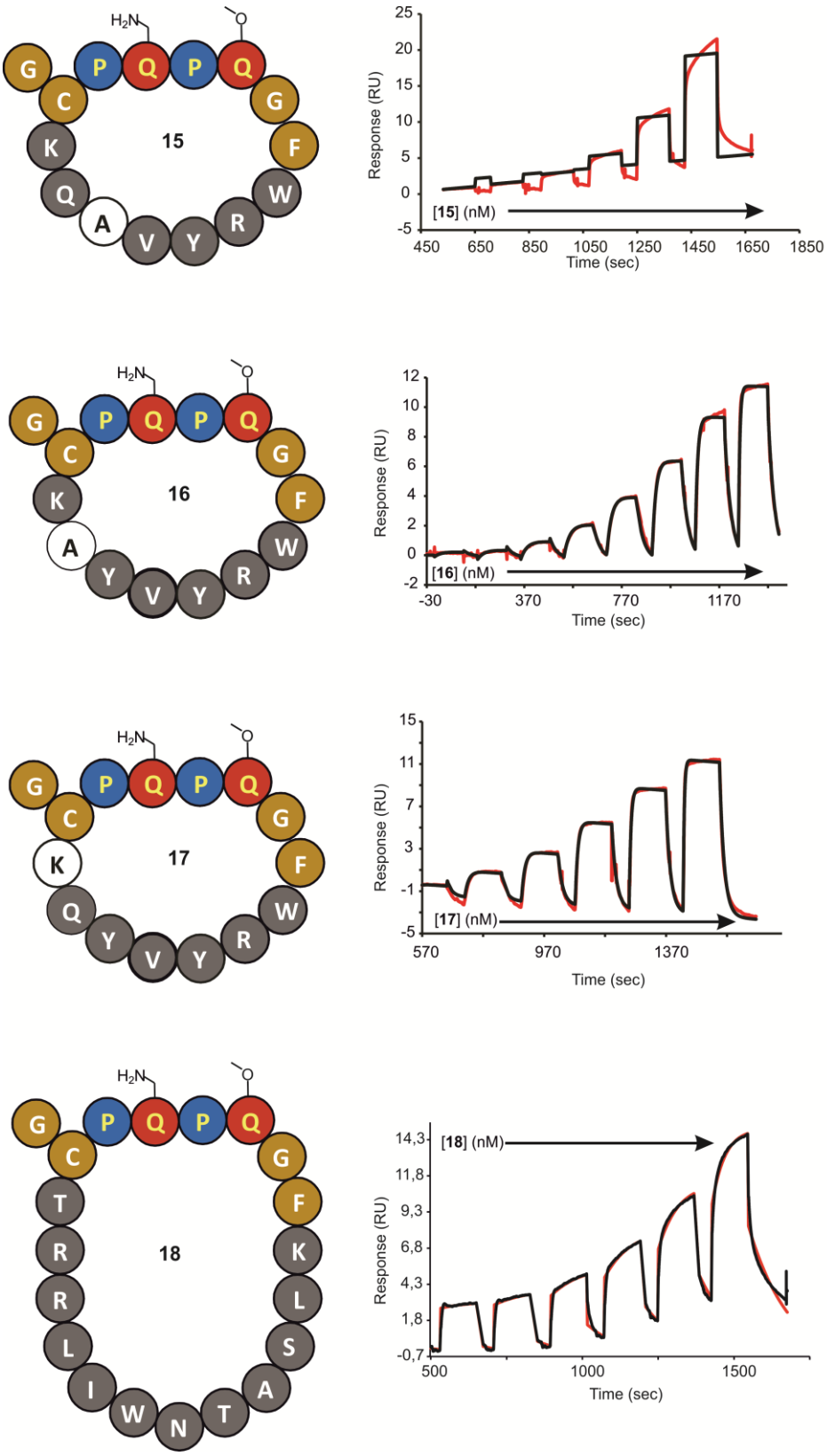

Figure S8 part 2. SPR sensorgams of Ala-scan compounds **15**-**18** used as analytes, while C-lobe was immobilized on CM5-sensor chips via amine coupling with the use of NHS/EDC activation. The sensorgrams could not be fitted for compound **15** and only a lower estimate of the K_d could be provided.

1.9. Figure S9

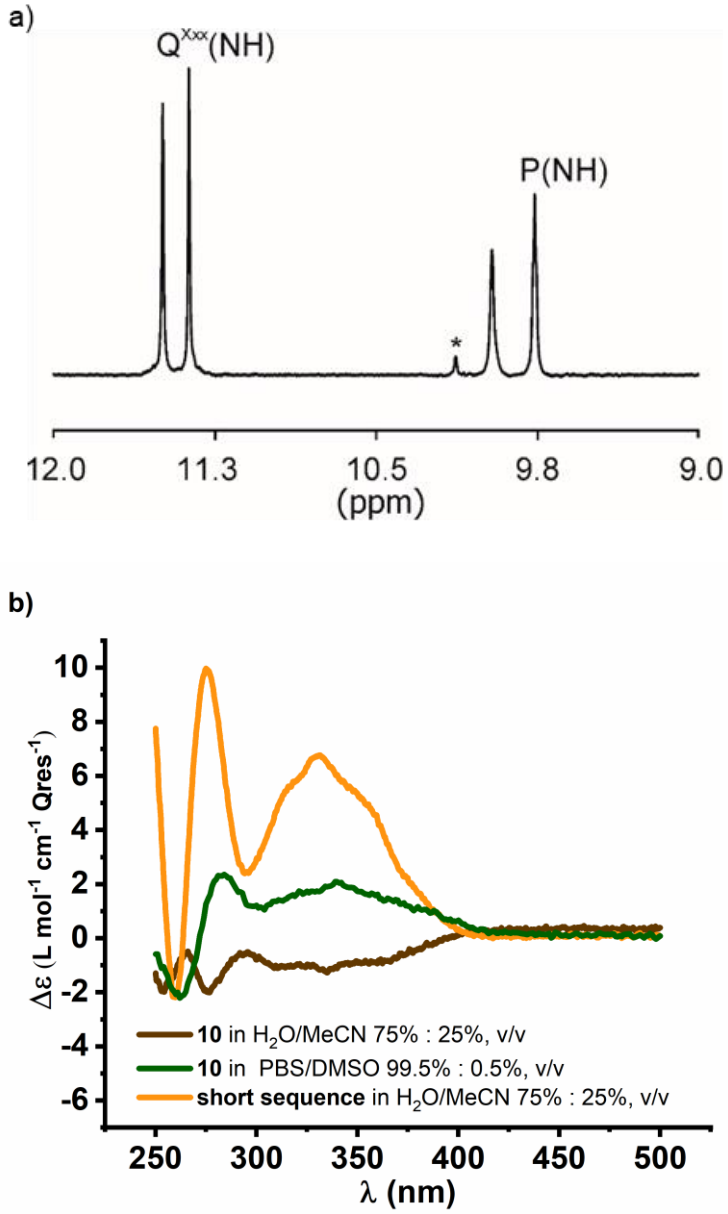

Figure S9. (a) Part of the ^{1}H NMR spectrum of **10** between 12.0–9.0 ppm in CD_3CN (25% (v/v) in H_2O, water suppression). The helically-folded, downfield-shifted protons of the quinoline amides are at ~11.5 ppm, and one of the two pyridine amides is at ~9.8 ppm. This significant downfield shift of amide proton resonances is a result of a hydrogen-bonded structure which is a typical indicator for helical folding.[11a] The adjacent signal at ~10.0 ppm belongs to the Trp7 N–H signal, and the asterisk (*) denotes an impurity. (b) CD spectrum of **10** at 25 °C in different solvents: recorded at a concentration of 242 µM in H_2O/MeCN (75:25 v/v); recorded at a concentration of 15 µM in 20 mM PBS buffer pH 7.4, containing 0.5% DMSO used for the initial dissolution of **10**. CD spectrum of a previously reported macrocyclic peptide-foldamer hybrid "short sequence" (CH_2–C(O)–PQ^{Asp}PQ^{Asp}GlyPhe(Lys)$_3$*Cys*Gly–OH, compound **3** from Dengler *et al*; italics represent elements connected by thioether macrocyclization)[15a] with *P* handedness bias is included for comparison.

1.10. Figure S10

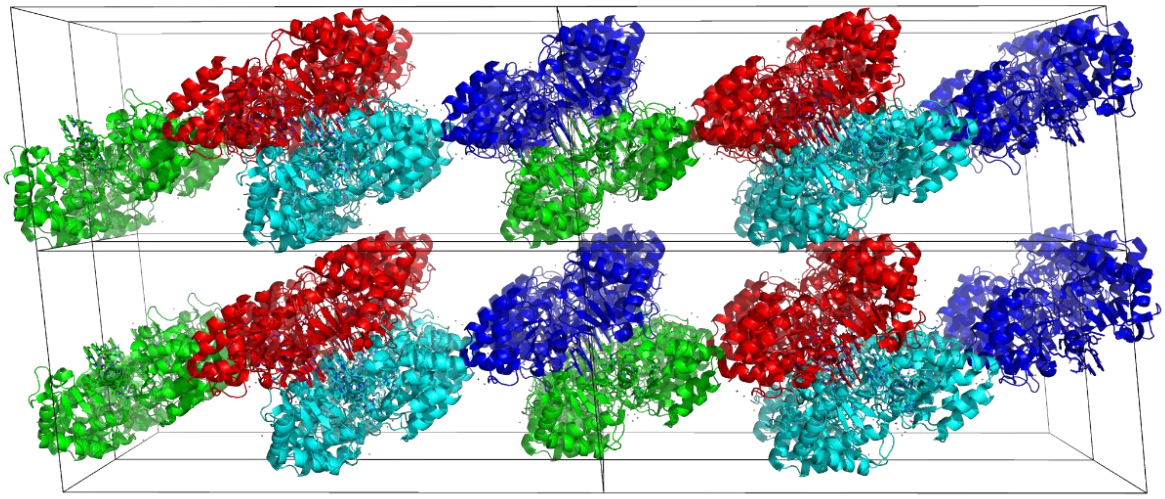

Figure S10. The crystal lattice of the C-lobe and ligand **10** complex. The asymmetric units in the unit cells are shown in green, red, cyan, and blue.

1.11. Figure S11

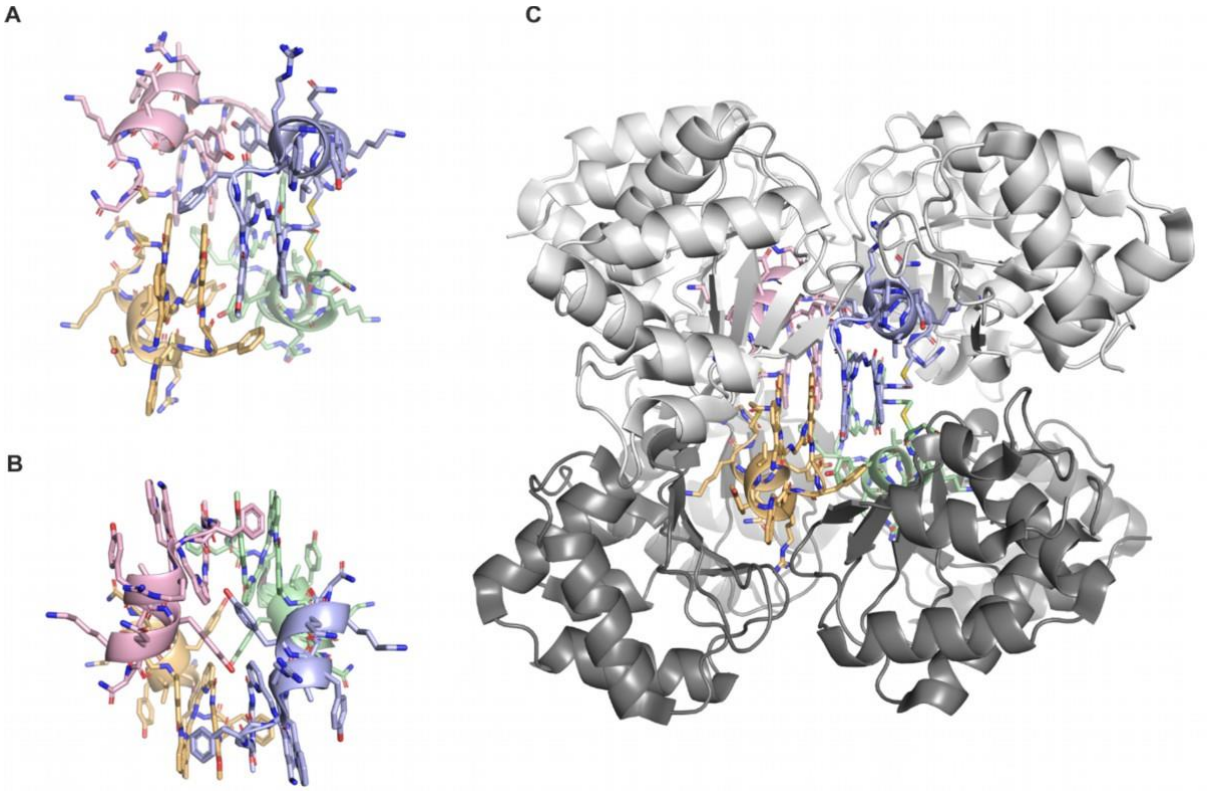

Figure S11. Crystal packing of the C-lobe and ligand **10** complex. Two views of a cluster of four macrocycles **10** showing stacking between (A) foldamers and (B) between Tyr11 residues. C) Cube formed by eight C-lobe proteins surrounding the cluster of four macrocycles.

1.12. Figure S12

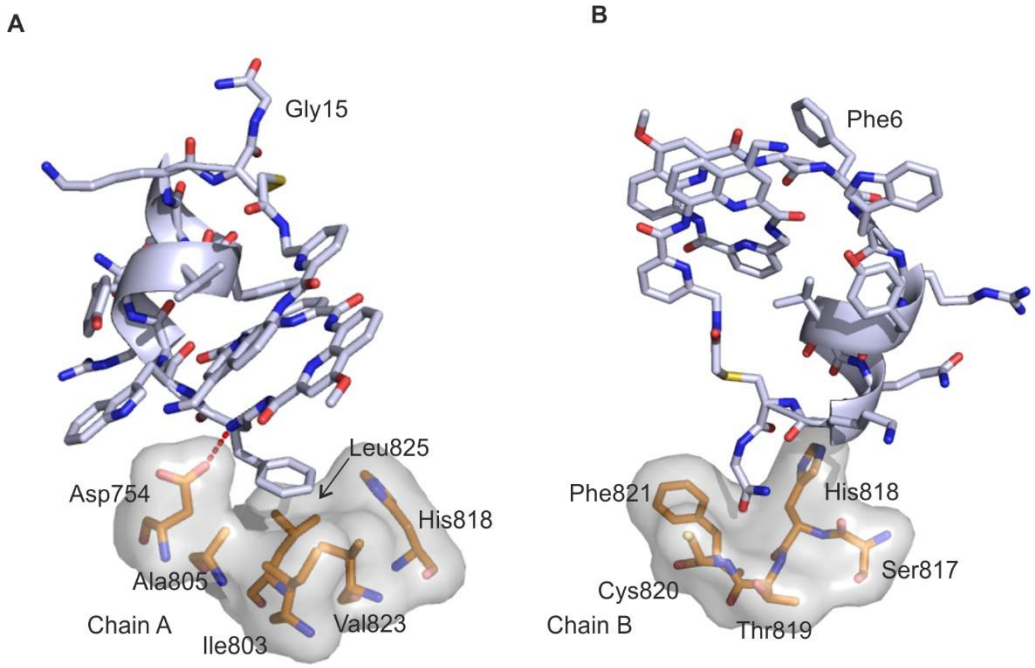

Figure S12. Representation of the contacts between the residues Phe6 and Gly15 in **10** and the C-lobe surface of chains A and B in the asymmetric unit, respectively.

1.13. Figure S13

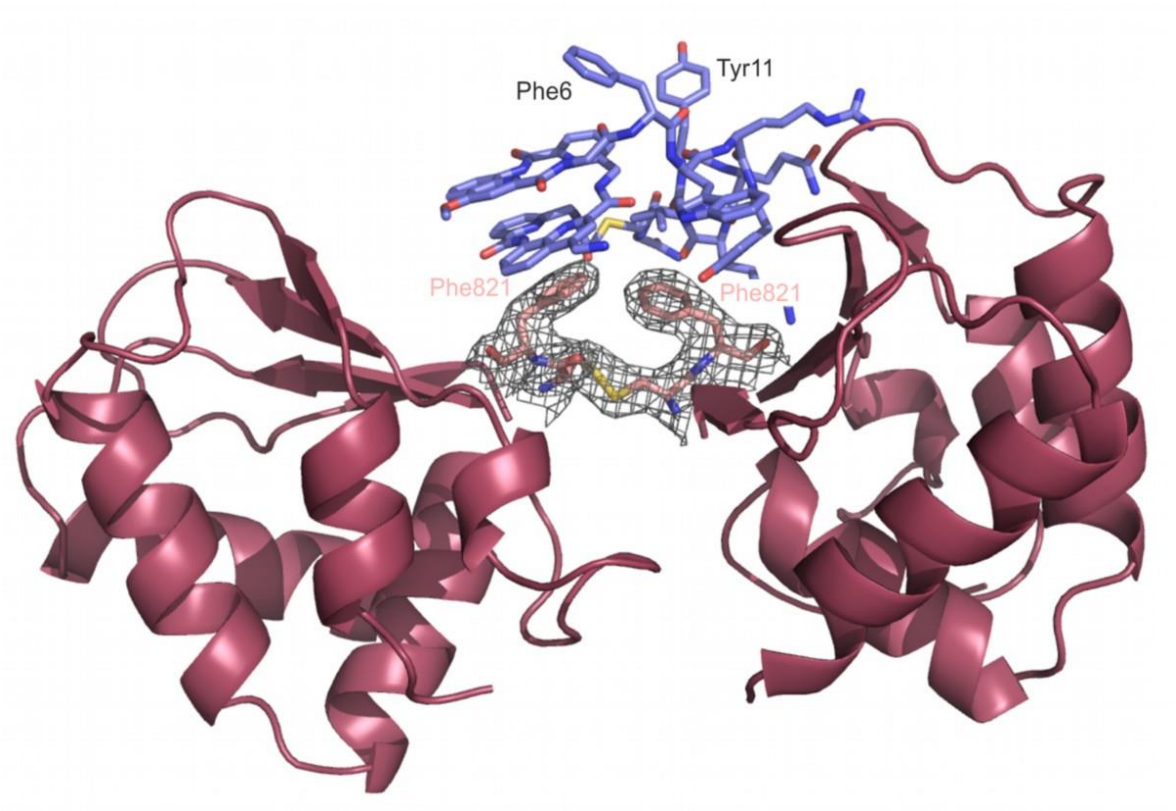

Figure S13. The disulfide bridge between Cys820 of chain C and Cys820 of the symmetry-related chain A' (right) in the crystal packing. The stacking of Phe821 (chain A') and foldamer units of the macrocyclic ligand **10** prevents binding of a second macrocycle on the cognate site of A' and promotes the 2:1 protein-ligand stoichiometry in the crystal. The Cys820 and Phe821 amino acid residues are shown with the 2Fo-2Fc electron density map at 1.0 σ for the disulfide.

1.14. Figure S14

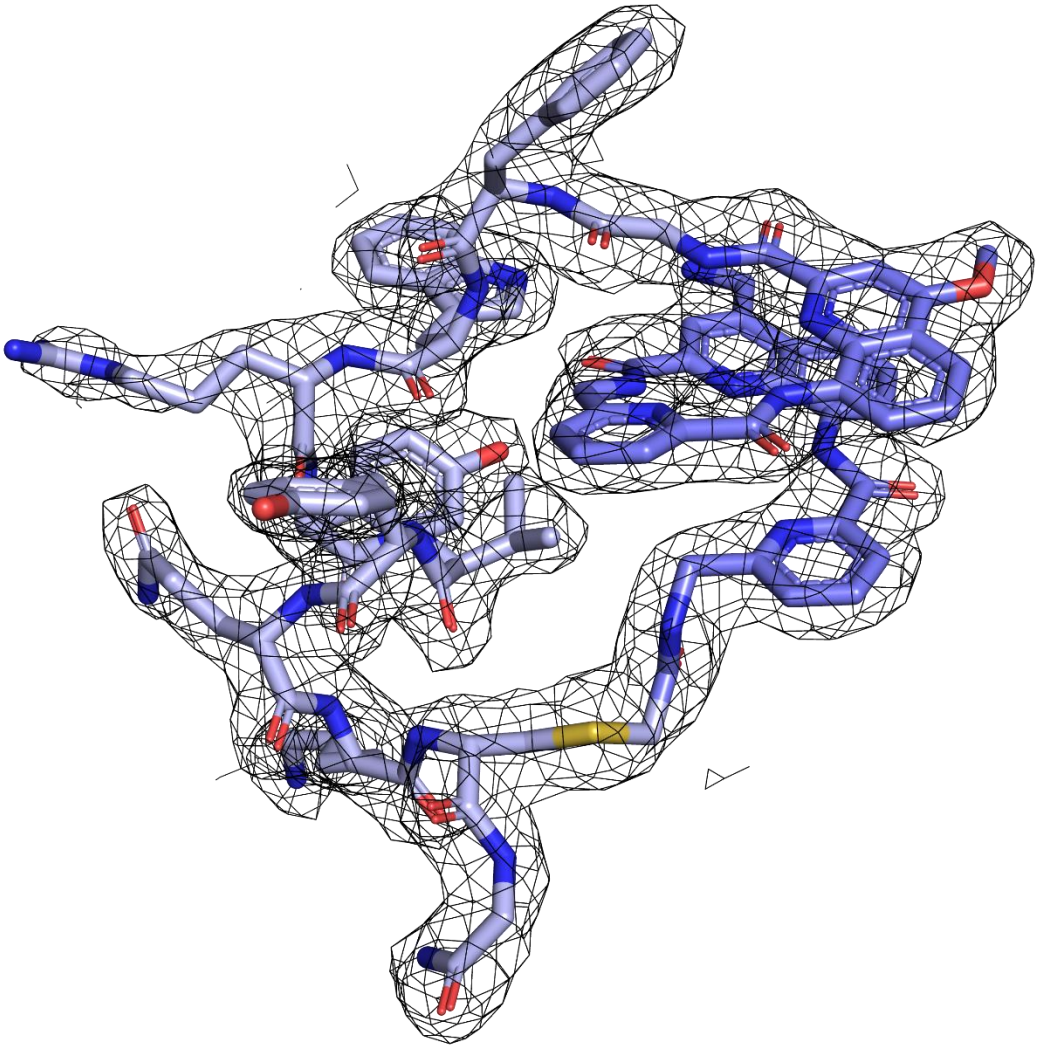

Figure S14. The weighted 2Fo-Fc electron density maps (black mesh) for the bound ligand **10** in the crystal structure are shown contoured at 1.0 σ.

1.15. Figure S15

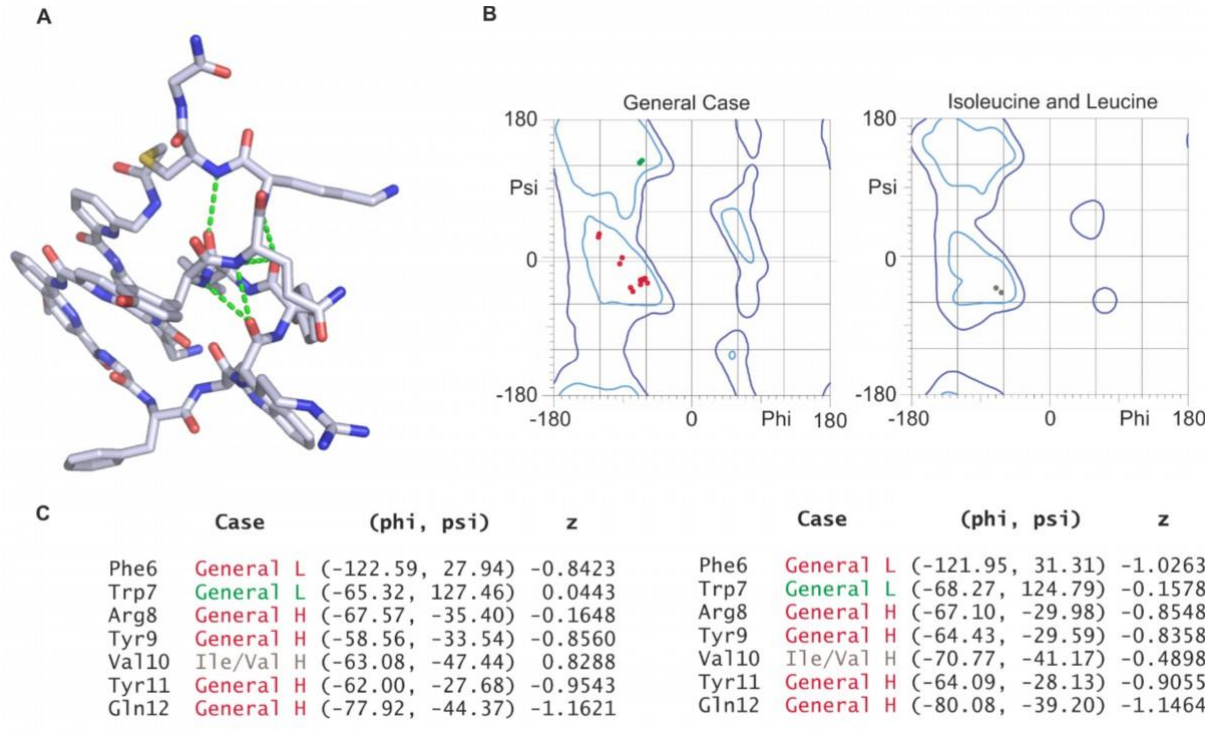

Figure S15. a) Intramolecular hydrogen bond network of the α-helix in **10**; B) Ramachandran plots obtained from MolProbity and C) Tables of Phi, Psi and Z data for each of the residues involved in the α-helix conformation and corresponding to the two hybrid molecules of **10** present in the asymmetric unit.

1.1. Figure S16

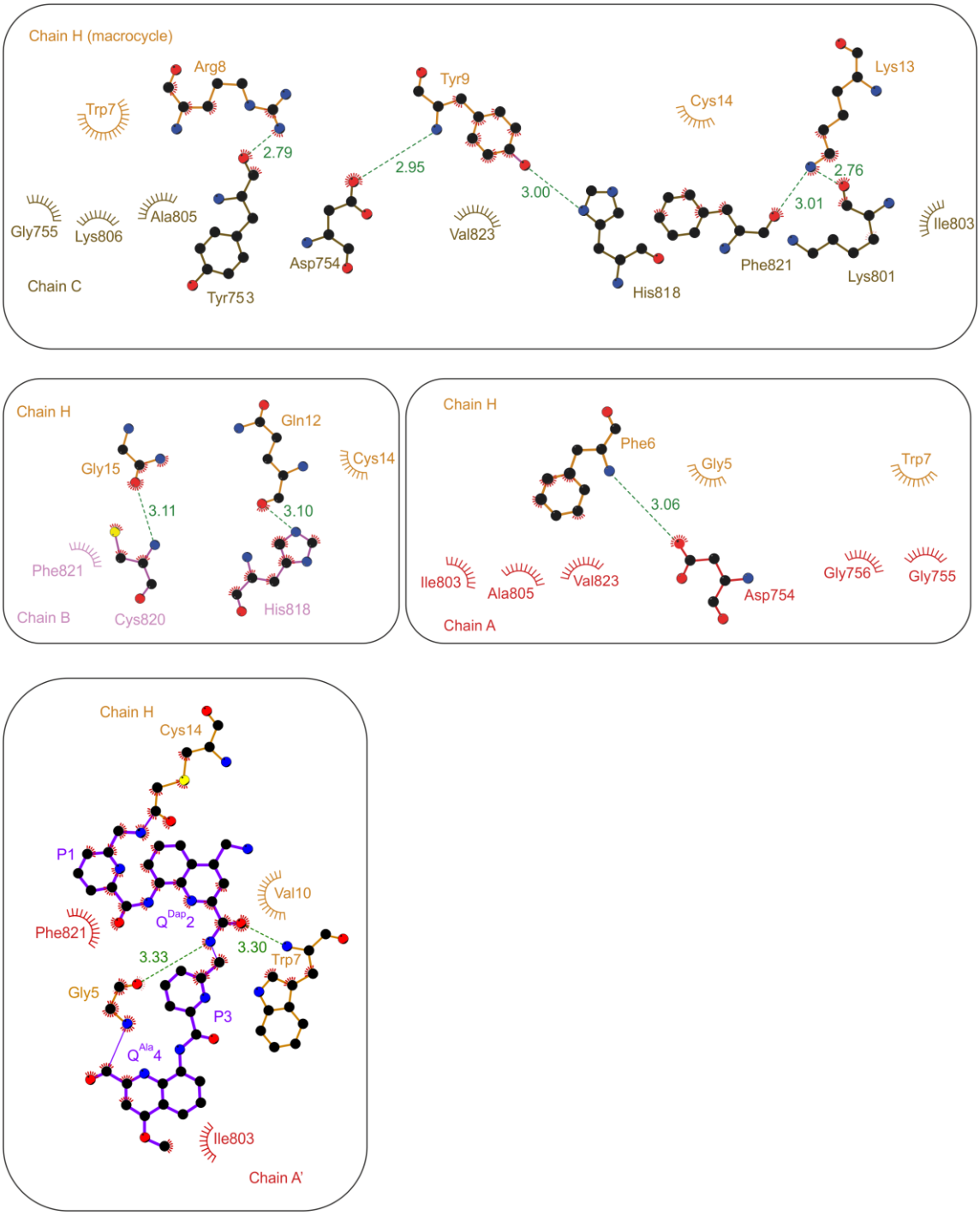

Figure S16. LigPlot representation of the crystal contacts between macrocycle **10** (chain H) and four distinct C-lobe protein chains (chains A, A', C and B). The top panel shows contacts between protein residues of chain C and the peptide residues that were converged during the display selection, constituting a binding area of 396 Å^2. The middle left panel show contacts between protein residues of chain B and the Gly15, Gln12, and Cys14 residues of the ligand, contact area of 5 Å^2. The middle right panel shows contacts between protein residues of chain A and Phe6, Gly5, and Trp7 of the ligand, contact area of 201 Å^2. The bottom panel shows interactions between the chain A' and the ligand **10**, contact area of 173 Å^2.The plots were generated using LigPlot v.14.5 software and the 7QPB PDB file.[22]

1.2. Figure S17

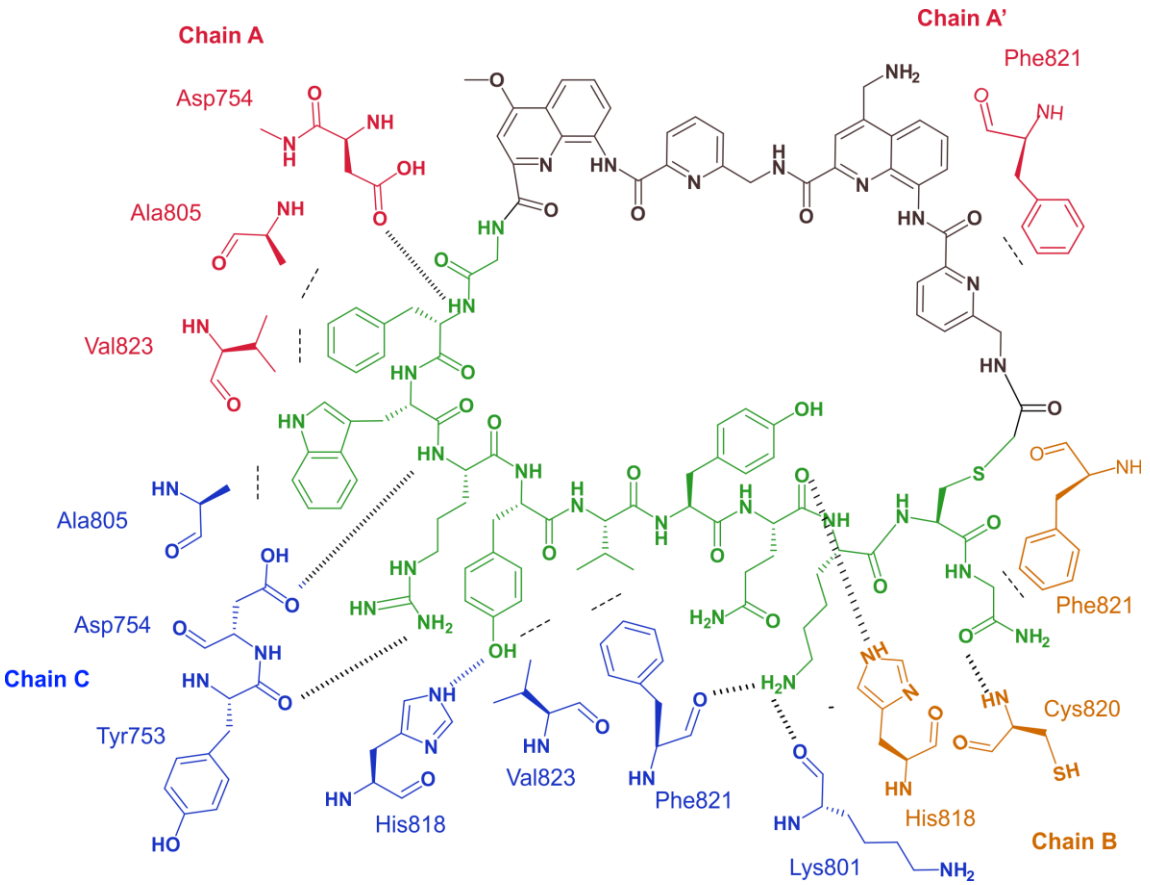

Figure S17. Overview of contacts between macrocycle **10** (chain H) and four C-lobe protein chains of the crystal lattice (A, A', B, C). The actual macrocycle binding site is on chain C. For more details, see **Figure S16**.

1.3. Figure S18

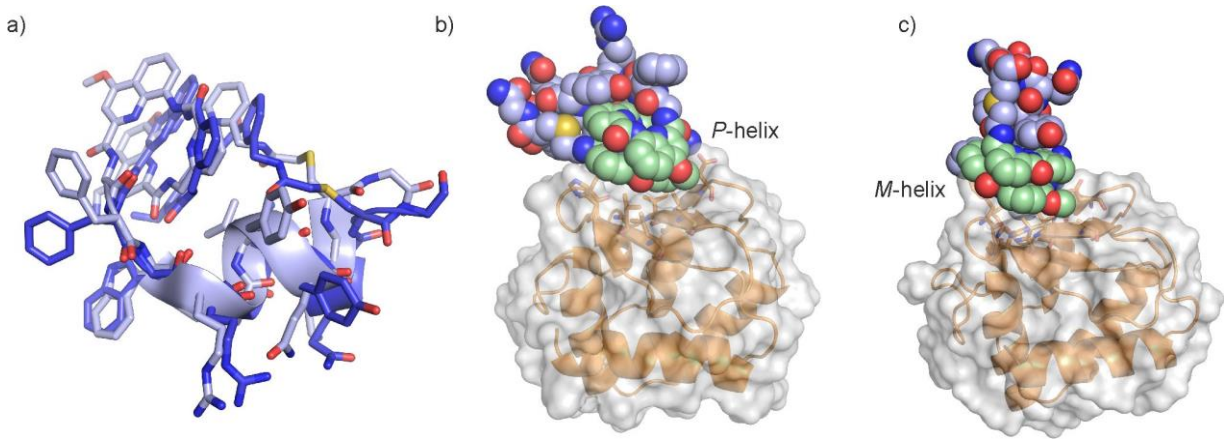

Figure S18. a) Overlay of **10** with a *P*-helical foldamer as found in complex with C-lobe in the crystal structure (dark blue) and of **10** with an *M*-helical foldamer as found in a snapshot of an MD simulation of its complex with C-lobe (gray). b) Snapshot of an MD simulation of **10** with a *P*-helical foldamer (green) showing a binding mode where the foldamer is in contact with the protein. c) Snapshot of an MD simulation of **10** with an *M*-helical foldamer (green) showing a configuration where the foldamer is in contact with the protein.

1.4. Figure S19

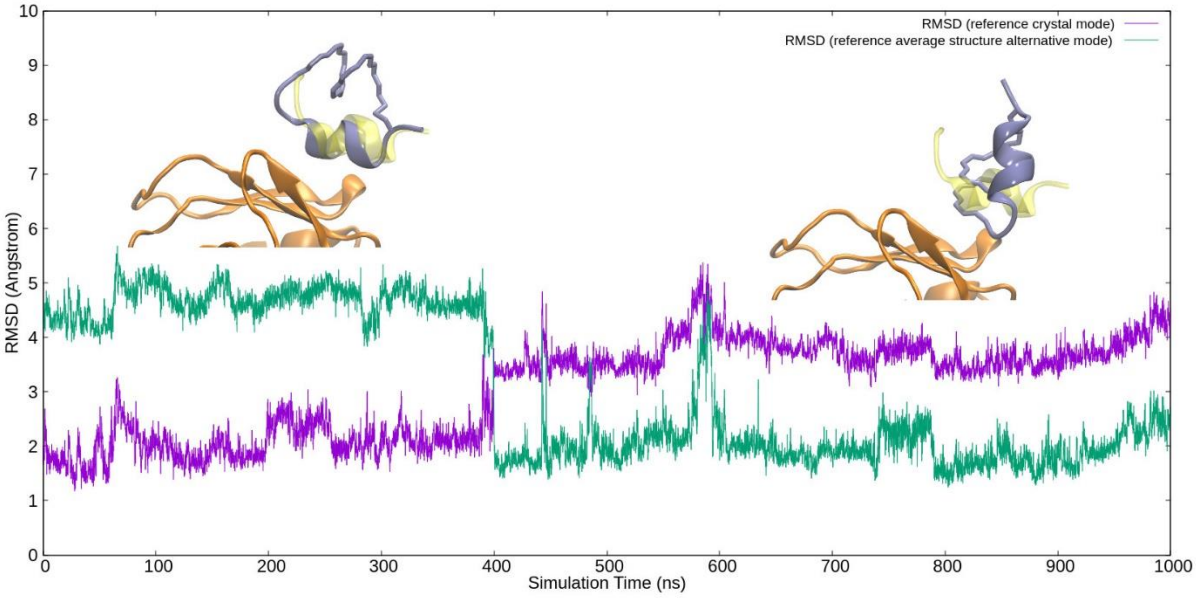

Figure S19. Root mean square displacement (RMSD) along a 1000 ns MD simulation trajectory for a *M* **10** with C-lobe complex. Purple line is RMSD with respect to the crystal structure (C-lobe and α-helix backbone atoms included in RMSD calculation). Green line is RMSD with respect to an average structure of all conformations in the alternative binding mode (as shown in **Figure 4c** of the main text, C-lobe, α-helix and foldamer backbone atoms included in RMSD calculation). Two snapshots represent the structures of crystal mode (left) and alternative mode (right, with foldamer helix in contact with the protein), in which the α-helix in crystal structure is shown in a transparent yellow representation as reference.

1.5. Figure S20

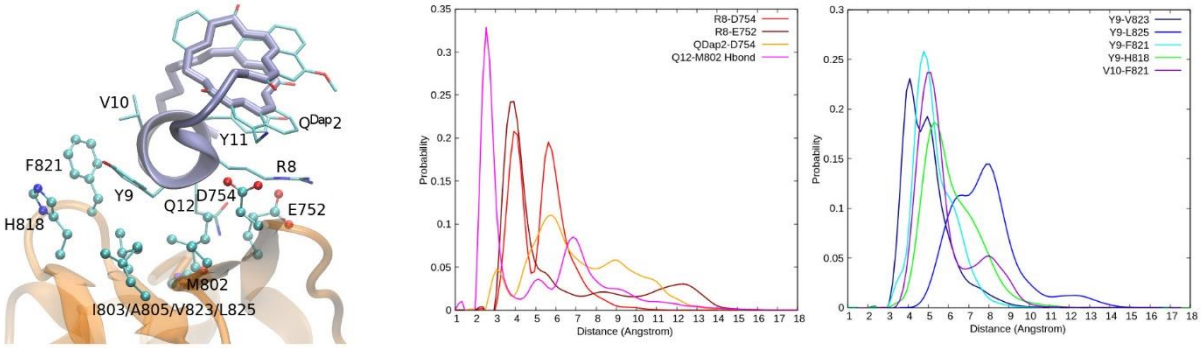

Figure S20. Snapshot and distance histograms for the *M* **10**-C-lobe complex at the binding mode similar to the crystal structure. Left: Representative snapshot. Middle: Salt bridge and hydrogen bond (Hbond) distance histograms, in which the side chain N atom in $Q^{Dap}2$ and guanidinium C atom in Arg8 of the macrocycle, and the carboxylate C atoms in Glu752 or Asp754 of C-lobe are used in the distance calculation. Hbond distance is between Gln12 side chain N of the macrocycle and Met802 backbone O atom of C-lobe. Right: Distance histograms for other contacts, in which the centers of masses of hydrophobic side chain groups of C-lobe (Val823, Leu825, Phe821, His818) and the macrocycle (Tyr9, Val10) are used in calculating the residue-residue distance. The probability of occurrence is normalized by the total number of conformations in this binding mode.

1.6. Figure S21

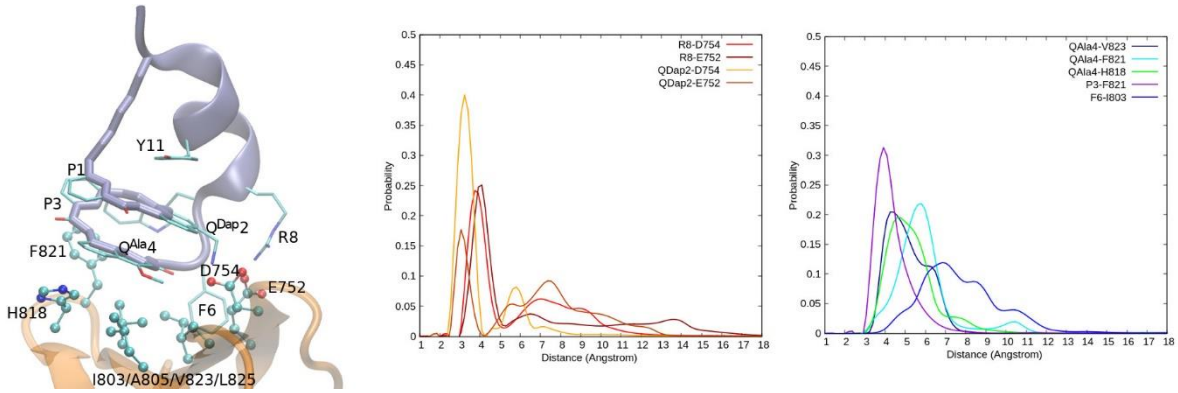

Figure S21. Snapshot and distance histograms for the *M* **10**-C-lobe complex at an alternative binding mode as shown in **Figure 4c** in the main text. Left: Representative snapshot. Middle: Salt bridge distance histograms, in which the side chain N atom in Q^{Dap} and guanidine C atom in Arg8 of the macrocycle, and the carboxylate C atoms in Glu752 or Asp754 of C-lobe are used in the distance calculation. Right: Distance histograms for other contacts, in which the centers of masses of hydrophobic side chain groups of C-lobe (Val823, Phe821, His818, Ile803) and of the macrocycle (Q^{Ala}4, P3, Phe6) are used in calculating the residue-residue distance. The probability of occurrence is normalized by the total number of conformations in this binding mode.

1.7. Figure S22

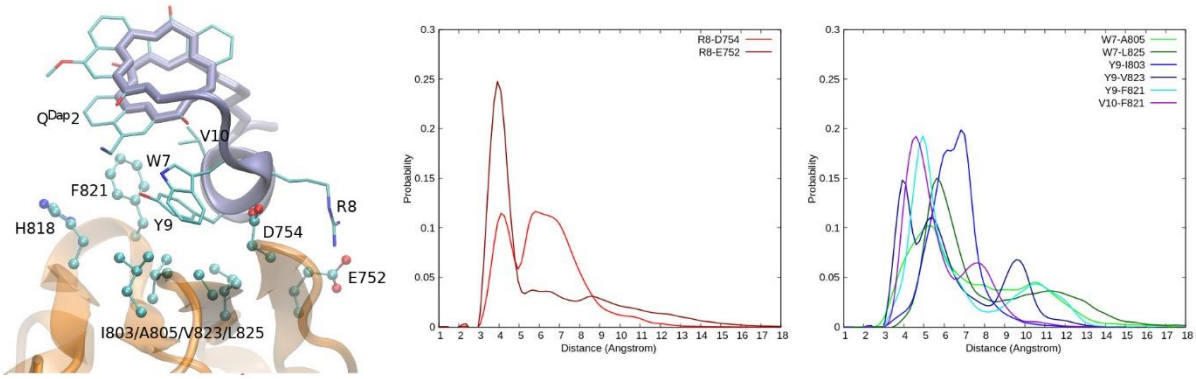

Figure S22. Snapshot and distance histograms for the *P* **10**-C-lobe complex at the binding mode resembling the crystal structure. Left: Representative snapshot. Middle: Salt bridge distance histograms, in which the guanidine C atom in Arg8 of the macrocycle and the carboxylate C atoms of Glu752 or Asp754 are used in the distance calculation. Right: Distance histograms for other contacts, in which the centers of masses of hydrophobic side chains of C-lobe (Ile803, Ala805, Val823, Leu825, Phe821) and of macrocycle residues (Trp7, Tyr9, Val10) are used in calculating the residue-residue distance. The probability of occurrence is normalized by the total number of conformations in this binding mode.

1.8. Figure S23

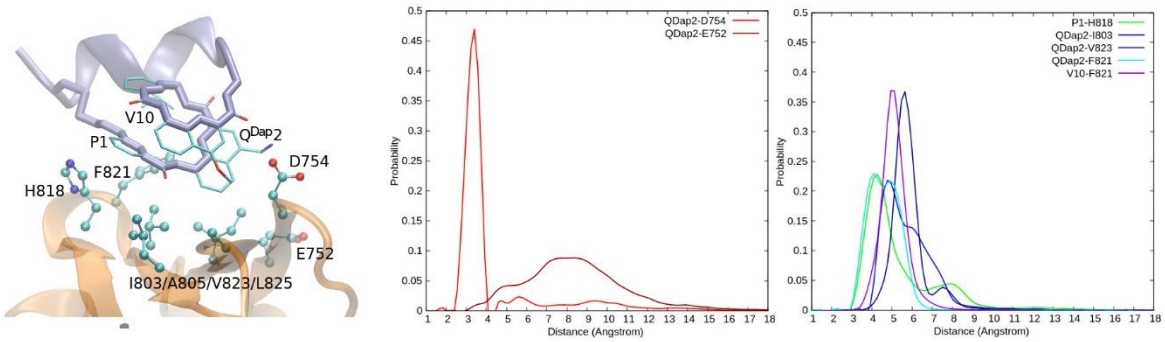

Figure S23. Snapshot and distance histograms for the *P* **10**-C-lobe complex at an alternative binding mode as shown in **Figure 4d** in the main text. Left: Representative snapshot. Middle: Salt bridge distance histograms, in which the side chain N atom in Q^{Dap} and the carboxylate C atoms in Glu752 or Asp754 are used in the distance calculation. Right: Distance histograms for other contacts, in which the centers of masses of hydrophobic side chain groups of C-lobe (Ile803, Val823, His818, Phe821) and foldamer residues (P1, $Q^{Dap}2$, Val10) are used in calculating the residue-residue distance. The probability of occurrence is normalized by the total number of conformations in this binding mode.

1.9. Figure S24

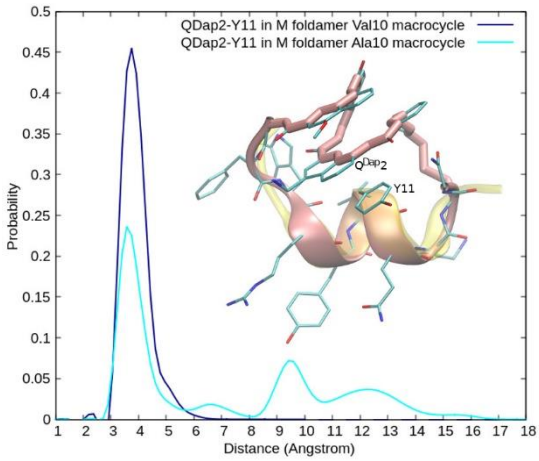

Figure S24. Histogram of the distance between COMs of aromatic rings of $Q^{Dap}2$ and Tyr11 for *M* **10** foldamer macrocycles. The insert in the graph is a snapshot showing stacking of Tyr11 and $Q^{Dap}2$ in the *M* Foldamer macrocycle. All MD trajectories are included (i.e. including all binding modes). The sequence labelled "Ala10" corresponds to the V10A mutant **14.**

1.10. Figure S25

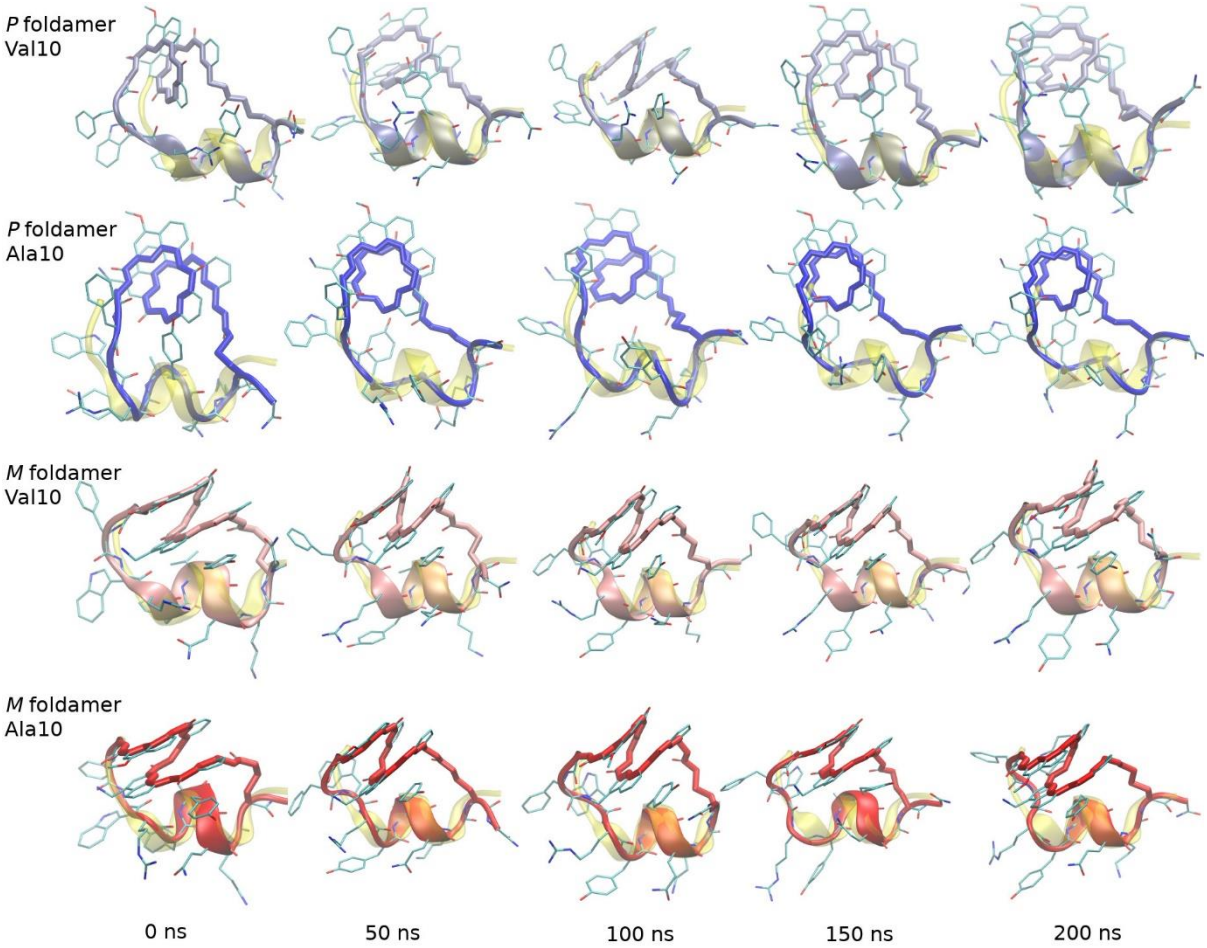

Figure S25. Snapshots of **10** in the first 200ns with C-lobe removed for clarity on macrocycle structures. The α-helix in transparent yellow is the crystal structure, used here as a reference. Sequence labelled "Ala10" correspond to the V10A mutant **14**.

2. Safety Statement

No unexpected or unusually high safety hazards were encountered.

3. Biochemistry and Structural Biology

3.1. Materials and general methods

All chemicals were purchased from Sigma-Aldrich at molecular biology grade or higher unless otherwise indicated. The pET28a(+) vector containing isoform I of human E6AP$_{741–852}$ ("C-lobe") with an N-terminal HRV3C protease-cleavable His$_6$-tag[15b] (sequence and plasmid map: **Figure S4**) was a kind gift from Dr. Sonja Lorenz (Max Planck Institute for Biophysical Chemistry) and sequence fidelity was confirmed by Sanger sequencing. One Shot™ BL21(DE3) Chemically Competent *E. coli* (C600003) and HisPur™ Ni-NTA Superflow Agarose (25217) were purchased from ThermoFisher Scientific. Econo-Column® gravity flow columns (7372551) were purchased from BioRad. Color Prestained Protein Standard (P7718S) was purchased from New England Biolabs.

Exclusively ultrapure water from an OmniaTap system (Stakpure) was used. Bacterial culture media and equipment were sterilized by autoclaving. Bacterial cultures were grown using a MaxQ-6000 shaking incubator (ThermoFisher Scientific). UV-Vis determination of protein concentration (280 nm), protein purity (260/280 nm), and OD_{600} were all measured on a NanoDrop™ One^C (ThermoFisher Scientific). Bacterial centrifugation was carried out on an Avanti JXN-26 Centrifuge (Beckman Coulter) using a JLA-8.1000 or JA-25.50 rotor. Probe sonication was carried out on a UP200St Ultrasonic Processor fitted with a S26d14 Sonotrode (Hielscher Ultrasonics) using 5 cycles of 2 min on (100% amplitude, 90% pulse) and 5 min rest.

Sodium-dodecyl sulfate-polyacrylamide gel electrophoresis (SDS-PAGE) was carried out on a BioRad system, including a PowerPac™ HC High-Current Power Supply and a Mini-PROTEAN® Tetra Vertical Electrophoresis Cell. 2× 10-, 12-, or 15-well gels with a 15% resolving gel and 4% stacking gel were prepared as follows:

Reagent	Resolving gel (15%)	Stacking gel (4%)
H_2O	3.625 mL	3.25 mL
Resolving/Stacking Buffer (SureCast, Thermo)	2.5 mL	1.25 mL
Acrylamide 30% (SureCast, Thermo)	3.75 mL	0.5 mL
Ammonium Persulfate (10% (w/v) in H_2O)	100 µL	25 µL
N,N,N',N'-tetramethylethylenediamine (TEMED)	10 µL	5 µL

Gel samples were prepared by mixing 3:1 with sample loading buffer (4×: Tris-HCl (200 mM) pH 6.8, bromophenol blue (0.04% (w/v)), glycerol (24% (v/v)), SDS (8% (w/v), β-mercaptoethanol (20% (v/v))) and boiling for 10 min. Gels were run at 85 V for 10 min then 180 V for 50 min and stained with Coomassie Brilliant Blue.

Size-exclusion chromatography (SEC) was carried out in a cold cabinet (Unichromat 1500) maintained at 15 °C on a custom Knauer fast protein liquid chromatography (FPLC) system coupled with a HiLoad® 16/600 Superdex® 75 pg column (Cytiva, 28989333). The column eluent was monitored by UV detection at 200, 220, 260, and 280 nm with a diode array detector and fractions were collected by a Foxy R1 Fraction Collector (Teledyne ISCO). Protein concentration and buffer exchange were performed using spin concentrators of various volume capacities (Amicon, 3 kDa

MWCO) according to manufacturer's instructions. Dialysis was performed using 3 kDa MWCO Slide-A-Lyzer™ G2 dialysis cassettes of various volume capacities (ThermoFisher Scientific) according to manufacturer's instructions.

3.2. Protein expression and purification

Isoform I of human $E6AP_{741–852}$ ("C-lobe") was expressed from a pET28a(+) vector with an N-terminal HRV3C protease-cleavable His_6-tag (**Figure S4**). The protein was expressed recombinantly from *E. coli* BL21(DE3) cells overnight at 18 °C in LB broth supplemented with kanamycin (50 µg mL^{-1}; Janssen) and induced at an OD_{600} of 0.6 with isopropyl-β-D-1-thiogalactopyranoside (IPTG, 0.5 mM). All subsequent steps were performed at 4 °C where possible. The cells were harvested by centrifugation (7,548 × g, 20 min), resuspended in lysis buffer (17.5 mL per 1 L culture; 50 mM Tris-HCl, pH 8.0, 100 mM NaCl, 5 mM imidazole, 1 mM DL-dithiothreitol (DTT), 0.1% (v/v) Triton X-100, 4% (v/v) glycerol), and lysed by probe sonication. The lysate was cleared by centrifugation (43,667 × g, 40 min) and incubated for 30 min with pre-equilibrated HisPur™ Ni-NTA Superflow Agarose (~2.5 mL slurry per 1 L culture). The agarose resin was applied to a gravity column, washed with wash buffer (100 mL; 50 mM Tris-HCl, pH 8.0, 400 mM NaCl, 5 mM imidazole, 1 mM DTT), and His_6-tagged protein eluted with elution buffer (50 mM Tris-HCl, pH 8.0, 400 mM NaCl, 250 mM imidazole, 1 mM DTT) by monitoring the absorption of the eluent at 280 nm. The purity of the eluent was determined by SDS-PAGE.

For isolation of protein with its associated His-tag, the eluate from the Ni-NTA column was further purified by SEC at a flow rate of 0.3–0.8 $mL.min^{-1}$ in SEC buffer (50 mM Tris-HCl, pH 7.4, 150 mM NaCl, 1 mM DTT) over Superdex 75 pg. Fractions corresponding to the protein of interest were analysed by SDS-PAGE for purity, combined, and concentrated.

For isolation of protein without its associated His-tag, the eluate from the Ni-NTA column was digested overnight by addition of HRV3C protease (Merck 71493; 20U per 1 mL crude protein) during dialysis into SEC buffer at 4 °C. The digested protein was incubated with Ni-NTA agarose as described above and eluted from the column with SEC buffer. The eluate was concentrated and purified further by SEC as described above.

3.3. *In vitro* translation

Preparation of eFx and $tRNA^{fMet}_{CAU}$

All oligonucleotides were purchased from Operon (Japan). DNA templates were assembled using reported protocols and after transcription, using T7 RNA polymerase, they resulted in the desired sequences.[23–26]

Microhelix

Microhelix RNA (mhRNA) was purchased from GeneDesign (Japan), being a mimic of the acceptor stem of tRNA (the site of aminoacylation), originally based on the acceptor stem of *E. coli* Asn tRNA.

Aminoacylation of mhRNA

3 µL H_2O, 1 µL mhRNA (250 µM), 1 µL eFx (250 µM) and 1 µL HEPES-KOH pH 8.4 (500 mM) were mixed, heated to 95 °C for 2 min and cooled to room temperature for 5 min. 2 µL $MgCl_2$ (3 M) was added and left for 5 min at room temperature. Solution was placed on ice until cold and the aminoacylation was initiated by adding 2 µL cyanomethyl substrate (25 µM) in DMSO. Reaction was incubated on ice for 2–12 hours, depending on the substrate; final concentrations: 25 µM

microhelix, 25 µM eFx and 5 mM cyanomethyl ester in 50 mM HEPES-KOH pH 8.4, 600 mM $MgCl_2$, 20% DMSO. The reaction was stopped by pelleting any insoluble substrate, collecting the substrate, adding 4 reaction volumes (40 µL) of 0.3 M NaOAc pH 5.2, and the product precipitated using 10 reaction volumes of EtOH (100 µL). The pellet was washed with 0.1 M NaOAc pH 5.2, 70% EtOH and analyzed by 20% denaturing acid PAGE (50 mM sodium acetate, 6 M urea). The RNA was stained with ethidium bromide and analyzed on an FLA-5100 (Fuji, Japan) and results are shown in **Figure S1**.

Aminoacylation of $tRNA^{fMet}_{CAU}$ *with foldamer substrates*

25 µM $tRNA^{fMet}_{CAU}$, 25 µM eFx and 5 mM cyanomethyl ester substrate were incubated in 50 mM HEPES-KOH pH 8.4, 600 mM $MgCl_2$ in 20% DMSO using the time originating from the "*Aminoacylation of mhRNA*" for each substrate (**Figure S1**).

Model mRNA templates (encoding for *f*MGGGTYY-*flag* & *f*MYAATAACA-*flag*)

The following primers were purchased by Eurofins genomics (Japan):

<u>Template encoding for fMYAATAA-*flag*</u>

P1: GGCGTAATACGACTCACTATAG

P2: TAATACGACTCACTATAGGGTTAACTTTAACAAGGAGAAAAACATGTAC

P3:

CGTCGTCGTCCTTGTAGTCAGCACAAGCAGCGGTAGCAGCGTACATGTTTTTCTCCTTGTTAAAG

P4: CGAAGCTTACTTGTCGTCGTCGTCCTTGTAGTC

<u>Template encoding for *f*MGGGTYYCA-*flag*</u>

P1: GGCGTAATACGACTCACTATAG

P2': TAATACGACTCACTATAGGGTTAACTTTAACAAGGAGAAAAACATGGGC

P3': CGTCGTCGTCCTTGTAGTCGTAGTAGGTGCCGCCGCCCATGTTTTTCTCCTTGTTAAAG

P4: CGAAGCTTACTTGTCGTCGTCGTCCTTGTAGTC

$P2^{(\prime)}$ was annealed with $P3^{(\prime)}$ and extended using *Taq* DNA polymerase. The resulting product was diluted 200 times with PCR reaction buffer and amplified by using P1 and P4 as the 5'- and 3'-primers, respectively. The DNA product was transcribed by T7 RNA polymerase and purified by 10% denaturing PAGE. The mRNA template was dissolved in water and its concentration was adjusted to 10 µM.

In vitro *translation and MALDI-TOF-MS*

A custom-made *in vitro* translation mixture was used, with the final concentrations of individual components: 1.2 µM ribosome, 0.1 µM T7 RNA polymerase, 4 µg mL^{-1} creatine kinase, 3 µg mL^{-1} myokinase, 0.1 µM pyrophosphatase, 0.1 µM nucleotidediphosphatase kinase, 2.7 µM IF1, 0.4 µM IF2, 1.5 µM IF3, 30 µM EF-Tu, 30 µM EFTs, 0.26 µM EF-G, 0.25 µM RF2, 0.17 µM RF3, 0.5 µM RRF, 0.6 µM MTF, 0.73 µM AlaRS, 0.03 µM ArgRS, 0.38 µM AsnRS, 0.02 µM CysRS, 0.06 µM GlnRS, 0.23 µM GluRS, 0.09 µM GlyRS, 0.02 µM HisRS, 0.4 µM IleRS, 0.04 µM LeuRS, 0.03 µM MetRS, 0.68 µM PheRS, 0.16 µM ProRS, 0.04 µM SerRS, 0.09 µM ThrRS, 0.03 µM TrpRS, 0.02 µM ValRS, 0.13 µM AspRS, 0.11 µM LysRS, 0.02 µM TyrRS. Additionally, 50 mM HEPES-KOH (pH 7.6), 100 mM potassium acetate, 2 mM GTP, 2 mM ATP, 1 mM CTP, 1 mM UTP, 20 mM creatine phosphate, 12 mM $Mg(OAc)_2$, 2 mM spermidine, 2 mM DTT, and 1.5 mg mL^{-1} *E. coli* total tRNA (Roche).

- For MALDI-TOF analysis (**Figure S2**): 5 of the 20 canonical amino acids were included at 500 µM, including Met, Asp, Tyr, Lys and Ala. Solutions containing the above plus 1.5 µM mRNA template and 25 µM foldamer-$tRNA^{Pro1E2}_{GGU}$ (prepared using eFx, above) were incubated for 30 min at 37 °C. The foldamer-peptide hybrid was isolated using anti-FLAG M2 affinity agarose gel (Sigma) and eluted using 0.2% TFA. Solution was mixed, 1:1, with a half-saturated solution (80% MeCN, 19.5% H_2O, 0.5% AcOH) of α-cyano-4-hydrocinnamic acid prior to spotting on a MALDI plate. Foldamer-peptide MALDI-TOF-MS analysis was performed by an UltrafleXtreme (Bruker Daltonics) in reflector/positive mode.
- For radioisotope quantification (**Figure S3**): 4 of the 20 canonical amino acids were included at 500 µM: Met, Tyr, Lys and Ala. 50 µM [^{14}C]Asp was added. *In vitro* translation was carried out as above. Translation reactions were stopped by adding an equal volume of stop solution [0.9 M Tris-HCl (pH 8.45), 8% SDS, 30% glycerol and 0.001% xylene cyanol] and incubating at 95 °C for 2 min. Then, the samples were analyzed by 15% tricine SDS-PAGE and autoradiography analyzed using a Typhoon FLA 7000 imager (GE Healthcare). Peptide yield was normalized by intensity of [^{14}C]Asp band. Note that FLAG-tag purification is not carried out during this experiment.

3.4. RaPID selection protocol

Two RNA libraries, consisting of 4–9 and 10–15 NNK codons, were prepared as previously described.[27] Briefly, RNA molecules were synthesized by T7 RNA polymerase reactions from DNA templates assembled by PCR and purified by PAGE. Furthermore, puromycin-linked mRNA was prepared by incubation with puromycin-linked oligonucleotide and T4 RNA ligase and was purified by phenol/chloroform extraction and ethanol precipitation. Oligonucleotides for both libraries and puromycin-linked oligonucleotide were previously reported.[28]

Ribosomal synthesis of the macrocyclic peptide libraries was performed as previously described.[27] In brief, for the initial selection, 1.2 mM puromycin-linked mRNA library was translated in a Met-deficient FIT reaction containing 25 mM of **7**-$tRNA_{fMet}$ for 30 min at 37 °C. The reaction was incubated at 25 °C for 12 min before disruption of the ribosome–mRNA complex by incubation at 37 °C for 30 min in the presence of 20 mM EDTA. The resulting peptide-linked mRNAs were then reverse-transcribed using RNase H-reverse transcriptase (Promega) for 1 h at 42 °C. The mixture was desalted by means of Sephadex G-25. Subsequently, brief passage of the reaction over His-Tag Dynabeads (Life Technologies) thrice was carried out to remove translation proteins from the library. Affinity screening was performed by three serial passages (counterselections, 30 min each at 4 °C) of the library over His-Tag Dynabeads (Life Technologies), followed by affinity selection against 200 nM His_6-C-lobe immobilized on the same beads for 30 min at 4 °C. cDNA was eluted from the beads by heating to 95 °C for 5 min and fractional recovery from the final counterselection (negative control) and affinity selection step were assessed by quantitative PCR using Sybr Green I on a LightCycler thermal cycler (Roche) and results are shown in **Figure 2d** and **Figure S5**. Enriched DNA libraries were recovered by PCR and used as input for transcription reactions to generate the mRNA library for the subsequent round of screening. After five iterative rounds of library synthesis, affinity selection, and recovery, the final DNA library was sequenced to identify C-lobe binders.

For high-throughput sequencing of the selections carried out, DNA samples were PCR-amplified with nesting primers,[28] purified using a Nucleospin column (Machery-Nagel), and sequenced using a MiSeq high-throughput sequencer (Illumina). Data analysis was performed using CLC sequence

viewer 8 software (Qiagen). Results for the top 20 hits from each library are shown in **Figure S6**, and for the top 50 hits is shown in **Extended Data 1**.

Clone assay: In this experiment we demonstrate the effect of the foldamer initiator on the binding to the protein modified beads, for the two different library sizes. mRNA sequences encoding for the top hits from the sequencing data underwent an additional round of selection. Peptides, linked to their genotype, were exposed sequentially to unmodified (Neg) and protein-modified (Pos) beads and recovery was again determined by qPCR in a manner similar to the selection experiment. In a subsequent experiment, the abiotic initiator was substituted with Trp (capable of undergoing cyclization) and the resulting peptides were treated as their "abiotic" counterparts. The results are shown in **Figure 2d** and **Figure S7**.

3.5. Circular dichroism (CD)

CD data were recorded on a Jasco J-810 spectrometer with 1 or 2 mm quartz cuvette. The exact concentration of macrocycle **10** in each sample was determined by taking the average absorbance value between 374.8–375.2 nm ($\overline{A}_{375}$) and applying it to the Beer-Lambert law:

$$[\mathbf{10}]\,(\mu M) = \frac{\overline{A}_{375} \cdot 10^6}{\varepsilon_{375} \cdot l}$$

Where ε_{375} is the extinction coefficient at 375 nm contributed by the Q monomers as previously reported (2 × 2,678 M^{-1} cm^{-1}), and l is the path length (cm) of the cuvette. The raw CD data in millidegrees (mdeg) was converted to molar extinction per number of quinoline (Q) residues ($\Delta\varepsilon$) by the following equation:

$$\Delta\varepsilon\,(L\,mol^{-1}cm^{-1}{Q_{res}}^{-1}) = \frac{mdeg}{[\mathbf{10}] \cdot 10^{-6} \cdot l \cdot 32980 \cdot n_{Q_{res}}}$$

Where $n_{Q_{res}}$ is the number of Q residues in the compound.

3.6. Protein-macrocycle crystallization

For co-crystallisation of C-lobe with compound **10**, the solutions of these components were kept at 4 °C and pre-mixed as follows. HRV3C-cleaved C-lobe was buffer exchanged into NaN_3 (0.05% (v/v)) in H_2O, concentrated, and mixed (final concentration: 6.7 mg mL^{-1}) with 1.1 eq. compound **10** in H_2O. The mixture was centrifuged (17,000 × g, 5 min, 4 °C) and the complex crystallized using the hanging drop technique in polyethylene glycol (PEG) 8,000 (7.2% (w/v)), sodium cacodylate (0.06 mM), $Ca(OAc)_2$ (0.06 mM), pH 5.5 at 4 °C with a complex solution to reservoir solution ratio of 1:1. The plate-like crystals were mounted in nylon loops, cryoprotected with glycerol (15% (v/v)) and flash cooled in liquid nitrogen.

3.7. Data collection and structure refinement

X-ray diffraction data were collected at beamline ID23-1 of the European Synchrotron Radiation Facility (ESRF, Grenoble) on a Dectris Eiger2 X 16M detector.[21] Data was processed using XDS package and the structure was solved by molecular replacement in Phase-MR using the C-lobe from the E6AP-UBCH7 complex as a search model (PDB ID: 1C4Z).[15a] The structure was further refined in iterative rounds of manual model building and refinement in Coot[29] and Phenix.[30] Jligand[31] was used to produce restrain files for the foldamer-peptide hybrid, and the ligand was modelled into

clearly feasible electron density map at the final stages of refinement. The structure was validated with MolProbity and deposited in the PDB under accession code 7QPB. The statistics of data collection and structure refinement are summarized in **Table S1**.

Table S1. Data collection and refinement statistics

Wavelength	
Resolution range	29.53 - 2.342 (2.426 - 2.342)
Space group	C 1 2 1
Unit cell	149.91 59.05 67.3 90 95.466 90
Total reflections	84596 (8078)
Unique reflections	24491 (2402)
Multiplicity	3.5 (3.4)
Completeness (%)	0.98 (0.97)
Mean I/sigma(I)	11.91 (1.91)
Wilson B-factor	50.30
R-merge	0.06614 (0.6111)
R-meas	0.07841 (0.7249)
CC1/2	0.998 (0.673)
CC*	0.999 (0.897)
Reflections used in refinement	24488 (2402)
Reflections used for R-free	1225 (120)
R-work	0.2152 (0.2840)
R-free	0.2632 (0.3344)
CC(work)	0.939 (0.770)
CC(free)	0.912 (0.679)
Number of non-hydrogen atoms	3753
macromolecules	3586
ligands	110
Protein residues	422
RMS(bonds)	0.015
RMS(angles)	1.05
Ramachandran favored (%)	98
Ramachandran allowed (%)	2.3

Ramachandran outliers (%)	0
Rotamer outliers (%)	0.26
Clashscore	3.31
Average B-factor	52.79
macromolecules	53.19
ligands	41.55
solvent	49.32

Statistics for the highest-resolution shell are shown in parentheses.

3.8. Surface plasmon resonance (SPR)

The binding of macrocyclic peptide-foldamer hybrids to the C-lobe of the E6AP HECT domain bearing a His_6 tag at its N-terminus was characterized by surface plasmon resonance (SPR) analysis on a Biacore 8K instrument (Cytiva) at 25 °C. The composition of the running buffer was HBS-P^+ buffer (0.1 M HEPES, pH 7.4, 1.5 M NaCl and 0.5% v/v Surfactant P20) containing 0.1% DMSO. The surface preparation of Series S Sensor Chip CM5 included activation of carboxymethyl groups on a dextran-coated chip by reaction with 1:1 ratio between 0.4 M 1-ethyl-3-(3-dimethylaminopropyl)-carbodiimide (EDC) and 0.1 M N-hydroxysuccinimide (NHS), followed by covalent bonding of the C-lobe to the chip surface via amide linkages and quenching of excess activated esters with 1 M ethanolamine according to manufacturer instructions (Cytiva). Reference channels were prepared in the same manner without immobilization with C-lobe and all the carboxymethyl groups were quenched with ethanolamine. The immobilized C-lobe on CM5 sensor chip was with a density of 1000 RU. Each macrocyclic foldamer-peptide hybrid was injected at a flow rate of 30 µL/min, contact time of 120 s, and dissociation time of 120 s. After each run, the chip was regenerated by injecting a regeneration buffer (Glycine pH 2.0) until the response returned to the original baseline level. The binding curves of the measurement channels (immobilized with C-lobe) were subtracted with that of reference channels (un-immobilized), and employed to derive affinity and kinetic constants. Binding sensorgrams were fitted to the standard 1:1 binding model with the Biacore Insight Evaluation software (Cytiva). Steady state values were fitted in OriginPro 2019b software to the quadratic 1:1 binding model[32] using the Langmuir equation.

$$RU = Rmax \times [macrocycle]/(K_d + [macrocycle])$$

Where *RU* is SPR response units, [macrocycle] is macrocycle concentration (nM), K_d is the dissociation constant (µM), and A_0 is a factor relating to total ligand concentration

The concentration ranges used for compounds **10**, **13**, **14** and **16** were 3.9, 7.81, 15.62, 31.25, 62.5, 125, 250 and 500 nM while for **11**, **12**, **15** and **17** the range of concentrations was from 31.25 to 1000 nM.

3.9. Molecular dynamics simulation setup

We carried out MD simulations on four macrocycle-C-lobe complexes. These are the two by two combinations of the *M* or *P* foldamer helix, with the α-helix or its V10A mutant (compound **14**). We built the initial structures of all four systems by adopting the positions and structures of C-lobe and α-helix in the crystal structure. The macrocycle with a foldamer helix was built using previously developed arylamide building blocks,[33] in combination with amino acid residues, including a modified cysteine residue, with the AMBER20 software package.[34] The α-helix structure (in both *M* and *P* macrocycles), as well as the *P* foldamer helix structure, were adjusted to reproduce and align with the crystal structure. Before solvation and equilibration, the foldamer helix also undergoes minimization while C-lobe and α-helix are kept fixed.

Each macrocycle-C-lobe complex was then solvated by explicit TIP3P water molecules in a periodic box measuring about 70 Å along each side. The ff14SB force field[35] was used for amino acid residues. The general AMBER force field (GAFF),[36] with improved torsional parameters,[33] was used for the aromatic foldamer. Following a standard RESP[37] charge fitting procedure, we also created a new cysteine unit with modified side chain to connect to the N-terminus of the foldamer helix. All systems were equilibrated using the same procedure involving minimization with solvent, heating and NPT simulation at 1 atm and 300K. Production runs using the NVT ensemble at 300K were then carried out for 500 to 1500 ns per run. For each system, 2-3 production runs were carried out in parallel using slightly different equilibrated structures (extracted at different times of the NPT equilibration run). The trajectories were then analyzed mainly using the cpptraj program in the AMBER20 package in terms of RMSD, distance, hydrogen bonding etc. as discussed.

3.10. Binding mode analysis

Binding mode analysis was carried out using a combination of visual inspection, RMSD calculations with respect to different reference structures (crystal structure or average structure of sections of trajectories with alternative binding mode), as well as analysis of specific residue to residue distances. **Figure S19** illustrates an example of a MD trajectory exhibits two binding modes. We then consolidated the conformations (*i.e.* sections of MD trajectories from all runs for the system) that belong to each binding mode for further analysis of the binding interactions. **Figure S20–S23** illustrate different binding modes found in the MD simulations of the *P* and *M* foldamer with Val10 α-helix macrocycle-C-lobe complexes. Residues that contribute to binding between macrocycle and C-lobe are shown and labelled specifically in the snapshot. Also shown in **Figure S20–S23** are distance histograms illustrating formation of salt bridges, as well as contacts between the aromatic and/or hydrophobic groups of the macrocycle and protein surface.

3.11. Role of Tyr11 in *M* foldamer macrocycles

The distance histogram in **Figure S24** clearly shows the persistent stacking of Tyr11 with $Q^{Dap}2$ in the *M* foldamer macrocycle with Val10. The stacking is not so constant in the macrocycle with the V10A mutant.

3.12. Destabilization of the α-helix in macrocycle with *P* foldamer and V10A mutation

Secondary structure analysis (**Table S2**) gives evidence on a significant destabilization of the α-helix (unwinding as shown in row 2 of **Figure S25**) upon the V10A mutation. For each **10**-C-lobe, the analysis is carried out on all MD trajectories, thus including all binding modes. The fraction of helicity is based on average over time and all parallel runs of each system. The same mutation has a moderate effect on the *M* macrocycle helix.

Table S2. Fraction of helicity (3-10 and α-helix) obtained from residue by residue secondary structure analysis.[38]

Macrocycles	*P* foldamer Val10 Total (3-10/α)	*M* foldamer Val10 Total (3-10/α)	*P* Foldamer V10A Total (3-10/α)	*M* foldamer V10A Total (3-10/α)
Trp7	0.01 (0.01/0.00)	0.00	0.00	0.00
Arg8	**0.67** (0.07/**0.60)**	**0.84** (0.00/**0.84)**	0.19 (0.06/0.14)	**0.59** (0.03/**0.56)**
Tyr9	**0.68** (0.07/**0.61)**	**0.88** (0.01/**0.87)**	0.22 (0.06/0.16)	**0.61** (0.03/**0.58)**
Val10 or Ala10	**0.78** (0.14/**0.64)**	**0.92** (0.02/**0.90)**	**0.62 (0.41**/0.21)	**0.81** (0.15/**0.66)**
Tyr11	**0.87** (0.21/**0.66)**	**0.95** (0.05/**0.90)**	**0.69 (0.43**/0.26)	**0.87** (0.20/**0.67)**
Gln12	**0.57** (0.21/**0.36)**	**0.75** (0.07/**0.68)**	**0.62 (0.42**/0.20)	**0.66** (0.21/**0.45)**
Lys13	**0.44** (0.14/**0.31)**	**0.53** (0.06/**0.47)**	**0.47** (0.21/0.16)	**0.46** (0.16/**0.30)**
Cys14	0.15 (0.02/0.13)	0.31 (0.02/0.29)	0.08 (0.00/0.08)	0.14 (0.03/0.11)

4. Chemical synthesis

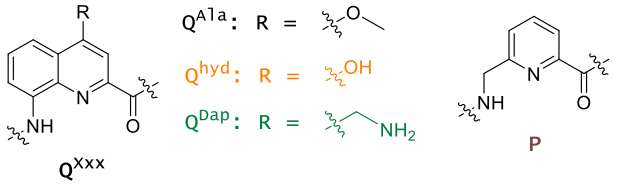

Foldamer-peptide hybrid sequences evaluated for *in vitro* translation:

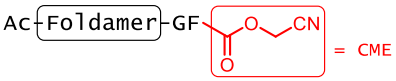

1: Ac-Q^{Ala}-P-Q^{Ala}-GF-CME

2: Ac-Q^{Dap}-P-Q^{Ala}-GF-CME

3: Ac-Q^{Hyd}-P-Q^{Ala}-GF-CME

4: Ac-P-Q^{Ala}-P-Q^{Ala}-GF-CME

5: Ac-P-Q^{Dap}-P-Q^{Ala}-GF-CME

6: Ac-P-Q^{Hyd}-P-Q^{Ala}-GF-CME

Foldamer-peptide hybrid sequences used as initiators for RaPID selection against protein target:

7: ClAc-P-Q^{Dap}-P-Q^{Ala}-GF-CME

8: ClAc-Q^{Hyd}-P-Q^{Ala}-GF-CME

9: ClAc-P-Q^{Hyd}-P-Q^{Ala}-GF-CME

Macrocyclic foldamer-peptide hybrids:

10: CH_2CO-P-Q^{Dap}-P-Q^{Ala}-GFWRYVYQKCG-NH_2
S

11: CH_2CO-P-Q^{Dap}-P-Q^{Ala}-GFARYVYQKCG-NH_2
S

12: CH_2CO-P-Q^{Dap}-P-Q^{Ala}-GFWAYVYQKCG-NH_2
S

13: CH_2CO-P-Q^{Dap}-P-Q^{Ala}-GFWRAVYQKCG-NH_2
S

14: CH_2CO-P-Q^{Dap}-P-Q^{Ala}-GFWRYAYQKCG-NH_2
S

15: CH_2CO-P-Q^{Dap}-P-Q^{Ala}-GFWRYVAQKCG-NH_2
S

16: CH_2CO-P-Q^{Dap}-P-Q^{Ala}-GFWRYVYAKCG-NH_2
S

17: CH_2CO-P-Q^{Dap}-P-Q^{Ala}-GFWRYVYQACG-NH_2
S

18: CH_2CO-P-Q^{Dap}-P-Q^{Ala}-GFKLSATNWILRRTCG-NH_2
S

Scheme S1. Foldamer-peptide hybrid sequences synthesized in the context of this study. The α-amino acid residues are written in one-letter code *e.g.* GF stands for Gly-Phe dipeptide and P in brown color stands for the pyridine unit.

4.1. Materials

Fmoc-Q^{Ala}-OH, Fmoc-Q^{OH}-OH, Fmoc-Q^{Dap}-OH and P monomers were prepared following reported synthetic protocols.[17,39,40]

If not otherwise mentioned, chemical reagents were purchased from Sigma-Aldrich. Fmoc-*N*-protected amino acids, benzotriazol-1-yl-oxytripyrrolidinophosphonium hexafluorophosphate (PyBOP), benzotriazol-1-yloxytris(dimethylamino)phosphonium hexafluorophosphate (BOP), 2-(1*H*-benzotriazol-1-yl)-1,1,3,3-tetramethyl-uronium-hexafluorophosphate (HBTU) and Biotin-PEG_4-COOH were purchased from IRIS Biotech. Solvents were purchased from Fisher Scientific (cyclohexane, ethyl acetate, dichloromethane (DCM), methanol and acetone, analytical grade), IRIS (*N*-methyl-2-pyrrolidinone (NMP)) or Carlo Erba (*N*,*N*-dimethylformamide (DMF) peptide grade) and used without further purification. Anhydrous tetrahydrofuran (THF) and anhydrous dichloromethane were obtained from MBRAUN SPS-800 solvent purification system. *N*,*N'*-diisopropylethylamine (DIPEA) was distilled over CaH_2 prior to use. Exclusively ultrapure water was used. Rink amide MBHA resin was purchased from CEM. SASRIN resin was purchased from IRIS biotech. H-(*L*)-Phe-2-CT-resin was purchased from Novabiochem. Silica column chromatography was performed on silica gel (230-400 mesh, 40-63 µm, Merck) and thin-layer chromatography (TLC) was performed on silica gel 60-F254 plates (Merck).

4.2. General methods for solid-phase synthesis

3.2.1 Solid-phase peptide synthesis (SPPS)

The peptide segments of compounds **1-9** were synthesized manually in a syringe reactor equipped with a filter on pre-loaded H-(*L*)-Phe-Chlorotrityl resin (manufacturer's loading: 0.54 $mmol.g^{-1}$; scale between 11 and 100 µmol). Fmoc-Gly-OH (3 eq. relative to resin loading) was coupled in the presence of HBTU (2.9 eq.) and DIPEA (6 eq.) in DMF at r.t. for 1 h and coupling was repeated once for 2 h.

The peptide segment for compounds **10**–**13** (**P10**–**P13** respectively) was synthesized using a Liberty Blue CEM® synthesizer at a scale of 50 µmol. Microwave couplings were performed twice at 50°C for 10 min with Fmoc-*N*-α-amino acid (5 eq. relative to the resin loading, 0.5 mmol), PyBOP (5 eq., 0.5 mmol), and DIPEA (10 eq. 1.0 mmol) in DMF (2.75 mL in total). Fmoc deprotection was performed twice with 20% (v/v) piperidine in DMF (2.0 mL) at 75°C (1 × 30 s and 1 × 180 s). The resin was washed with DMF (2 × 2 mL) after the two consecutive deprotection steps and one time with DMF (3 mL) in between coupling and deprotection steps.

3.2.2 Manual solid-phase foldamer synthesis (SPFS) for compounds 1–9, 13a

SPFS for compounds **1**–**9** (including acid chloride activation, HBTU coupling and Fmoc deprotection) was undertaken according to reported protocols.[9a]

3.2.3 Automated SPFS of foldamer-peptide hybrids 11a and 12a

The automated SPFS was carried out on a Chorus PurePep synthesizer according to the recently published protocols.[41] The scale used was 25 µmol on 10 ml size reaction vessel.

3.2.4 Solid-phase foldamer synthesis (SPFS) of F10

The SPFS of foldamer fragment of **10** (**F10**) was carried out on a Discover-Bio CEM® microwave oven in open vessel mode as previously described[15a] on Fmoc-Gly-SASRIN resin (manufacturer's loading: 0.79 mmol g^{-1}) by using the *in situ* activation strategy on a 200 µmol scale.

3.2.5 Fragment condensation

F10 was next coupled *via* a fragment condensation approach (Figure S2) on the resin-bound peptide **P10** on a 0.050 mmol scale. To remove any remaining moisture, **F10** was lyophilized prior to coupling. **F10** (50 mg, 0.047 mmol, 0.94 eq.) was then dissolved in dry NMP (0.4 mL) and dry THF (1.0 mL) together with DIPEA (35 µL, 0.2 mmol, 4 eq.) and BOP (44 mg, 0.1 mmol, 2 eq.). After pre-activation for 3 min, the coupling solution was added to the resin-bound H-Phe-peptide **P10** under N_2 atmosphere. The mixture was stirred for 24 h at r.t. by monitoring the progress of the reaction via HPLC analysis. The resin solution was filtered off and washed with DMF (3 x 3 mL). To facilitate HPLC purification, remaining unreacted resin-bound H-Phe-peptide **P10** was acetylated (**Method 3.2.6**).

3.2.6 N-terminal acetylation

Unreacted N-terminal aliphatic amines were acetylated with a solution of acetic anhydride in DCM (50% (v/v), 1 mL per 100 mg resin). The resin was incubated with this reaction mixture for 10 min with mechanical shaking at r.t. For the N-terminal aromatic amines of the Q monomers, the reaction time was extended to 16 h at r.t. and DIPEA (5 eq.) was added to the reaction mixture.

3.2.7 N-terminal chloroacetylation

For N-terminal chloroacetylation, the resin was incubated with a solution of chloroacetic anhydride (10 eq.) together with DIPEA (20 eq.) in dry DCM or DMF for 15 min at r.t. with mechanical shaking. This step was repeated once without washing in between. For the aromatic amine of Q monomers, the reaction time was extended to 30 min (twice). The resin solution was filtered off, washed with DCM and dried under a stream of nitrogen.

3.2.8 Cleavage of resin-bound oligomers

For Cys-containing foldamer-peptide hybrids (**10a**–**12a**), the Rink amide resin was treated with the cleavage cocktail (10-15 mL per gram of resin) consisting of trifluoroacetic acid (TFA)/triisopropylsilane (TIS)/ethane-1,2-dithiol (EDT)/H_2O (92.5:2.5:2.5:2.5, v/v/v/v) at r.t. for 120 min. Precipitation and subsequent centrifugation of the foldamer-peptide hybrids and fragments were performed in cold Et_2O. The precipitates were dried under a stream of nitrogen, dissolved in an acetonitrile/water mixture and lyophilized. For the cleavage of protected foldamer fragments (**1a**–**9a**), the corresponding chlorotrityl or SASRIN resin was treated with a solution (20 mL per gram of resin) of hexafluoroisopropanol (HFIP) in dry DCM (60% (v/v)) for 60 min at r.t. This cleavage step was repeated once giving a better recovery yield without loss of purity of the crude. Foldamer fragment **F10** was cleaved with a solution of HFIP in dry DCM (30:70, v/v) for 2 x 60 min at r.t.

3.2.9 Cyanomethyl ester (CME) installation

The CME ester was installed on the crude cleavage products of foldamer-Gly-Phe-OH fragments (precursors of **1**-**6** and **7**-**9**). The foldamer-Gly-Phe-OH was dissolved in anhydrous DMF directly followed by the addition of freshly distilled DIPEA (6 eq.) or pre-dried potassium carbonate (6 eq.) and bromo acetonitrile (6 eq.). The reaction mixture was stirred for 2 h at r.t. under inert N_2

atmosphere. The progression of the reaction was monitored by TLC (EtOAc/cyclohexane mixtures). The crude protected CME adducts were extracted with EtOAc and washed once with 5% (v/v) citric acid in water and twice with saturated aqueous (sat. aq.) NaCl. The organic layer was dried over $MgSO_4$, filtered over cotton, and concentrated under reduced pressure. The remaining DMF was azeotroped with toluene (3×) and crude CME esters were purified by silica column chromatography (ethylacetate/cyclohexane mixtures or MeOH/DCM mixtures, yields: 37%-89%).

3.2.10 Boc/*tert*-Bu deprotection of CME containing foldamer-peptide hybrids

Deprotection of Boc and *t*Bu protecting groups was performed by dissolving the foldamer-Gly-Phe-CEM esters in a mixture of TFA:DCM:TIS (50:48:2 v/v/v) and stirring at r.t. for 2 h. The solvents were removed by evaporation and the pure solid compounds were obtained after trituration in Et_2O.

4.3. General methods for NMR, HRMS, HPLC analysis and purification

^{1}H NMR spectra were recorded on Avance III HD 400 MHz Bruker BioSpin and Avance III HD 500 MHz Bruker BioSpin spectrometers. All chemical shifts are reported in ppm and calibrated against residual solvent signals of DMSO-d_6 (δ 2.50 ppm) and $CDCl_3$ (δ 7.26 ppm). In the case of ^{1}H NMR spectra recorded in H_2O/CH_3CN, 3-(trimethylsilyl)propionic-2,2,3,3-d_4 acid sodium salt (TPS) was added to the medium and calibrated against δ 0.00. Coupling constants (*J*) are reported in Hz. Signal multiplicities were abbreviated as *s*, singlet; *d*, doublet; *t*, triplet; *q*, quartet, and *m*, multiplet.

High-resolution electrospray mass spectra for compounds **1**–**9** were recorded on a Thermo Finnigan LTQ FT Ultra FourierTransform Ionen Cyclotron Resonance Mass Spectrometer by direct infusion of the analyte dissolved in either DCM or aqueous media in positive or negative ionization mode. Mass spectra for compounds **10**–**12** were recorded on a Bruker microTOF II by direct infusion from aqueous media in either positive or negative ionization mode. The instrument was calibrated in positive and negative mode by direct infusion of a calibration solution (Agilent Technologies ESI-L Low Concentration Tuning Mix).

RP-HPLC analyses, as well as semi-preparative purification, were performed on an Ultimate 3000 HPLC System (ThermoFisher Scientific). Preparative RP-HPLC purification was performed on a Waters system with a 2707 Autosampler, a 2489 UV/Visible detector, a 2545 Quaternary Gradient Module and a Fraction Collector III. For analytical analysis, a Nucleodur C18 Gravity column (4 × 100 mm, 5 µm, Macherey-Nagel) was used, and semi-preparative purifications were performed on a Nucleodur C18 Gravity column (10 × 250 mm, 5 µm, Macherey-Nagel). A Nucleodur C8 Gravity column (4 × 50 mm, 5 µm, Macherey-Nagel) was also used in analytical mode and for semi-preparative purification, the Nucleodur C8 Gravity column (10 × 100 mm, 5 µm, Macherey-Nagel) was employed. Semi-preparative purification was performed with an automated fraction collector system from ThermoFisher Scientific. Preparative purifications were performed on a VP 125/21 Nucelodor C18 HTec column (21 × 125 mm, 5 µm, Macherey-Nagel). When using acidic conditions 0.1% (v/v) TFA was added to the aqueous mobile phase (referred to as mobile phase A) and to acetonitrile (referred to as mobile phase B). For analytical RP-HPLC analysis, a flow rate of 1.0 $mL.min^{-1}$ was applied, semi-preparative purification on RP-HPLC was performed at a flow rate of 5.0 $mL.min^{-1}$, and preparative purification was performed at 25 $mL.min^{-1}$. The column eluent was monitored by UV detection at 214, 254, and/or 300 nm with a diode array detector.

4.4. Experimental procedures for chemical synthesis

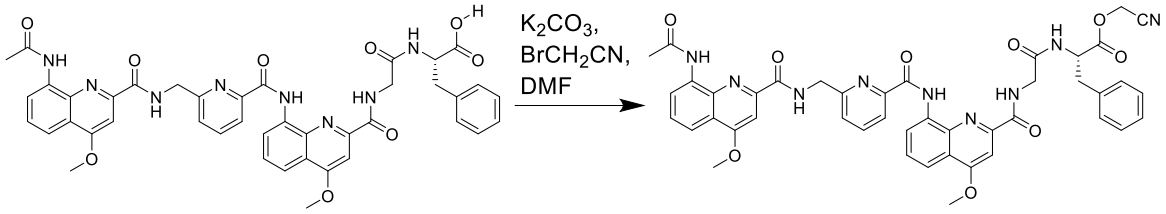

1a **1**

Compound 1a: Compound **1a** was prepared on a preloaded H-(L)-Phe-2-CT resin (0.60 mmol/g) using SPPS (**Method 3.2.1**) and SPFS (**Method 3.2.2**) synthesis protocols on an 0.011 mmol scale. After final acetylation (**Method 3.2.6**) and resin cleavage (**Method 3.2.8**) with HFIP:DCM (60:40, v/v), a crude brown powder was recovered in 44% yield (3.9 mg) and was used directly in subsequent reactions without further purification steps.

Compound 1: Compound **1** was synthesized from carboxylic acid **1a** (3.9 mg, 4.9 µmol) using the general cyanomethyl installation protocol (**Method 3.2.9**). The obtained crude residue was purified by silica gel column chromatography using a mixture of EtOAc and cyclohexane starting from 50% to 100% (v/v) EtOAc. After evaporating the corresponding fractions, compound **3** was obtained as a white solid (1.7 mg, 41%). ^{1}H NMR (500 MHz, Chloroform-*d*) δ 11.93 (s, 1H), 9.60 (s, 1H), 9.46 (s, 1H), 9.06 (dd, *J* = 7.7, 1.3 Hz, 1H), 8.67 (d, *J* = 7.7 Hz, 1H), 8.59 (t, *J* = 5.5 Hz, 1H), 8.31 (dd, *J* = 7.6, 1.1 Hz, 1H), 7.98 – 7.94 (m, 2H), 7.84 (dd, *J* = 16.3, 8.1 Hz, 2H), 7.74 (s, 1H), 7.64 (t, *J* = 8.1 Hz, 1H), 7.55 (s, 1H), 7.50 – 7.45 (m, 1H), 7.18 (p, *J* = 3.6 Hz, 3H), 6.92 – 6.86 (m, 2H), 4.96 – 4.90 (m, 1H), 4.76 (dd, *J* = 15.0, 6.2 Hz, 1H), 4.69 (d, *J* = 15.6 Hz, 1H), 4.61 – 4.52 (m, 1H), 4.45 (d, *J* = 15.7 Hz, 1H), 4.36 (dd, *J* = 17.0, 6.4 Hz, 1H), 4.29 – 4.21 (m, 1H), 4.15 (s, 3H), 4.13 (s, 3H), 2.94 (dd, *J* = 14.0, 5.5 Hz, 1H), 2.82 (dd, *J* = 14.0, 7.6 Hz, 1H), 1.88 (s, 3H). HRMS (ESI$^+$): *m/z* calculated for $C_{44}H_{39}N_9O_9$ $[M+H]^+$ 838.2944 found 838.2945.

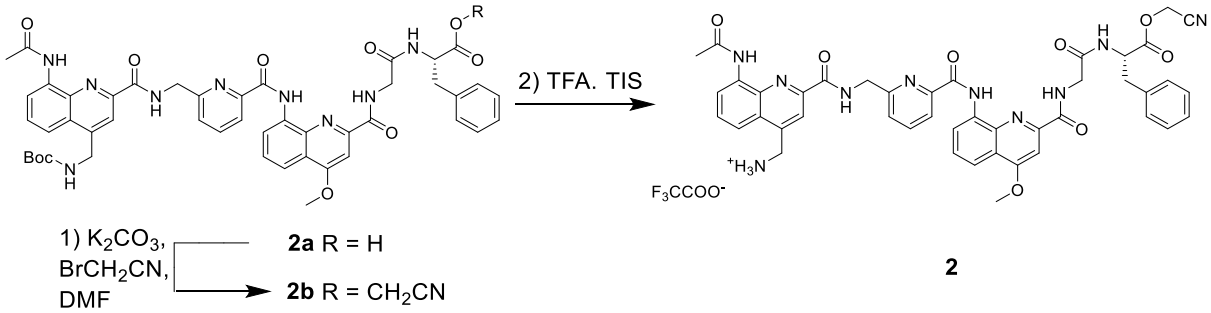

Compound 2a: Compound **2a** was prepared on a preloaded H-(L)-Phe-2-CT resin (0.60 mmol/g) using SPPS (**Method 3.2.1**) and SPFS (**Method 3.2.2**) synthesis protocols on an 0.011 mmol scale. After final acetylation (**Method 3.2.6**) and resin cleavage (**Method 3.2.8**) with HFIP:DCM (60:40, v/v), a crude brown powder was recovered in 42% yield (4.1 mg) and was used directly in subsequent reactions without further purification steps.

Compound 2b: Compound **2b** was synthesized from carboxylic acid **2a** (4.1 mg, 4.6 µmol) using the general cyanomethyl installation protocol (**Method 3.2.9**). The obtained crude residue was purified by silica gel column chromatography using a mixture of EtOAc in cyclohexane starting from 30% to 100% (v/v) EtOAc. After evaporating the corresponding fractions, compound **2b** was obtained as a white solid (3.8 mg, 89%). ^{1}H NMR (500 MHz, $CDCl_3$/DMSO) δ 11.75 (s, 1H), 9.67 (s, 1H), 9.45 (t, *J* = 6.1 Hz, 1H), 8.83 (dd, *J* = 7.7, 1.3 Hz, 1H), 8.49 (dd, *J* = 15.6, 8.2 Hz, 2H), 8.39 (d, *J* = 6.0 Hz, 1H), 8.10 (s, 1H), 8.05 (dd, *J* = 7.6, 1.2 Hz, 1H), 7.76 – 7.72 (m, 2H), 7.67 (dd, *J* = 7.7, 1.2 Hz, 1H), 7.49 (dd, *J* = 8.5, 1.2 Hz, 1H), 7.43 – 7.38 (m, 1H), 7.38 – 7.34 (m, 2H), 6.98 – 6.96 (m, 3H), 6.71 – 6.65 (m, 2H), 6.14 (s, 1H), 4.62 (d, *J* = 5.6 Hz, 2H), 4.55 (dd, *J* = 9.0, 5.0 Hz, 1H), 4.48 (dd, *J* = 15.0, 8.0 Hz, 2H), 4.28 (d, *J* = 6.2 Hz, 1H), 4.23 (d, *J* = 15.7 Hz, 1H), 4.12 (d, *J* = 5.2 Hz, 2H), 3.93 (s, 3H), 2.65-2.55 (m, 2H), 1.60 (s, 3H), 1.30 (s, 9H). HRMS (ESI$^+$): *m/z* calculated for $C_{49}H_{48}N_{10}O_{10}$ $[M+H]^+$ 937.3628 found 937.3626.

Compound 2: Compound **2** was synthesized from cyanomethyl ester **2b** (1.4 mg, 1.5 µmol) using the general deprotection protocol (**Method 3.2.10**) in a TFA:DCM:TIS mixture. The obtained white powder was used without further purification (0.7 mg, 0.7 µmol, 50%).^{1}H NMR (500 MHz, DMSO-d_6) δ 12.12 (s, 1H), 10.23 (s, 1H), 10.18 (t, *J* = 6.1 Hz, 1H), 8.96 (dd, *J* = 7.7, 1.3 Hz, 1H), 8.90 (t, *J* = 6.2 Hz, 1H), 8.79 (d, *J* = 7.6 Hz, 1H), 8.74 (dd, *J* = 7.8, 1.2 Hz, 1H), 8.51 (s, 3H), 8.37 (s, 1H), 8.19 (dd, *J* = 7.6, 1.2 Hz, 1H), 8.13 (t, *J* = 7.7 Hz, 1H), 7.92 (dd, *J* = 8.4, 1.4 Hz, 1H), 7.86 (dd, *J* = 8.5, 1.3 Hz, 1H), 7.79 – 7.69 (m, 4H), 7.61 (s, 1H), 7.11 – 7.05 (m, 5H), 4.92 – 4.82 (m, 4H), 4.69 (s, 2H), 4.59 (td, *J* = 8.1, 6.0 Hz, 1H), 4.23 (dd, *J* = 16.9, 6.3 Hz, 1H), 4.17 (s, 3H), 4.16 – 4.12 (m, 1H), 2.96 (dd, *J* = 13.7, 6.0 Hz, 1H), 2.90 (dd, *J* = 13.8, 8.6 Hz, 1H), 2.13 (s, 3H). HRMS (ESI$^+$): *m/z* calculated for $C_{44}H_{41}N_{10}O_8$ $[M+H]^+$ 837.3103 found 837.3100.

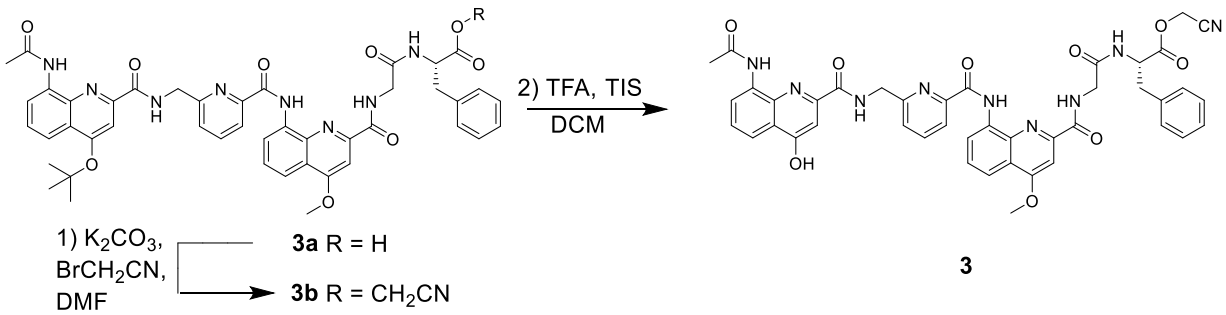

Compound 3a: Compound **3a** was prepared on a preloaded H-(L)-Phe-2-CT resin (0.60 mmol/g) using SPPS (**Method 3.2.1**) and SPFS (**Method 3.2.2**) synthesis protocols on an 0.011 mmol scale. After final acetylation (**Method 3.2.6**) and resin cleavage (**Method 3.2.8**) with HFIP/DCM (60:40, v/v), a crude brown powder was recovered in 54% yield (5.0 mg) and was used directly in subsequent reactions without further purification steps.

Compound 3b: Compound **3b** was synthesized from carboxylic acid **3a** (5.0 mg, 5.0 µmol) using the general cyanomethyl installation protocol (**Method 3.2.9**). The obtained crude residue was purified by silica gel column chromatography using a mixture of EtOAc in cyclohexane starting from 50% to 100% (v/v) EtOAc. After evaporating the corresponding fractions, compound **3b** was obtained as a white solid (1.2 mg, 37%). ^{1}H NMR (500 MHz, Chloroform-*d*) δ 11.97 (s, 1H), 9.61 (s, 1H), 9.43 (t, *J* =

6.1 Hz, 1H), 9.07 (dd, *J* = 7.7, 1.3 Hz, 1H), 8.69 – 8.60 (m, 2H), 8.30 (dd, *J* = 7.7, 1.1 Hz, 1H), 7.99 – 7.93 (m, 2H), 7.89 – 7.85 (m, 2H), 7.83 (dd, *J* = 7.7, 1.2 Hz, 1H), 7.64 (t, *J* = 8.1 Hz, 1H), 7.56 (s, 1H), 7.49 – 7.44 (m, 1H), 7.20 – 7.15 (m, 3H), 6.89 (dd, *J* = 6.5, 2.8 Hz, 2H), 6.41 (d, *J* = 8.8 Hz, 1H), 4.92 (ddd, *J* = 8.7, 7.5, 5.6 Hz, 1H), 4.76 – 4.68 (m, 2H), 4.62 (dd, *J* = 14.8, 5.9 Hz, 1H), 4.37 (d, *J* = 15.6 Hz, 1H), 4.35 – 4.25 (m, 2H), 4.13 (s, 3H), 2.93 (dd, *J* = 14.1, 5.7 Hz, 1H), 2.82 (dd, *J* = 14.0, 7.5 Hz, 1H), 1.88 (s, 3H), 1.71 (s, 9H). HRMS (ESI$^+$): *m/z* calculated for $C_{47}H_{45}N_9O_9$ $[M+H]^+$ 880.3413 found 880.3416

Compound 3: Compound **3** was synthesized from cyanomethyl ester **3b** (1.2 mg, 1.3 µmol) using the general deprotection protocol (**Method 3.2.10**) in a TFA:DCM:TIS mixture. The obtained white powder was used without further purification (0.5 mg, 0.6 µmol, 54%). ^{1}H NMR (500 MHz, DMSO-d_6) δ 12.16 (s, 1H), 11.93 (s, 1H), 10.10 (s, 1H), 10.06 (t, *J* = 6.2 Hz, 1H), 8.97 (dd, *J* = 7.7, 1.3 Hz, 1H), 8.88 (t, *J* = 6.2 Hz, 1H), 8.79 (d, *J* = 7.5 Hz, 1H), 8.65 (dd, *J* = 7.8, 1.3 Hz, 1H), 8.18 (dd, *J* = 7.6, 1.2 Hz, 1H), 8.12 (t, *J* = 7.7 Hz, 1H), 7.93 (dd, *J* = 8.4, 1.3 Hz, 1H), 7.81 (dd, *J* = 8.4, 1.4 Hz, 1H), 7.76 – 7.71 (m, 2H), 7.65 (s, 2H), 7.52 (t, *J* = 8.1 Hz, 1H), 7.11 – 7.04 (m, 5H), 4.86 (d, *J* = 4.4 Hz, 2H), 4.84 – 4.79 (m, 2H), 4.59 (td, *J* = 8.0, 6.4 Hz, 1H), 4.25 (dd, *J* = 17.0, 6.4 Hz, 1H), 4.17 (s, 3H), 4.17 – 4.12 (m, 1H), 2.99 – 2.84 (m, 2H), 2.12 (s, 3H). HRMS (ESI$^-$): *m/z* calculated for $C_{43}H_{37}N_9O_9$ $[M–H]^-$ 822.2641 found 822.2641.

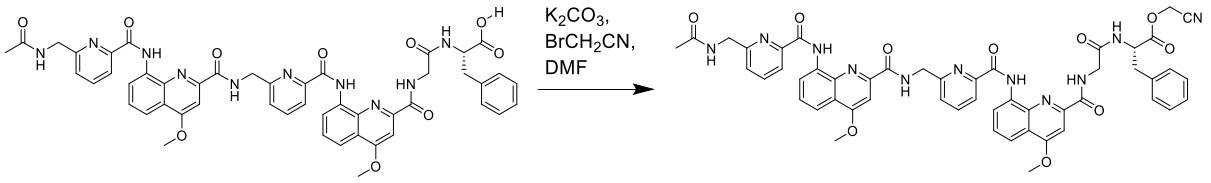

4a **4**

Compound 4a: Compound **4a** was prepared on a preloaded H-(L)-Phe-2-CT resin (0.60 mmol/g) using SPPS (**Method 3.2.1**) and SPFS (**Method 3.2.2**) synthesis protocols on an 0.011 mmol scale. After final acetylation (**Method 3.2.6**) and resin cleavage (**Method 3.2.8**) with HFIP:DCM (60:40, v/v), a crude brown powder was recovered in 25% yield (2.5 mg) and was used directly in subsequent reactions without further purification steps.

Compound 4: Compound **4** was synthesized from carboxylic acid 4**a** (2.5 mg, 2.7 µmol) using the general cyanomethyl installation protocol (**Method 3.2.9**). The obtained crude residue was purified by silica gel column chromatography using a mixture of MeOH in DCM starting from 1% to 6% (v/v) MeOH. After evaporating the corresponding fractions, compound 4 was obtained as a white solid (2.0 mg, 76%). ^{1}H NMR (500 MHz, Chloroform-*d*) δ 11.73 (s, 1H), 11.63 (s, 1H), 9.51 (d, *J* = 5.3 Hz, 1H), 8.58 (ddd, *J* = 14.6, 7.7, 1.3 Hz, 2H), 8.32 (s, 1H), 8.19 (d, *J* = 7.6 Hz, 1H), 8.03 (t, *J* = 7.7 Hz, 1H), 8.00 (d, *J* = 7.6 Hz, 1H), 7.97 (dd, *J* = 8.5, 1.3 Hz, 1H), 7.93 (dd, *J* = 8.4, 1.3 Hz, 1H), 7.86 (t, *J* = 7.7 Hz, 1H), 7.76 (s, 1H), 7.71 (d, *J* = 7.7 Hz, 1H), 7.61 – 7.57 (m, 1H), 7.51 – 7.46 (m, 1H), 7.29 (d, *J* = 9.7 Hz, 1H), 7.23 (d, *J* = 4.9 Hz, 1H), 7.12 – 7.06 (m, 3H), 6.96 (dd, *J* = 6.7, 2.9 Hz, 2H), 6.44 (d, *J* = 7.7 Hz, 1H), 6.36 (s, 1H), 5.04 (d, *J* = 5.0 Hz, 2H), 4.82 – 4.77 (m, 1H), 4.65 (d, *J* = 15.6 Hz, 1H), 4.54 (d, *J* = 15.6 Hz, 1H), 4.21 (s, 3H), 4.09 (s, 3H), 3.93 (t, *J* = 5.9 Hz, 2H), 3.90 – 3.83 (m, 1H), 3.75 (dd, *J* = 16.0, 5.1 Hz, 1H), 3.02 – 2.93 (m, 2H), 1.77 (s, 3H). HRMS (ESI$^+$): *m/z* calculated for $C_{51}H_{45}N_{11}O_{10}$ $[M+H]^+$ 972.3424 found 972.3419.

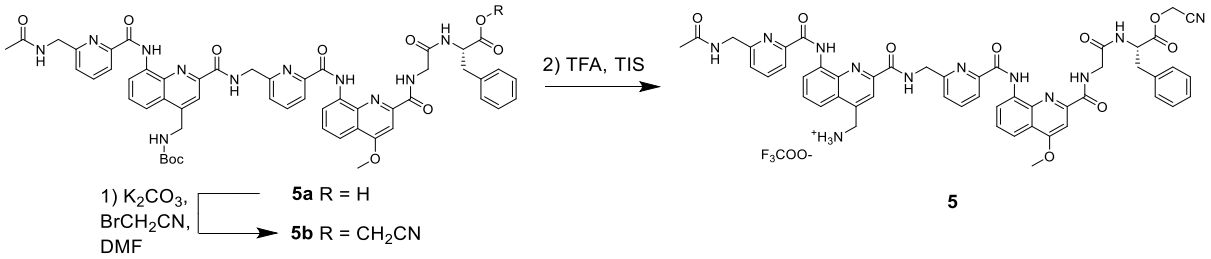

Compound 5a: Compound **5a** was prepared on a preloaded H-(L)-Phe-2-CT resin (0.60 mmol/g) using SPPS (**Method 3.2.1**) and SPFS (**Method 3.2.2**) synthesis protocols on an 0.011 mmol scale. After final acetylation (**Method 3.2.6**) and resin cleavage (**Method 3.2.8**) with HFIP:DCM (60:40, v/v), a crude brown powder was recovered in 27% yield (3.0 mg) and was used directly in subsequent reactions without further purification steps.

Compound 5b: Compound **5b** was synthesized from carboxylic acid **5a** (3.0 mg, 3.0 µmol) using the general cyanomethyl installation protocol (**Method 3.2.9**). The obtained crude residue was purified by silica gel column chromatography using a mixture of MeOH in DCM starting from 1% to 5% (v/v) MeOH. After evaporating the corresponding fractions, compound **5b** was obtained as a white solid (1.5 mg, 48%). ^{1}H NMR (500 MHz, DMSO-d_6) δ 11.83 (s, 1H), 11.78 (s, 1H), 9.53 (d, *J* = 5.8 Hz, 1H), 8.57 (d, *J* = 7.3 Hz, 1H), 8.54 (dd, *J* = 7.8, 3.4 Hz, 2H), 8.46 (t, *J* = 5.9 Hz, 1H), 8.19 (s, 1H), 8.14 – 8.10 (m, 2H), 8.06 (d, *J* = 7.5 Hz, 1H), 7.99 (t, *J* = 7.7 Hz, 1H), 7.90 (d, *J* = 7.6 Hz, 1H), 7.86 (dd, *J* = 8.5, 1.6 Hz, 2H), 7.79 (d, *J* = 7.7 Hz, 1H), 7.63 (dt, *J* = 11.7, 7.9 Hz, 3H), 7.37 (dd, *J* = 7.7, 1.1 Hz, 1H), 7.20 (s, 1H), 7.12 – 7.07 (m, 5H), 4.97 (d, *J* = 5.4 Hz, 2H), 4.85 (d, *J* = 1.0 Hz, 2H), 4.75 (d, *J* = 5.9 Hz, 2H), 4.50 (q, *J* = 7.2 Hz, 1H), 4.10 (s, 3H), 3.84 (qd, *J* = 16.8, 5.7 Hz, 2H), 3.62 (d, *J* = 5.8 Hz, 2H), 2.91 (dd, *J* = 7.3, 3.9 Hz, 2H), 1.64 (s, 3H), 1.44 (s, 9H). HRMS (ESI$^-$): *m/z* calculated for $C_{56}H_{54}N_{12}O_{11}$ [M–H]$^-$ 1069.3962 found 1069.3979.

Compound 5: Compound **5** was synthesized from cyanomethyl ester **5b** (1.5 mg, 1.4 µmol) using the general deprotection protocol (**Method 3.2.10**) in a TFA:DCM:TIS mixture. The obtained white powder was used without further purification (0.6 mg, 0.6 µmol, 40 %). ^{1}H NMR (500 MHz, DMSO-d_6) δ 11.77 (s, 1H), 11.76 (s, 1H), 9.61 (t, *J* = 5.2 Hz, 1H), 8.55 – 8.46 (m, 7H), 8.40 (s, 1H), 8.17 – 8.11 (m, 2H), 8.06 (d, *J* = 7.5 Hz, 1H), 8.01 (t, *J* = 7.7 Hz, 1H), 7.91 (dd, *J* = 10.3, 8.0 Hz, 2H), 7.85 (dd, *J* = 8.4, 1.3 Hz, 1H), 7.80 (d, *J* = 7.9 Hz, 1H), 7.71 (t, *J* = 8.1 Hz, 1H), 7.62 (t, *J* = 8.1 Hz, 1H), 7.38 (d, *J* = 7.7 Hz, 1H), 7.12 – 7.06 (m, 6H), 4.99 (d, *J* = 5.1 Hz, 2H), 4.86 (s, 2H), 4.72 (s, 2H), 4.48 (q, *J* = 7.2 Hz, 1H), 4.09 (s, 4H), 3.89 – 3.78 (m, 2H), 3.57 (d, *J* = 5.9 Hz, 2H), 2.96 – 2.86 (m, 2H), 1.67 (s, 3H). HRMS (ESI$^+$): *m/z* calculated for $C_{51}H_{48}N_{12}O_9$ [M+H]$^+$ 971.3583 found 971.3587.

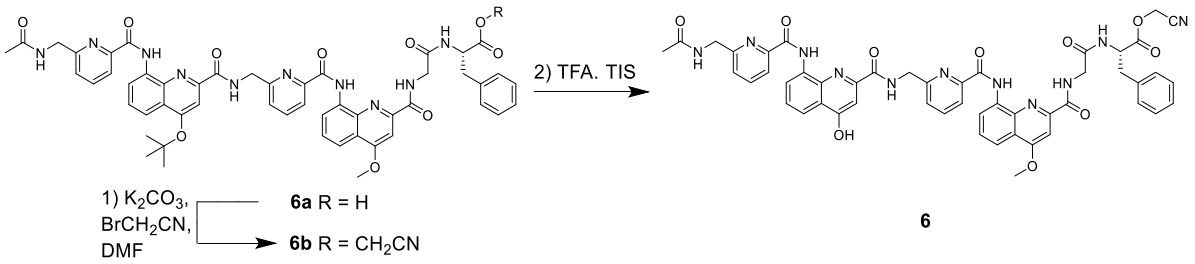

Compound 6a: Compound **6a** was prepared on a preloaded H-(L)-Phe-2-CT resin (0.60 mmol/g) using SPPS (**Method 3.2.1**) and SPFS (**Method 3.2.2**) synthesis protocols on an 0.011 mmol scale. After final acetylation (**Method 3.2.6**) and resin cleavage (**Method 3.2.8**) with HFIP:DCM (60:40, v/v), a crude brown powder was recovered in 28% yield (3.0 mg) and was used directly in subsequent reactions without further purification steps.

Compound 6b: Compound **6b** was synthesized from carboxylic acid **6a** (3.0 mg, 3.1 µmol) using the general cyanomethyl installation protocol (**Method 3.2.9**). The obtained crude residue was purified by silica gel column chromatography using a mixture of MeOH in DCM starting from 1% to 5% (v/v) MeOH. After evaporating the corresponding fractions, compound **4b** was obtained as a white solid (1.5 mg, 48%). ^{1}H NMR (500 MHz, Chloroform-*d*) δ 11.79 (s, 1H), 11.66 (s, 1H), 9.45 (t, *J* = 5.2 Hz, 1H), 8.63 (dd, *J* = 7.7, 1.3 Hz, 1H), 8.57 (dd, *J* = 7.7, 1.3 Hz, 1H), 8.34 (t, *J* = 5.6 Hz, 1H), 8.20 (dd, *J* = 7.6, 1.0 Hz, 1H), 8.02 (t, *J* = 7.2 Hz, 1H), 8.00 – 7.96 (m, 2H), 7.92 (dd, *J* = 8.5, 1.3 Hz, 1H), 7.90 (s, 1H), 7.83 (t, *J* = 7.7 Hz, 1H), 7.70 (dd, *J* = 7.8, 1.0 Hz, 1H), 7.59 (dd, *J* = 8.4, 7.7 Hz, 1H), 7.48 – 7.43 (m, 1H), 7.10 – 7.05 (m, 3H), 6.96 – 6.91 (m, 2H), 6.45 (d, *J* = 7.8 Hz, 1H), 6.31 (t, *J* = 5.4 Hz, 1H), 5.05 (t, *J* = 4.5 Hz, 2H), 4.78 (dt, *J* = 7.8, 6.1 Hz, 1H), 4.60 (d, *J* = 15.6 Hz, 1H), 4.49 (d, *J* = 15.6 Hz, 1H), 4.09 (s, 3H), 3.91 (dd, *J* = 5.6, 4.3 Hz, 2H), 3.85 (dd, *J* = 16.2, 5.4 Hz, 1H), 3.74 (dd, *J* = 16.4, 5.3 Hz, 1H), 2.99 – 2.90 (m, 2H), 1.76 (s, 8H), 1.74 (s, 3H). HRMS (ESI$^+$): *m/z* calculated for $C_{54}H_{51}N_{11}O_{11}$ $[M+H]^+$ 1014.3893 found 1014.3894.

Compound 6: Compound **6** was synthesized from cyanomethyl ester **6b** (1.5 mg, 1.5 µmol) using the general deprotection protocol (**Method 3.2.10**) in a TFA:DCM:TIS mixture. The obtained white powder was used without further purification (0.5 mg, 0.5 µmol, 35 %). ^{1}H NMR (500 MHz, DMSO-d_6) δ 12.06 (s, 1H), 11.89 (s, 1H), 11.73 (s, 1H), 9.49 (t, *J* = 5.3 Hz, 1H), 8.62 (d, *J* = 7.3 Hz, 1H), 8.51 (ddd, *J* = 16.7, 7.7, 1.3 Hz, 2H), 8.46 (t, *J* = 5.7 Hz, 1H), 8.15 – 8.05 (m, 3H), 7.97 (t, *J* = 7.7 Hz, 1H), 7.90 – 7.82 (m, 3H), 7.80 – 7.75 (m, 1H), 7.65 (s, 1H), 7.62 (t, *J* = 8.0 Hz, 1H), 7.50 (t, *J* = 8.0 Hz, 1H), 7.35 (dd, *J* = 7.8, 1.1 Hz, 1H), 7.21 (s, 1H), 7.15 – 7.06 (m, 6H), 4.93 (d, *J* = 5.4 Hz, 2H), 4.86 (d, *J* = 0.9 Hz, 2H), 4.49 (q, *J* = 7.3 Hz, 1H), 4.08 (s, 3H), 3.92 (dd, *J* = 17.0, 5.8 Hz, 1H), 3.83 (dd, *J* = 17.1, 5.6 Hz, 1H), 3.59 (d, *J* = 6.0 Hz, 2H), 2.93 (dd, *J* = 13.8, 6.5 Hz, 1H), 2.88 (dd, *J* = 13.7, 8.0 Hz, 1H), 1.63 (s, 3H). HRMS (ESI$^-$): *m/z* calculated for $C_{50}H_{43}N_{11}O_{10}$ $[M–H]^-$ 956.3122 found 956.3123.

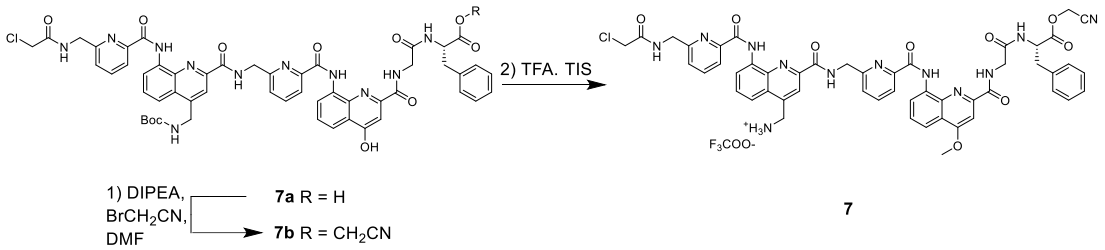

Compound 7a: Compound **7a** was prepared from H-(L)-Phe-2-CT resin on a 0.1 mmol scale (185 mg, manufacturer's loading: 0.54 mmol g^{-1}) using SPPS (**Method 3.2.1**) and SPFS (**Method 3.2.2**) synthesis protocols followed by final chloroacetylation (**Method 3.2.7**). The crude product obtained from resin cleavage (**Method 3.2.8**) was used directly in subsequent reaction without further purification (100 mg, 94%). ^{1}H NMR (500 MHz, DMSO-d_6) δ 12.67 (s, 1H), 11.78 (s, 1H), 11.75 (s, 1H), 9.54 (t, *J* = 5.2 Hz, 1H), 8.52 – 8.49 (m, 2H), 8.43 (t, *J* = 5.8 Hz, 1H), 8.22 (d, *J* = 7.8 Hz, 1H), 8.18 (s, 1H), 8.14 (t, *J* = 7.7 Hz, 1H), 8.05 (t, *J* = 7.7 Hz, 2H), 8.01 (t, *J* = 7.7 Hz, 1H), 7.91 (dd, *J* = 7.6, 1.1 Hz, 1H), 7.85 (dt, *J* = 8.5, 1.8 Hz, 2H), 7.79 (dd, *J* = 7.8, 1.0 Hz, 1H), 7.67 – 7.64 (m, 1H), 7.63 – 7.59 (m, 2H), 7.38 (dd, *J* = 7.8, 1.1 Hz, 1H), 7.16 (s, 1H), 7.10 – 7.05 (m, 5H), 4.97 (t, *J* = 4.5 Hz, 2H), 4.75 (d, *J* = 5.9 Hz, 2H), 4.43 – 4.34 (m, 1H), 4.09 (s, 3H), 3.93 (s, 2H), 3.89 – 3.81 (m, 1H), 3.75 (dd, *J* = 16.8, 5.6 Hz, 1H), 3.67 (d, *J* = 5.9 Hz, 2H), 2.92 (dd, *J* = 13.7, 5.7 Hz, 1H), 2.83 (dd, *J* = 13.7, 7.7 Hz, 1H), 1.44 (s, 9H). HRMS (ESI$^-$): *m/z* calculated for $C_{53}H_{50}ClN_{11}O_{11}$ $[M–H]^-$ 1064.3464 found 1064.3445.

Compound 7b: Compound **7b** was synthesized from carboxylic acid **7a** (100 mg, 0.1 mmol) the general cyanomethyl installation protocol (**Method 3.2.9**). The obtained crude residue was purified by silica gel column chromatography using a mixture of acetone in DCM starting from 20% to 40% (v/v) acetone. After evaporating the corresponding fractions, compound **8b** was obtained as a white solid (52 mg, 52%). ^{1}H NMR (500 MHz, DMSO-d_6) δ 11.78 (s, 1H), 11.75 (s, 1H), 9.55 (t, *J* = 5.3 Hz, 1H), 8.57 (d, *J* = 7.3 Hz, 1H), 8.53 – 8.48 (m, 3H), 8.40 (t, *J* = 5.8 Hz, 1H), 8.19 (s, 1H), 8.14 (t, *J* = 7.7 Hz, 1H), 8.06 (d, *J* = 7.6 Hz, 1H), 8.01 (t, *J* = 7.7 Hz, 1H), 7.92 – 7.89 (m, 1H), 7.85 (dt, *J* = 8.4, 1.5 Hz, 2H), 7.80 (dd, *J* = 7.8, 1.0 Hz, 1H), 7.67 – 7.59 (m, 3H), 7.38 (dd, *J* = 7.7, 1.1 Hz, 1H), 7.15 – 7.07 (m, 6H), 4.96 (d, *J* = 5.4 Hz, 2H), 4.86 (d, *J* = 1.2 Hz, 2H), 4.75 (d, *J* = 5.9 Hz, 2H), 4.50 (q, *J* = 7.2 Hz, 1H), 4.09 (s, 3H), 3.93 (s, 2H), 3.88 – 3.75 (m, 2H), 3.65 (d, *J* = 5.9 Hz, 2H), 2.97 – 2.88 (m, 2H), 1.44 (s, 9H). HRMS (ESI$^-$): *m/z* calculated for $C_{56}H_{53}ClN_{12}O_{11}$ $[M–H]^-$ 1103.3573 found 1103.3564.

Compound 7: For the synthesis of compound **7**, the total **7b** was directly submitted to the general deprotection protocol (**Method 3.2.10**) in a TFA:DCM:TIS mixture. The obtained white powder was used without further purification (43 mg, 0.042 mmol, 91%). ^{1}H NMR (500 MHz, DMSO-d_6) δ 11.72 (s, 1H), 11.71 (s, 1H), 9.61 (t, *J* = 5.0 Hz, 1H), 8.56 (s, 3H), 8.52 – 8.43 (m, 5H), 8.40 (s, 1H), 8.16 (t, *J* = 7.7 Hz, 1H), 8.07 – 8.01 (m, 2H), 7.91 (td, *J* = 7.6, 1.1 Hz, 2H), 7.83 (ddd, *J* = 12.6, 8.1, 1.2 Hz, 2H), 7.73 – 7.67 (m, 1H), 7.64 – 7.59 (m, 1H), 7.40 (dd, *J* = 7.8, 1.0 Hz, 1H), 7.14 – 7.05 (m, 6H), 4.98 (d, *J* = 5.0 Hz, 2H), 4.87 (d, *J* = 1.0 Hz, 2H), 4.72 (d, *J* = 5.8 Hz, 2H), 4.48 (td, *J* = 7.7, 6.5 Hz, 1H), 4.08 (s, 3H), 3.95 (s, 2H), 3.86 – 3.76 (m, 2H), 3.59 (d, *J* = 5.8 Hz, 2H), 2.92 (qd, *J* = 13.8, 7.1 Hz, 2H). HRMS (ESI$^-$): *m/z* calculated for $C_{51}H_{45}ClN_{12}O_9$ $[M–H]^-$ 1005.3194 found 1005.3209.

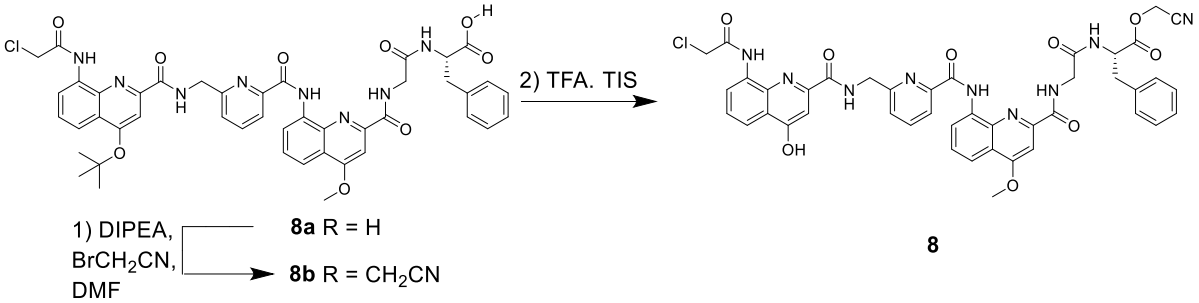

Compound 8a: Compound **8a** was prepared from H-(L)-Phe-2-CT resin on a 0.1 mmol scale (210 mg, manufacturer's loading: 0.54 mmol g^{-1}) using SPPS (**Method 3.2.1**) and SPFS (**Method 3.2.2**) synthesis protocols followed by final chloroacetylation (**Method 3.2.7**). The crude product obtained from resin cleavage (**Method 3.2.8**) was used directly in subsequent reaction without further purification. ^{1}H NMR (500 MHz, DMSO-d_6) δ 12.70 (s, 1H), 12.14 (s, 1H), 10.39 (s, 1H), 9.92 (t, *J* = 6.0 Hz, 1H), 8.96 (dd, *J* = 7.7, 1.3 Hz, 1H), 8.83 (t, *J* = 6.1 Hz, 1H), 8.58 (dd, *J* = 7.8, 1.3 Hz, 1H), 8.51 (d, *J* = 8.0 Hz, 1H), 8.19 (dd, *J* = 7.7, 1.1 Hz, 1H), 8.14 (t, *J* = 7.7 Hz, 1H), 8.05 (d, *J* = 7.6 Hz, 1H), 7.92 (dd, *J* = 8.4, 1.3 Hz, 1H), 7.86 (dd, *J* = 8.5, 1.3 Hz, 1H), 7.81 – 7.77 (m, 2H), 7.75 – 7.70 (m, 1H), 7.62 – 7.55 (m, 2H), 7.09 – 7.02 (m, 5H), 4.91 – 4.81 (m, 2H), 4.48 (td, *J* = 8.1, 5.6 Hz, 1H), 4.36 – 4.27 (m, 2H), 4.26 – 4.19 (m, 1H), 4.15 (s, 3H), 4.09 (dd, *J* = 17.0, 5.9 Hz, 1H), 2.93 (dd, *J* = 13.8, 5.6 Hz, 1H), 2.82 (dd, *J* = 13.8, 8.2 Hz, 1H), 1.62 (s, 9H). HRMS (ESI$^-$): *m/z* calculated for $C_{45}H_{42}ClN_8O_9$ [M–H]$^-$ 873.2769 found 873.2763.

Compound 8b and **8**: Compound **8b** was synthesized from carboxylic acid **8a** (43 mg, 0.05 mmol) using the general cyanomethyl installation protocol (**Method 3.2.9**). For the synthesis of compound **8**, the obtained crude residue **8b** was directly submitted to the general deprotection protocol (**Method 3.2.10**) in a TFA:DCM:TIS mixture. The crude compound was dissolved in DCM in which impurities precipitated within 24 h. The mixture was filtered and the filtrate was evaporated, redissolved and purified by semi-preparative HPLC using a gradient from 55–80% over 15 min at 25 °C on an RP-18 column. (16 mg, 37 %). ^{1}H NMR (500 MHz, DMSO-d_6) δ 12.15 (s, 1H), 12.04 (s, 1H), 10.37 (s, 1H), 9.89 (t, *J* = 6.1 Hz, 1H), 8.95 (dd, *J* = 7.7, 1.3 Hz, 1H), 8.83 (t, *J* = 6.1 Hz, 1H), 8.76 (d, *J* = 7.4 Hz, 1H), 8.57 (dd, *J* = 7.8, 1.3 Hz, 1H), 8.18 (dd, *J* = 7.6, 1.1 Hz, 1H), 8.12 (t, *J* = 7.7 Hz, 1H), 7.92 (dd, *J* = 8.5, 1.3 Hz, 1H), 7.87 (dd, *J* = 8.4, 1.3 Hz, 1H), 7.76 – 7.71 (m, 2H), 7.65 (s, 1H), 7.58 (s, 1H), 7.55 (t, *J* = 8.1 Hz, 1H), 7.11 – 7.04 (m, 5H), 4.87 (d, *J* = 1.5 Hz, 2H), 4.85 (d, *J* = 6.1 Hz, 2H), 4.56 (td, *J* = 7.9, 6.6 Hz, 1H), 4.36 (d, *J* = 1.4 Hz, 2H), 4.20 (dd, *J* = 17.0, 6.3 Hz, 1H), 4.15 (s, 3H), 4.11 (dd, *J* = 17.0, 5.9 Hz, 1H), 2.95 (dd, *J* = 13.7, 6.4 Hz, 1H), 2.89 (dd, *J* = 13.8, 8.2 Hz, 1H). HRMS (ESI$^-$): *m/z* calculated for $C_{43}H_{36}ClN_9O_9$ [M–H]$^-$ 856.2252 found 856.2244.

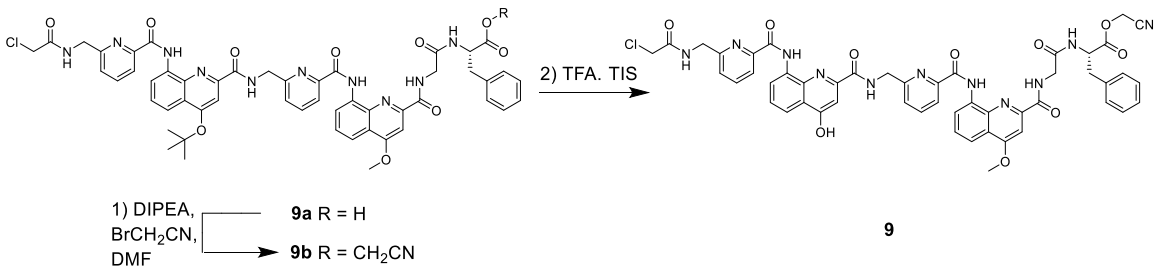

Compound 9a: Compound **9a** was prepared from H-(L)-Phe-2CT resin on a 0.1 mmol scale (185 mg, manufacturer's loading: 0.54 mmol g^{-1}) using SPPS (**Method 3.2.1**) and SPFS (**Method 3.2.2**) synthesis protocols followed by final chloroacetylation (**Method 3.2.7**). The crude product obtained from resin cleavage (**Method 3.2.8**) was used directly in subsequent reaction without further purification (110 mg, 98%). ^{1}H NMR (500 MHz, Chloroform-*d*) δ 11.72 (s, 1H), 11.52 (s, 1H), 9.53 (t, *J* = 5.1 Hz, 1H), 8.53 (d, *J* = 7.6 Hz, 1H), 8.46 – 8.41 (m, 1H), 8.31 (t, *J* = 5.4 Hz, 1H), 8.13 (d, *J* = 7.6 Hz, 1H), 7.94 (dd, *J* = 14.8, 7.8 Hz, 3H), 7.86 (dd, *J* = 8.4, 1.3 Hz, 1H), 7.82 (s, 1H), 7.79 (t, *J* = 7.7 Hz, 1H), 7.62 (d, *J* = 7.8 Hz, 1H), 7.54 (t, *J* = 8.1 Hz, 1H), 7.42 (t, *J* = 5.5 Hz, 1H), 7.38 (t, *J* = 8.1 Hz, 1H), 7.20 (d, *J* = 7.7 Hz, 1H), 7.12 (s, 1H), 7.05 – 6.99 (m, 5H), 6.74 (d, *J* = 7.4 Hz, 1H), 5.03 – 4.97 (m, 2H), 4.66 (q, *J* = 6.5 Hz, 1H), 4.02 (s, 3H), 3.98 (t, *J* = 4.0 Hz, 1H), 3.90 (dd, *J* = 16.8, 5.1 Hz, 1H), 3.85 (s, 2H), 3.79 (dd, *J* = 15.9, 5.0 Hz, 1H), 3.70 (dd, *J* = 15.9, 5.2 Hz, 1H), 3.04 – 2.96 (m, 1H), 2.93 – 2.86 (m, 1H), 1.71 (s, 9H). HRMS (ESI$^-$): *m/z* calculated for $C_{52}H_{48}ClN_{10}O_{10}$ [M–H]$^-$ 1007.3249 found 1007.3232.

Compound 9b: Compound **9b** was synthesized from carboxylic acid **9a** (110 mg, 0.1 mmol) the general cyanomethyl installation protocol (**Method 3.2.9**). The obtained crude residue was purified by silica gel column chromatography using a mixture of acetone in DCM starting from 20% to 40% (v/v) acetone. After evaporating the corresponding fractions, compound **9b** was obtained as a white solid (49 mg, 47%). ^{1}H NMR (500 MHz, DMSO-d_6) δ 11.83 (s, 1H), 11.62 (s, 1H), 9.55 (t, *J* = 5.1 Hz, 1H), 8.66 (d, *J* = 7.3 Hz, 1H), 8.47 (t, *J* = 5.9 Hz, 1H), 8.43 (ddd, *J* = 7.7, 2.9, 1.4 Hz, 2H), 8.34 (t, *J* = 5.6 Hz, 1H), 8.16 (t, *J* = 7.7 Hz, 1H), 8.07 (dd, *J* = 7.7, 1.0 Hz, 1H), 7.99 (t, *J* = 7.7 Hz, 1H), 7.87 – 7.80 (m, 4H), 7.79 (s, 1H), 7.62 – 7.57 (m, 1H), 7.53 – 7.49 (m, 1H), 7.37 (dd, *J* = 7.8, 1.0 Hz, 1H), 7.17 – 7.10 (m, 5H), 7.08 (s, 1H), 5.00 – 4.89 (m, 2H), 4.88 (s, 2H), 4.50 (td, *J* = 7.8, 6.6 Hz, 1H), 4.06 (s, 3H), 3.92 (s, 2H), 3.82 (qd, *J* = 17.1, 5.6 Hz, 2H), 3.56 (d, *J* = 5.9 Hz, 2H), 2.93 (qd, *J* = 13.8, 7.3 Hz, 2H), 1.69 (s, 9H). HRMS (ESI$^-$): *m/z* calculated for $C_{54}H_{49}ClN_{11}O_{10}$ [M–H]$^-$ 1046.3358 found 1046.3349.

Compound 9: For the synthesis of compound **9**, the total **9b** was directly submitted to the general deprotection protocol (**Method 3.2.10**) in a TFA:DCM:TIS mixture. The obtained white powder was used without further purification (47 mg, 0.042 mmol, 87 %). ^{1}H NMR (500 MHz, DMSO-d_6) δ 12.05 (s, 1H), 11.86 (s, 1H), 11.67 (s, 1H), 9.51 (t, *J* = 5.2 Hz, 1H), 8.63 (d, *J* = 7.3 Hz, 1H), 8.51 – 8.45 (m, 3H), 8.40 (t, *J* = 5.7 Hz, 1H), 8.14 (t, *J* = 7.7 Hz, 1H), 8.07 (d, *J* = 7.4 Hz, 1H), 8.00 (t, *J* = 7.7 Hz, 1H), 7.91 – 7.81 (m, 3H), 7.79 (d, *J* = 7.8 Hz, 1H), 7.64 (s, 1H), 7.61 (t, *J* = 8.1 Hz, 1H), 7.48 (t, *J* = 8.0 Hz, 1H), 7.37 (d, *J* = 7.7 Hz, 1H), 7.16 (s, 1H), 7.15 – 7.07 (m, 5H), 4.92 (d, *J* = 5.3 Hz, 2H), 4.87 (d, *J* = 1.1 Hz, 2H), 4.49 (q, *J* = 7.4 Hz, 1H), 4.07 (s, 3H), 3.91 (s, 2H), 3.90 – 3.78 (m, 2H), 3.61 (d, *J* = 5.9 Hz, 2H), 2.92 (qd, *J* = 13.8, 7.3 Hz, 2H).HRMS (ESI$^-$): *m/z* calculated for $C_{50}H_{41}ClN_{11}O_{10}$ [M–H]$^-$ 990.2732 found 990.2721.

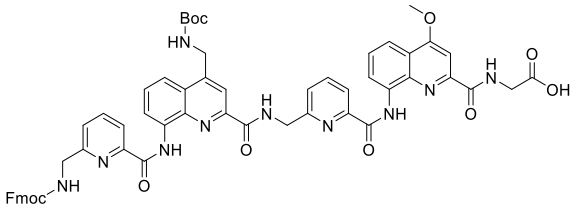

F10

Foldamer fragment F10: **F10** was synthesized on a preloaded Fmoc-Gly-SASRIN resin (loading: 0.61 mmol/g) using the general SPFS procedure (**Method 3.2.4**) on a 0.2 mmol scale. **F10** was recovered in 70% yield (150 mg) after cleavage (**Method 3.2.8**) using 6 mL of HFIP/DCM (30:70, v/v) mixture for 1 h at r.t. and was used without any further purification. ^{1}H NMR (500 MHz, DMSO-d_6) δ 12.67 (s, 1H), 11.86 (s, 1H), 11.77 (s, 1H), 9.60 (d, *J* = 6.0 Hz, 1H), 8.52 (d, *J* = 7.7 Hz, 1H), 8.47 (d, *J* = 7.8 Hz, 1H), 8.43 (d, *J* = 6.2 Hz, 1H), 8.17 (s, 1H), 8.10 (t, *J* = 7.6 Hz, 1H), 8.02 (dd, *J* = 14.4, 7.3 Hz, 2H), 7.92 (d, *J* = 7.5 Hz, 1H), 7.88 – 7.81 (m, 2H), 7.79 (d, *J* = 7.7 Hz, 1H), 7.75 (d, *J* = 7.6 Hz, 2H), 7.70 (t, *J* = 6.1 Hz, 1H), 7.64 (t, *J* = 8.0 Hz, 2H), 7.58 (t, *J* = 8.1 Hz, 1H), 7.44 (d, *J* = 7.5 Hz, 2H), 7.32 (t, *J* = 7.7 Hz, 3H), 7.17 (dd, *J* = 14.7, 7.4 Hz, 3H), 5.00 (d, *J* = 5.2 Hz, 2H), 4.74 (d, *J* = 5.9 Hz, 2H), 4.19 – 4.16 (m, 1H), 4.12 (d, *J* = 6.9 Hz, 2H), 4.08 (s, 3H), 4.03 (t, *J* = 6.9 Hz, 1H), 3.87 (d, *J* = 6.0 Hz, 2H), 3.62 (d, *J* = 6.0 Hz, 2H), 1.45 (s, 9H).HRMS (ESI$^-$) *m/z* calculated for $C_{58}H_{53}N_{10}O_{11}$ $[M+H]^+$ 1065.3890 found 1065.4042.

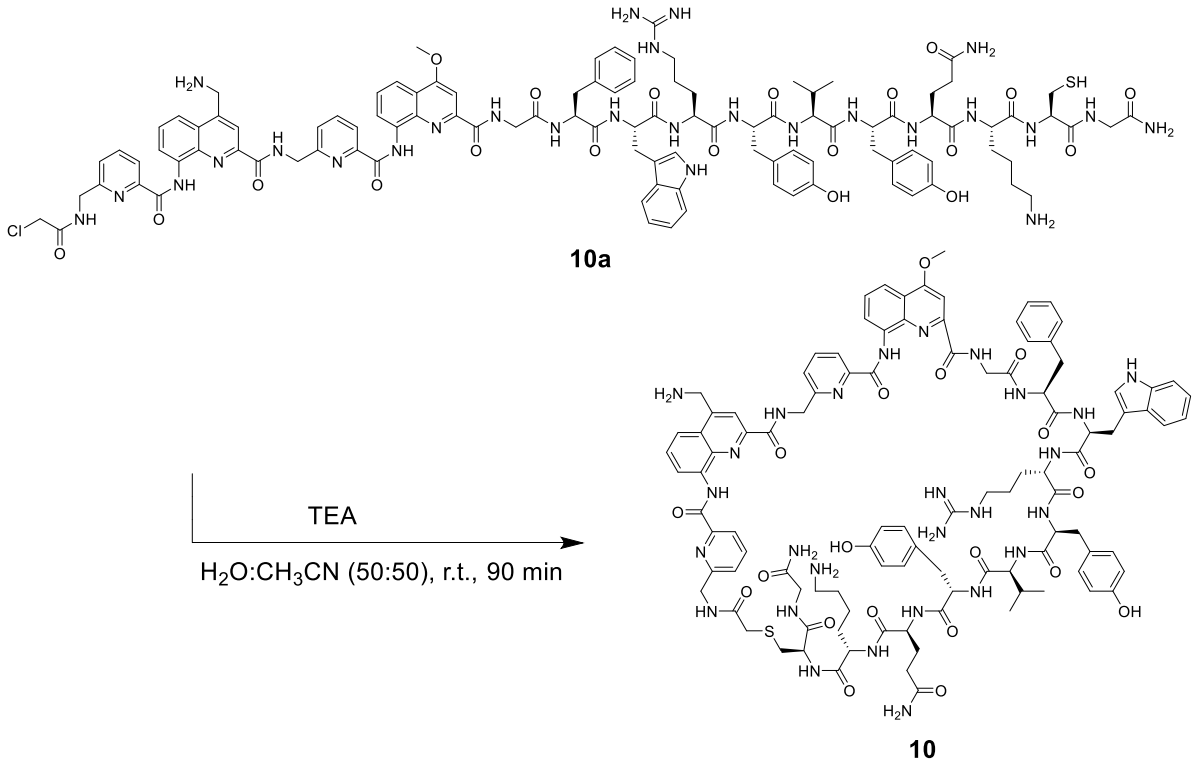

Compound 10a: Resin-bound Fmoc-Phe-Trp(Boc)-Arg(Pbf)-Tyr(tBu)-Val-Tyr(tBu)-Gln(Trt)-Lys(Boc)-Cys(Trt)-Gly-NH- was first prepared from Rink amide resin (0.33 mmol/g) using a CEM Liberty Blue microwave automated peptide synthesizer (**Method 3.2.1**) on a 0.1 mmol scale. Fragment condensation (**Method 3.2.5**) with foldamer fragment **F10** was next performed on a 50 µmol scale of deprotected resin-bound peptide. After Fmoc deprotection (piperidine (20% (v/v)) in DMF, 2 mL, 2× 5 min), final chloroacetylation (**Method 3.2.7**) and TFA cleavage (**Method 3.2.8**), crude **10a** (118 mg, 94%) was directly engaged in the macrocyclization reaction without further purification. HRMS (ESI$^+$): *m/z* calculated for $C_{105}H_{123}ClN_{27}O_{20}S$ $[M+H]^+$ 2149.8875 found 2149.9112

Compound 10: Total compound **10** was dissolved in 88 mL CH_3CN (50% (v/v) in H_2O) to a 0.5 mM dilution and triethylamine (6 mL, 0.5 M) was added. After 90 min at r.t. without agitation and monitoring the reaction by HPLC, the reaction mixture was concentrated under reduced pressure and acidified with an equimolar volume of TFA. Remaining solvents were evaporated by lyophilization and the crude macrocycle was purified by using semi-preparative RP-HPLC with a

gradient from 30–50% solvent B over 15 minutes at 50 °C on a 250 mm C18 column to give **10** as a colorless solid. For further studies, 2× lyophilization from HCl (0.1 M) provided compound **10** as an HCl salt. (12 mg, 10%). ^{1}H NMR was performed in CD_3CN (25% (v/v) in H_2O) with water suppression. ^{1}H NMR (500 MHz, Acetonitrile-d_3) δ 11.49 (s, 1H), 11.37 (s, 1H), 9.96 (s, 1H), 9.76 (t, *J* = 4.4 Hz, 1H), 8.37 (d, *J* = 7.1 Hz, 1H), 8.28 (s, 1H), 8.25 (s, 1H), 8.14 (d, *J* = 8.6 Hz, 1H), 8.07 (t, *J* = 8.1 Hz, 4H), 8.00 (d, *J* = 8.2 Hz, 1H), 7.97 – 7.89 (m, 5H), 7.84 – 7.79 (m, 2H), 7.76 (d, *J* = 7.5 Hz, 1H), 7.62 (dt, *J* = 19.8, 8.7 Hz, 3H), 7.52 (dd, *J* = 14.6, 8.1 Hz, 3H), 7.42 (d, *J* = 10.9 Hz, 2H), 7.40 – 7.34 (m, 3H), 7.32 (d, *J* = 9.3 Hz, 3H), 7.20 (dd, *J* = 23.5, 8.6 Hz, 1H), 7.04 (m, 9H), 6.96 – 6.89 (m, 6H), 6.85 – 6.77 (m, 1H), 6.74 – 6.65 (m, 6H), 6.62 (s, 1H), 4.80-4.40 (water suppression region), 3.97 (s, 2H), 3.84 (qd, *J* = 17.1, 6.5 Hz, 2H), 3.65 – 3.52 (m, 2H), 3.30 – 3.16 (m, 4H), 3.16 – 3.01 (m, 4H), 3.01 – 2.82 (m, 11H), 2.82 – 2.64 (m, 4H), 2.34 – 2.16 (m, 3H), 1.95 (q, *J* = 8.1, 7.5 Hz, 1H), 1.87 – 1.58 (m, 5H), 1.48 – 1.14 (m, 5H), 0.98 (s, 1H), 0.78 (m, 8H). HRMS (ESI$^+$): *m/z* calculated for $C_{105}H_{122}N_{27}O_{27}S$ $[M+H]^+$ 2113.9108 found 2113.9446.

Compounds 11-17: The resin-bound Ala-scan peptides (see scheme 1) were first prepared on low loading Rink amide resin (0.33 mmol/g) using a CEM Liberty Blue microwave automated peptide synthesizer on a 50 μmol scale. The resin-bound peptides was next slipped into two equal portions, and the foldamer segment was introduced via SPFS on the Chorus synthesizer (**Method 3.2.3**) on a 25 μmol scale. After final Fmoc deprotection (piperidine (20% (v/v)) in DMF, 2 mL, 2× 5 min), chloroacetylation (**Method 3.2.7**) and TFA cleavage (**Method 3.2.8**) crudes **11a-17a** were directly engaged in the macrocyclization reaction without further purification (see detailed protocol for compound **10** to give rise to macrocycles **11**-**17**.

Compd.	**Yield (%)**	**HRMS (ESI$^+$): *m/z* calculated for z=2**	**found**
11	5.1	$C_{97}H_{116}N_{26}O_{20}S$, 1000.1022	999.9471
12	10.8	$C_{102}H_{114}N_{24}O_{20}S$, 1015.114	1014.9300
13	3.7	$C_{99}H_{117}N_{27}O_{19}S$, 1011.6206	1011.4532
14	10.5	$C_{103}H_{117}N_{27}O_{20}S$, 1043.6418	696.9532*
15	8.4	$C_{99}H_{117}N_{27}O_{19}S$, 1011.6206	674.6088*
16	6.1	$C_{103}H_{118}N_{26}O_{19}S$, 1029.1427	1028.9519
17	2.2	$C_{102}H_{114}N_{26}O_{20}S$, 1029.1211	1028.9364

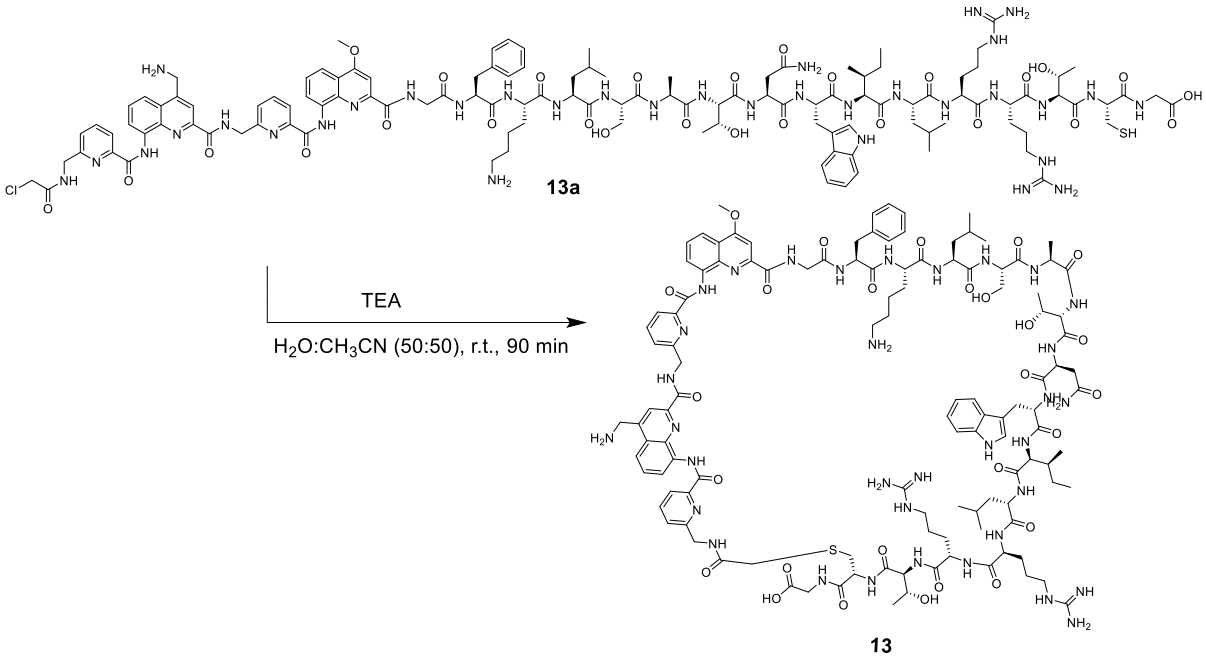

Compound 18a: Peptide Fmoc-Gly-Phe-Lys(Boc)-Leu-Ser(*t*Bu)Ala-Thr(*t*Bu)-Asn(Trt)-Trp(Boc)-Ile-Leu-Arg(Pbf)-Arg(Pbf)-Thr(*t*Bu)-Cys(Trt)-Gly-NH- was first prepared from Rink amide resin (0.33 mmol/g) using a CEM Liberty Blue microwave automated peptide synthesizer on a 100 μmol scale. The foldamer segment was then assembled manually with the Liberty bio microwave oven (**Method 3.2.2**) on a 50 μmol scale. After Fmoc deprotection, final chloroacetylation (**Method 3.2.7**) and TFA cleavage (**Method 3.2.8**), crude **18a** (157 mg, quantitative) was directly engaged in the macrocyclization reaction without further purification. HRMS (ESI$^+$): *m/z* calculated for $C_{119}H_{161}ClN_{34}O_{27}S$ $[M+2H]^{2+}$ 1283.5888 found 1283.6198.

Compound 18: Compound **18a** (38 mg, 0.5mM) was dissolved in 50 mL H_2O/acetonitrile (1:1, v/v) and Et_3N (6.8 mL) was added to reach a final concentration of 0.5 M. The mixture was quickly stirred and left without agitation. After stirring at r.t. for 90 min and monitoring the reaction by RP-HPLC, the reaction mixture was acidified with an equimolar volume of TFA and concentrated under reduced pressure. Remaining solvents were evaporated by lyophilization and the crude macrocycle was purified by using preparative RP-HPLC with a gradient from 30–50% solvent B over 20 min at r.t. on a 125 mm C18 column to give **18** as a white solid. For further studies, 2× lyophilization from HCl (0.1 M) provided compound **18** as an orange HCl salt. (19.3 mg, 15.3%). ^{1}H NMR was performed in CD_3CN (50% (v/v) in H_2O) with water suppression. HRMS (ESI$^+$): *m/z* calculated for $C_{119}H_{160}N_{34}O_{27}S$ $[M+2H]^{2+}$ 1265.6372 found 1265.6004.

4.5. ^{1}H NMR spectra and HPLC profiles

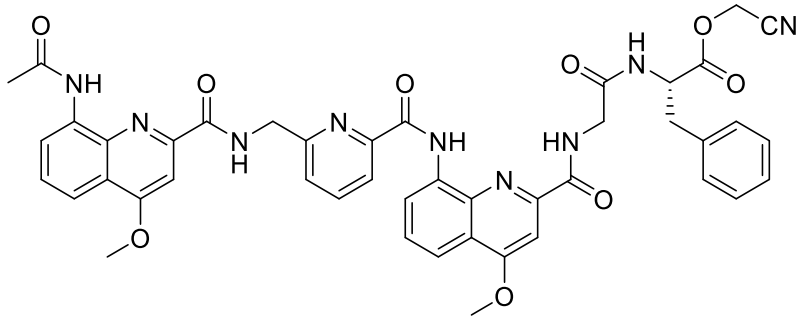

1

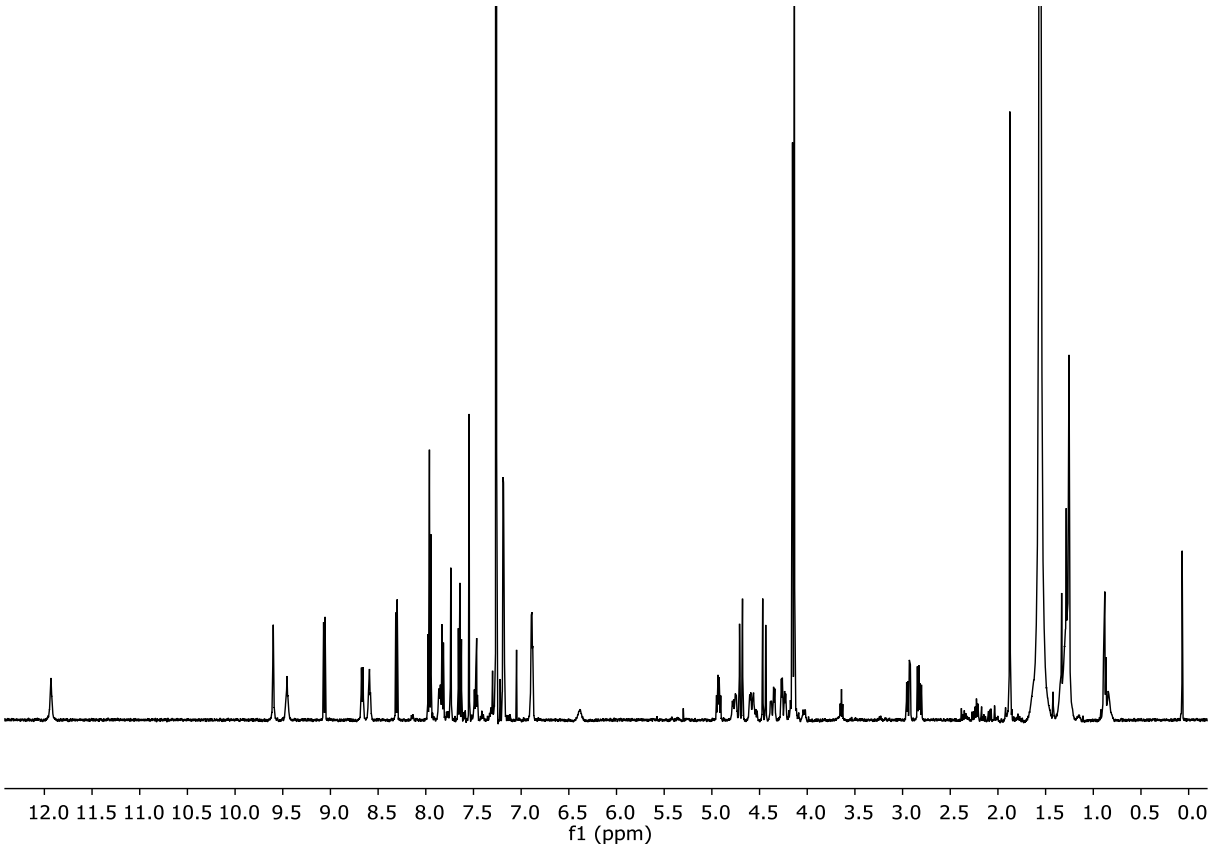

^{1}H NMR spectrum (500 MHz, $CDCl_3$, 25 °C) of **1**.

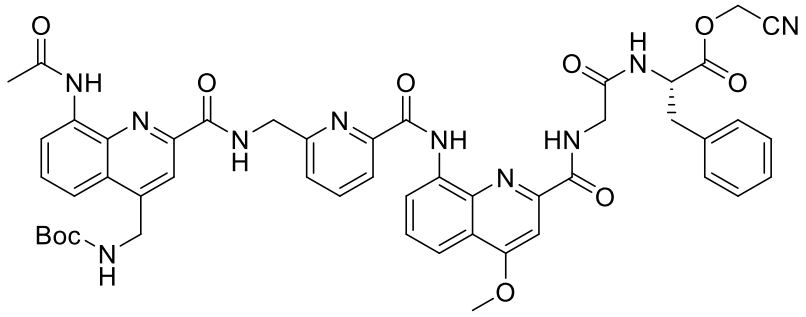

2b

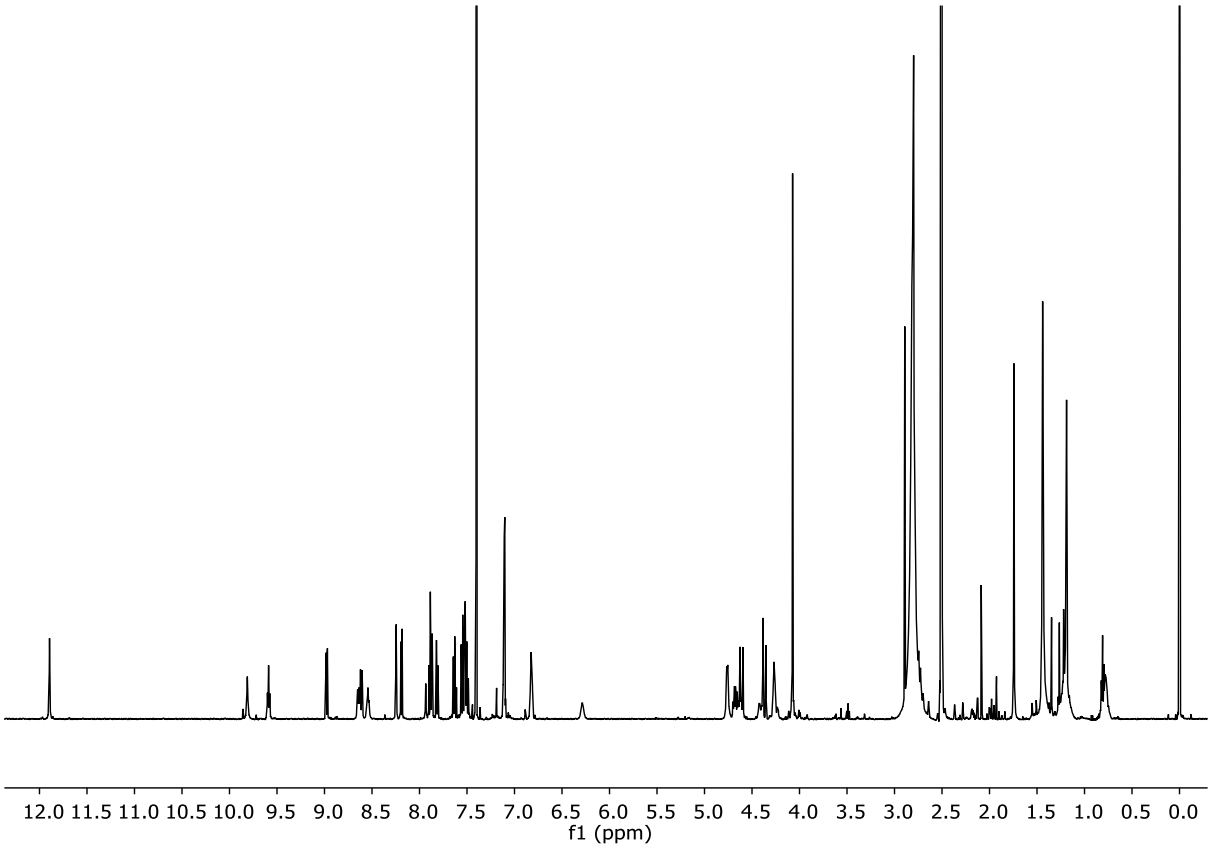

^{1}H NMR spectrum (500 MHz, $CDCl_3$, 25 °C) of **2b**.

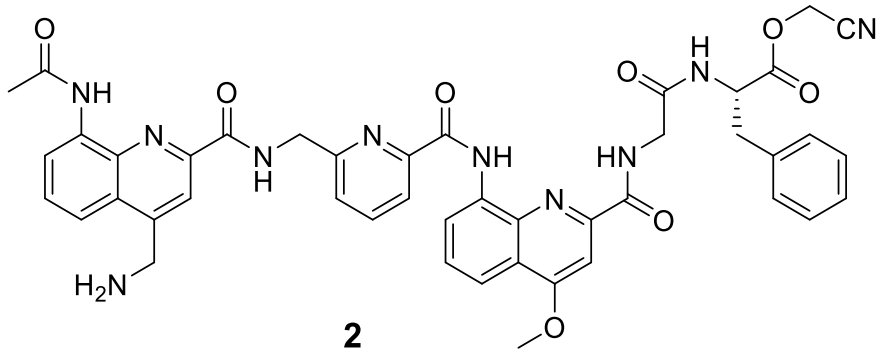

2

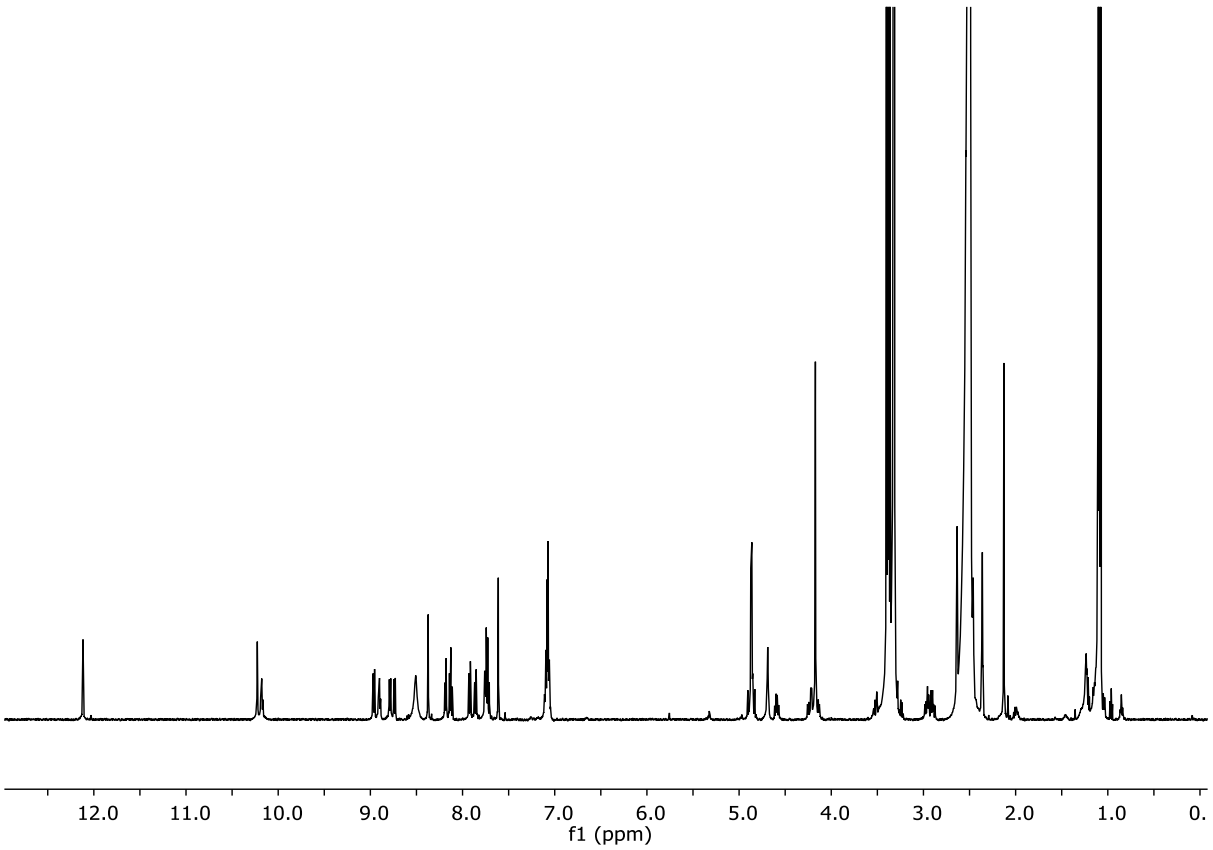

^{1}H NMR spectrum (500 MHz, DMSO-d_6, 25 °C) of **2**.

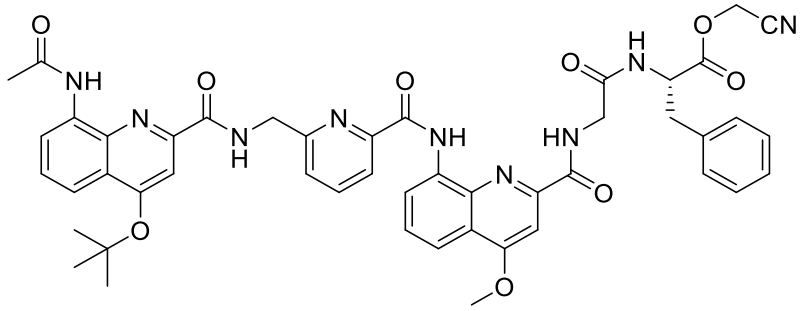

3b

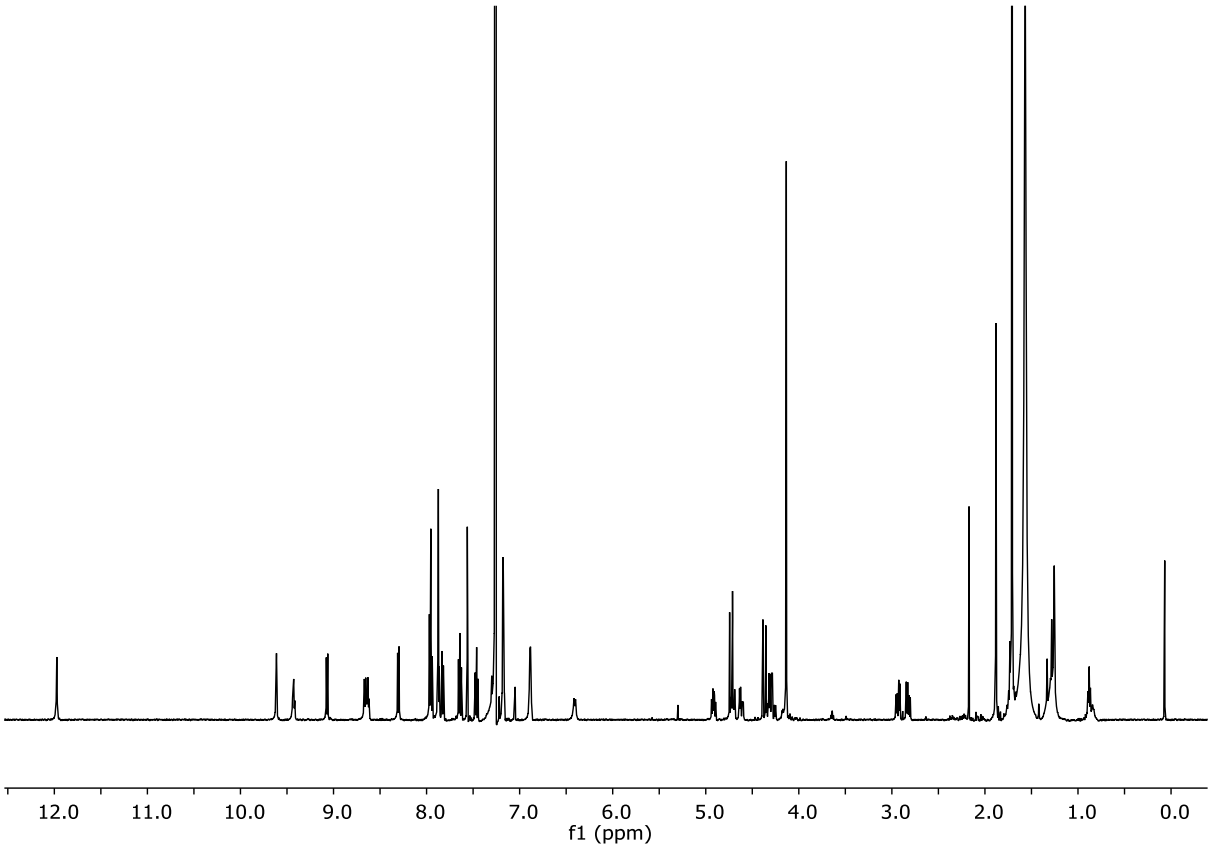

^{1}H NMR spectrum (500 MHz, $CDCl_3$, 25 °C) of **3b**.

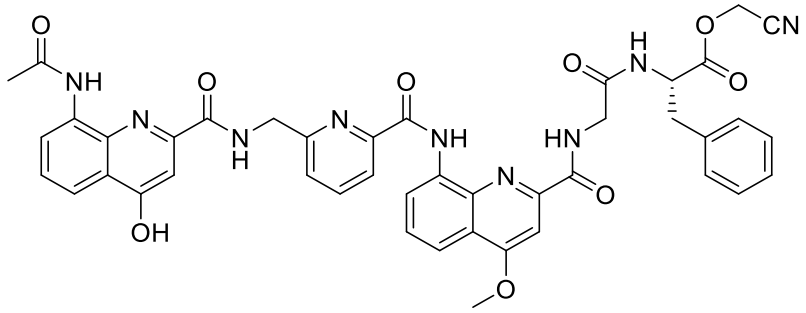

3

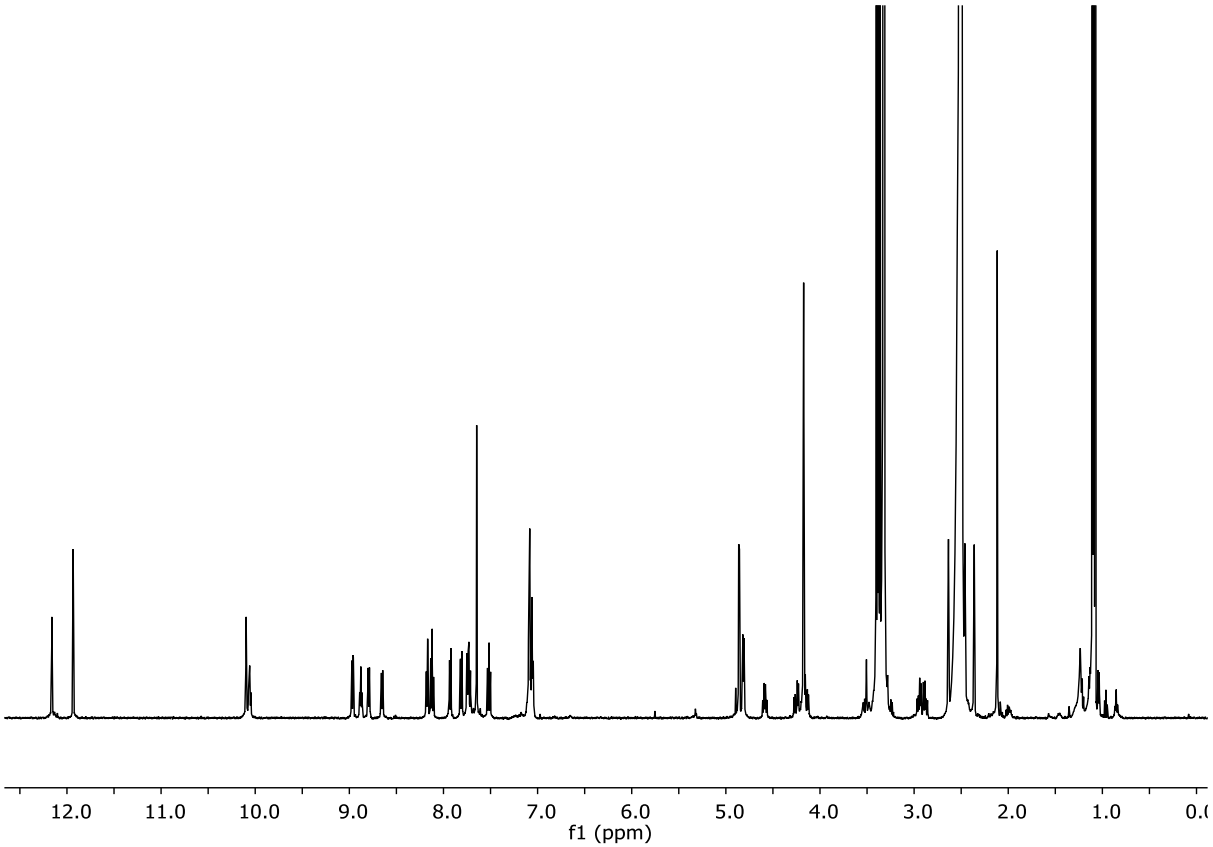

^{1}H NMR spectrum (500 MHz, DMSO-d_6, 25 °C) of **3**.

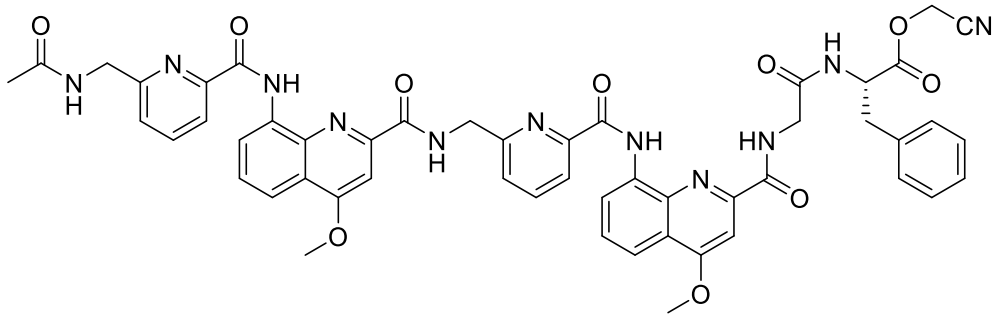

4

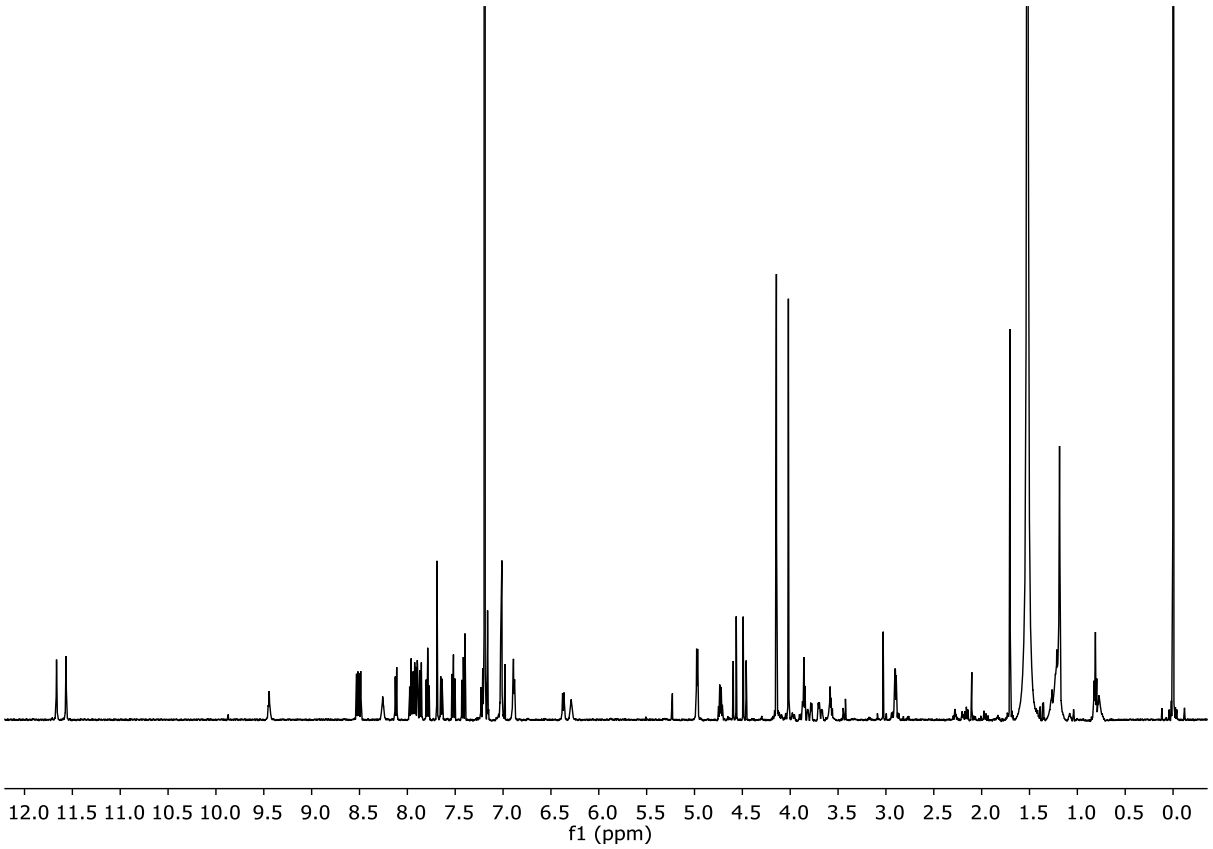

^{1}H NMR spectrum (500 MHz, $CDCl_3$, 25 °C) of **4**.

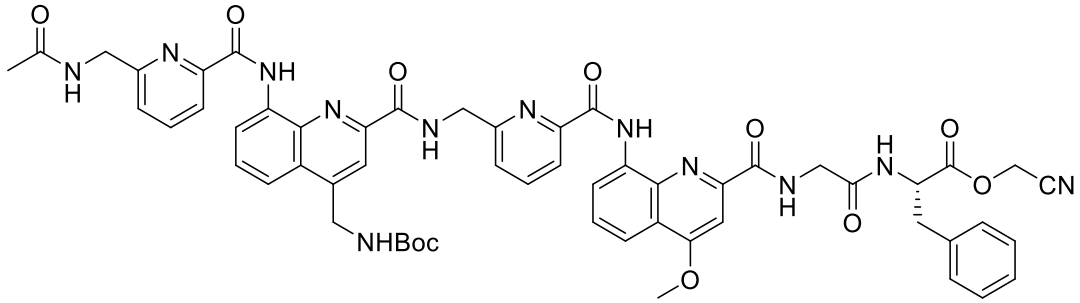

5b

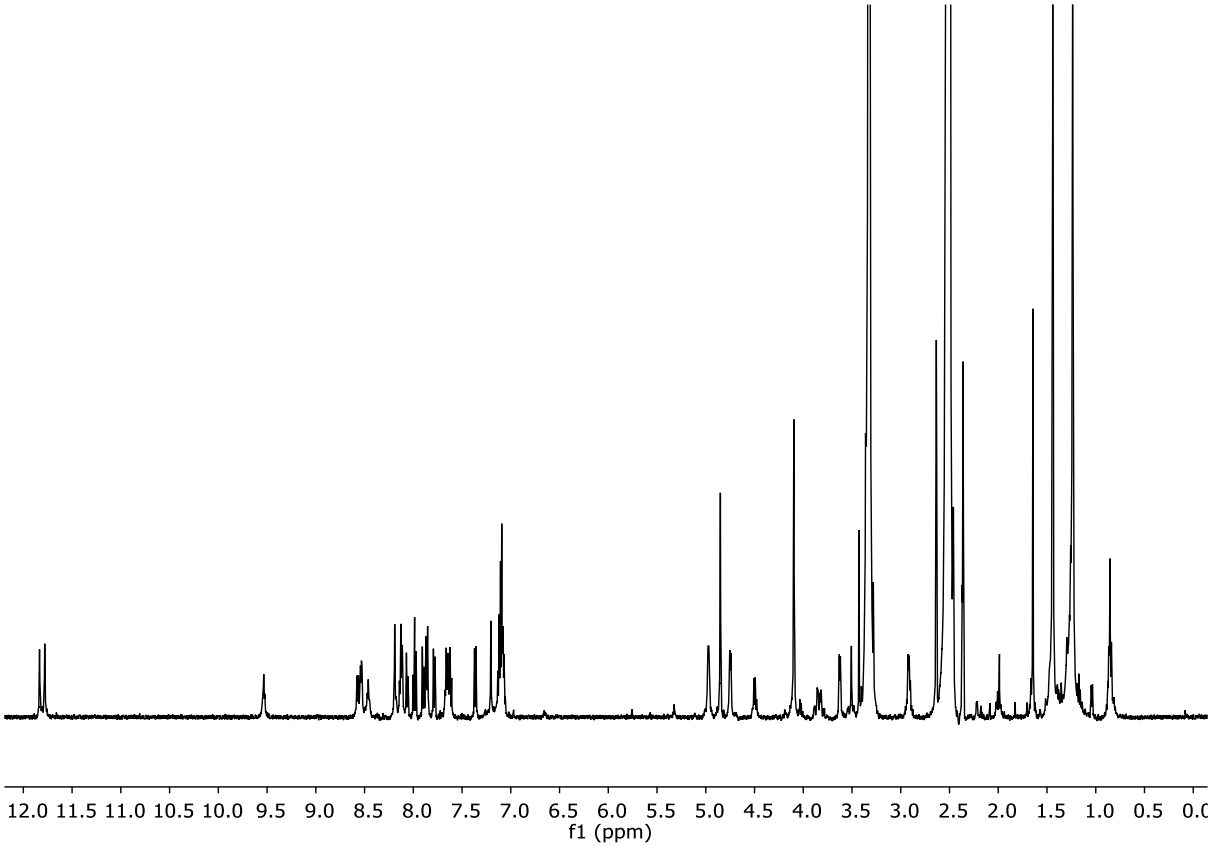

^{1}H NMR spectrum (500 MHz, $CDCl_3$, 25 °C) of **5b**.

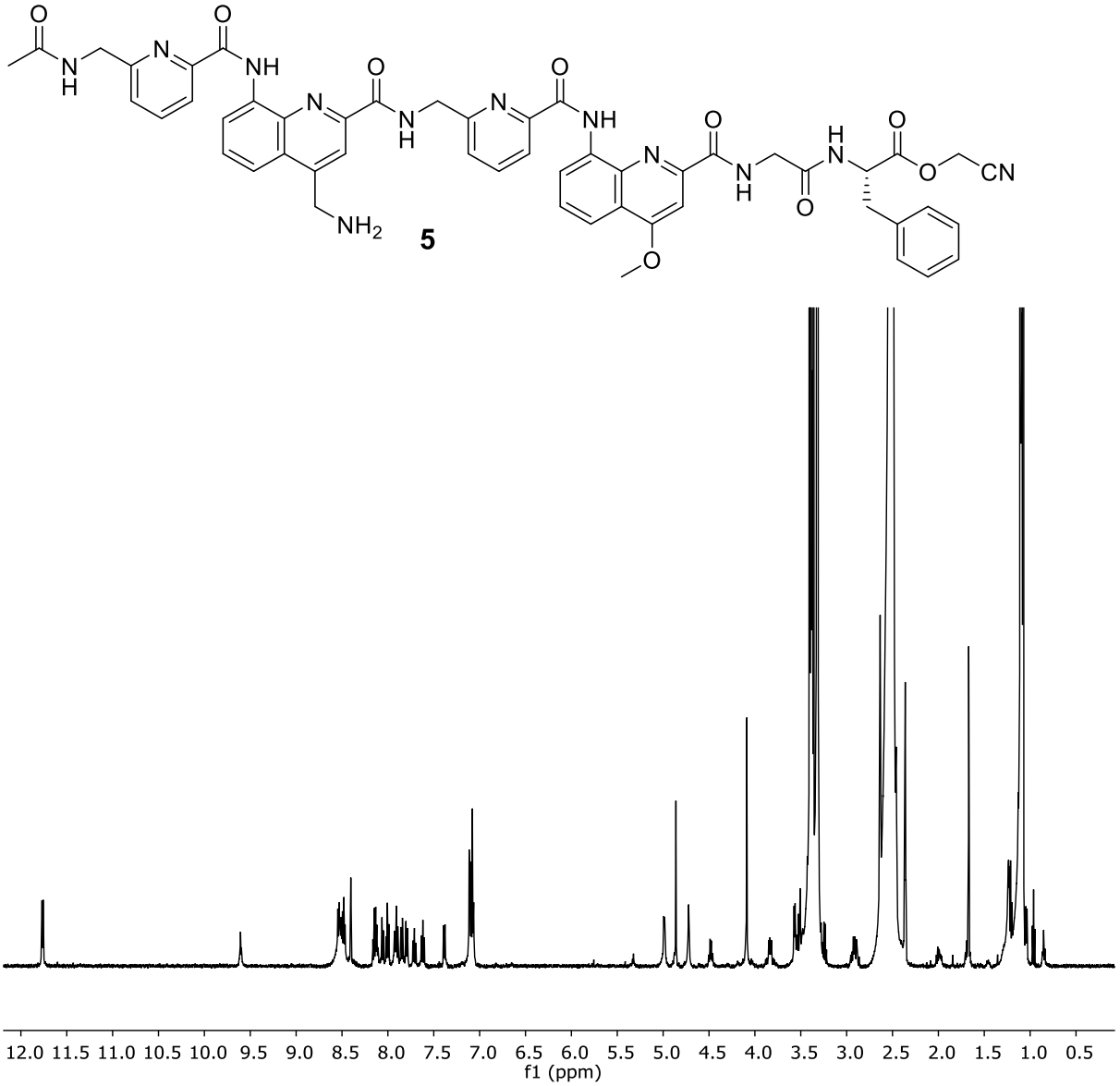

^{1}H NMR spectrum (500 MHz, DMSO-d_6, 25 °C) of **5**.

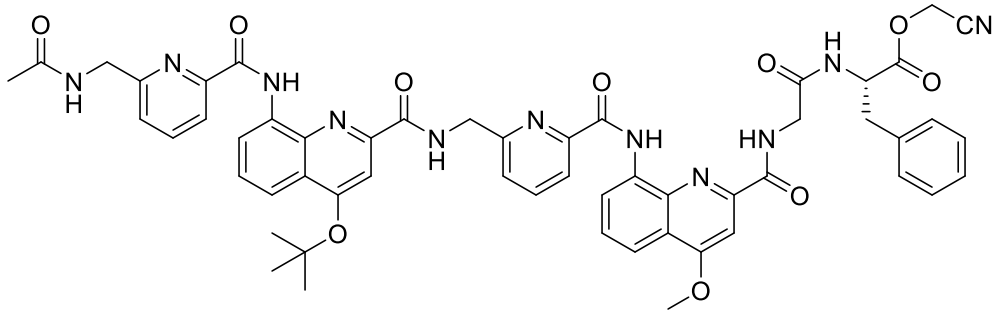

6b

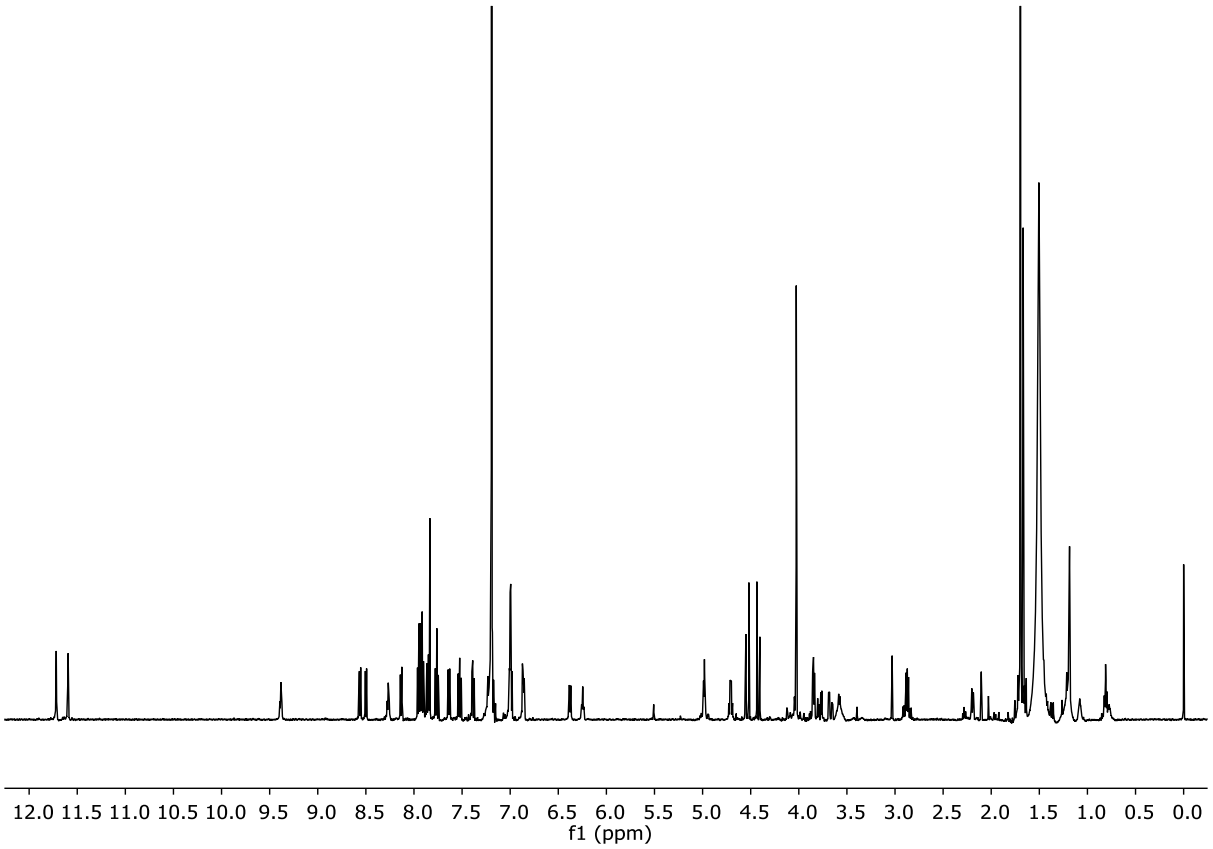

^{1}H NMR spectrum (500 MHz, $CDCl_3$, 25 °C) of **6b**.

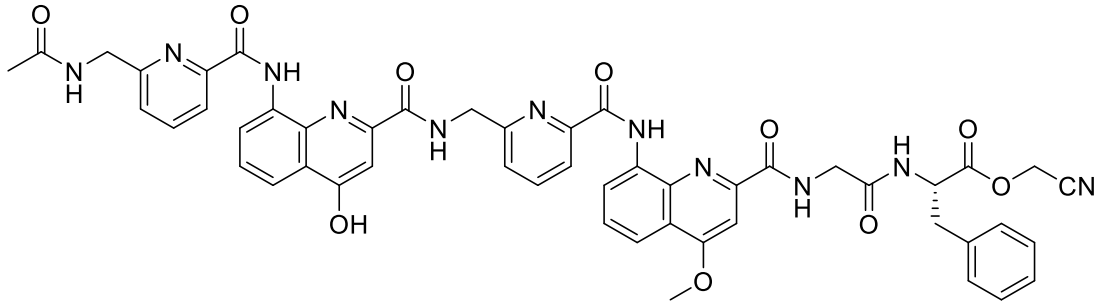

6

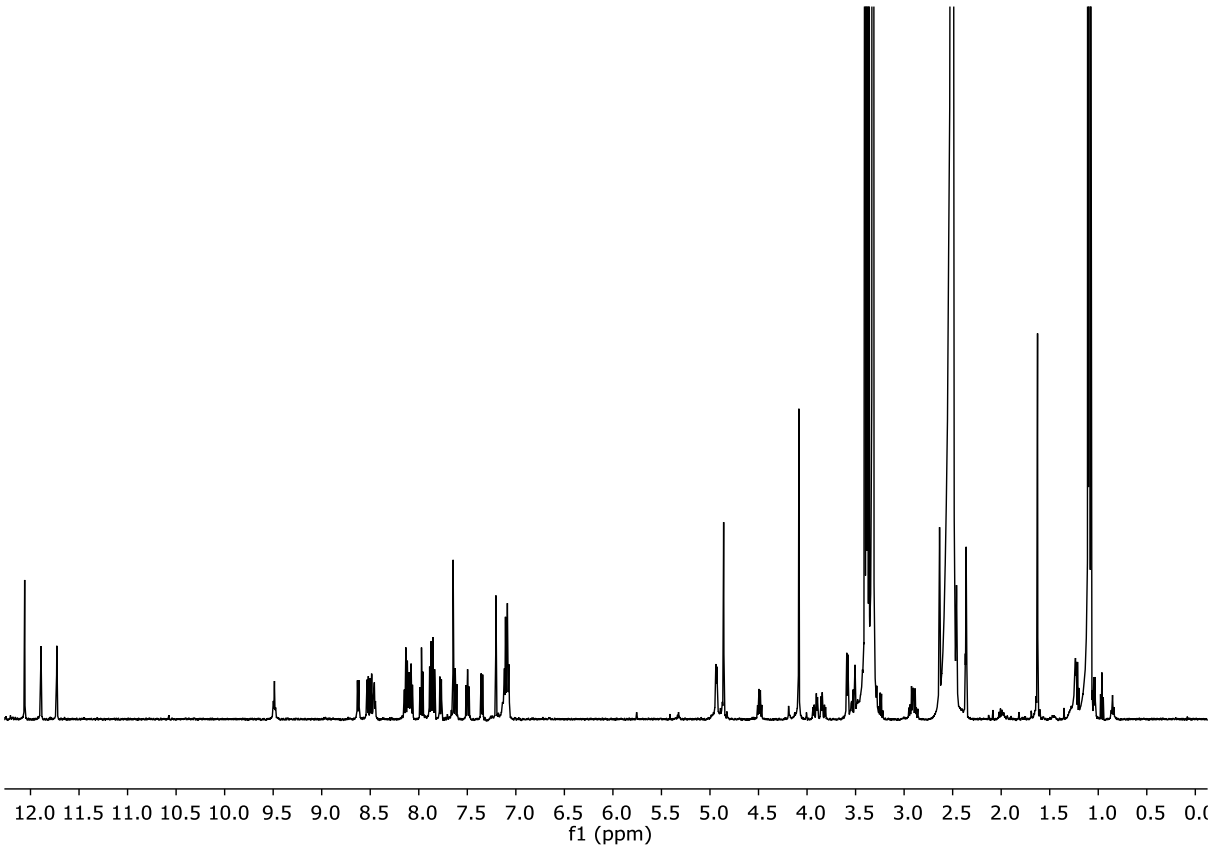

^{1}H NMR spectrum (500 MHz, DMSO-d_6, 25 °C) of **6**.

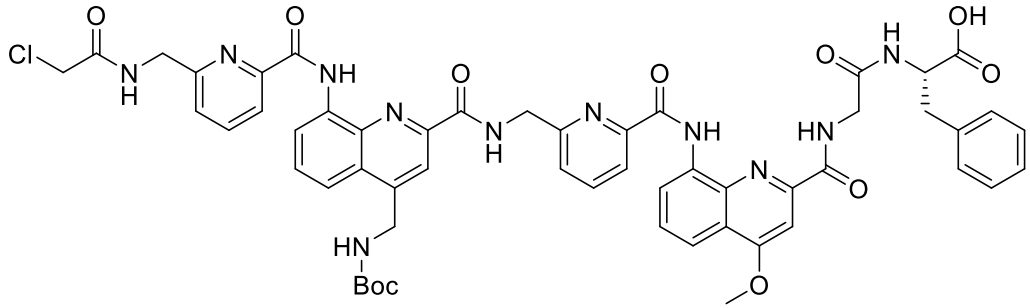

7a

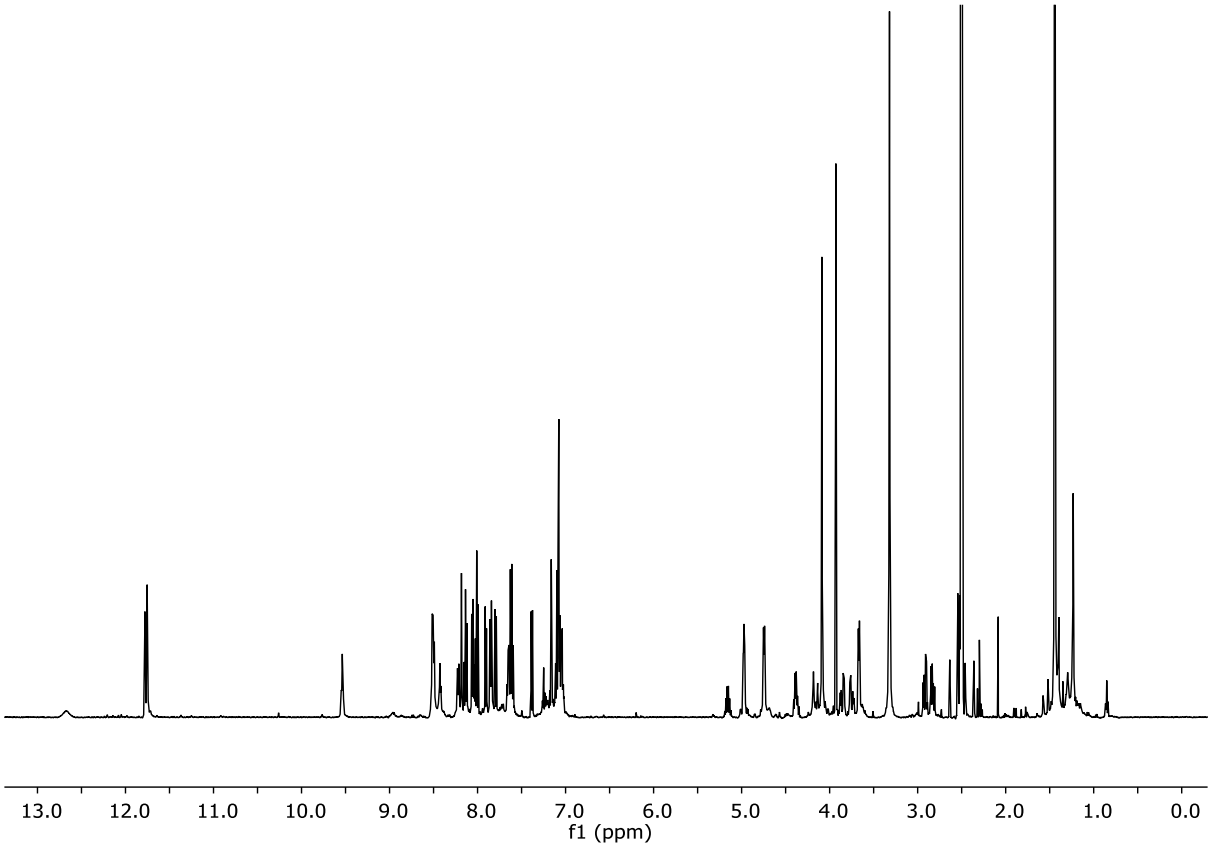

^{1}H NMR spectrum (500 MHz, DMSO-d_6, 25 °C) of **7a**.

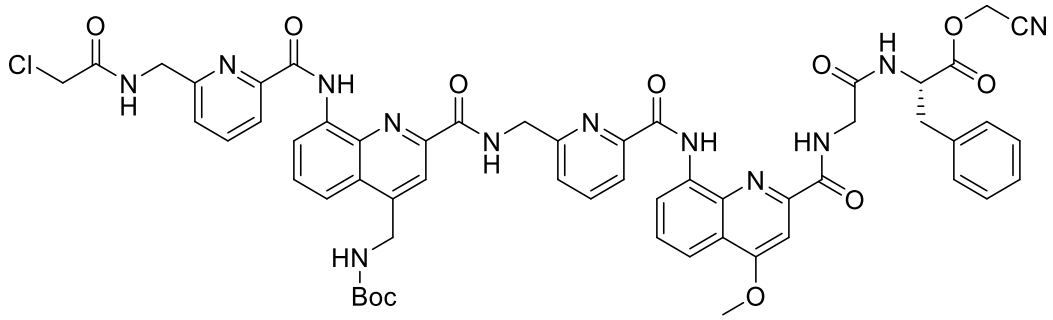

7b

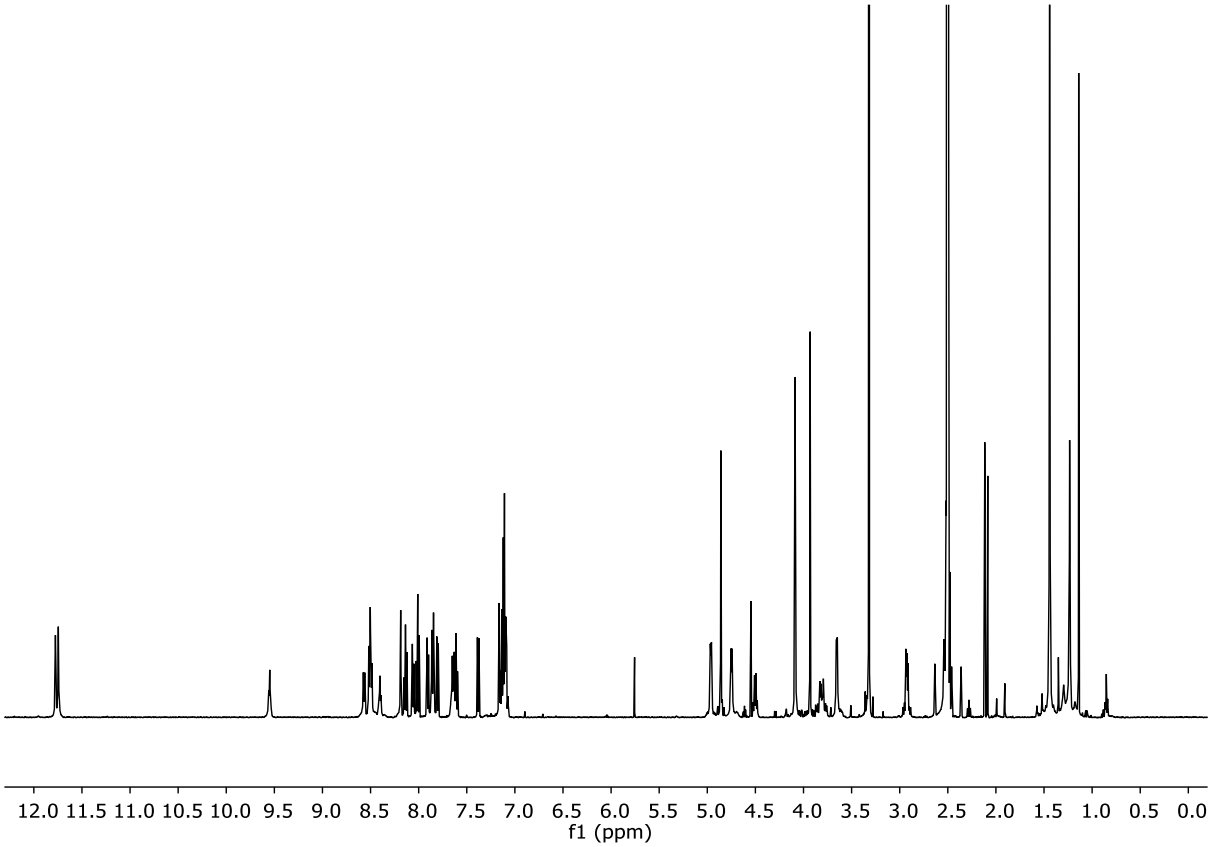

^{1}H NMR spectrum (500 MHz, DMSO-d_6, 25 °C) of **7b**.

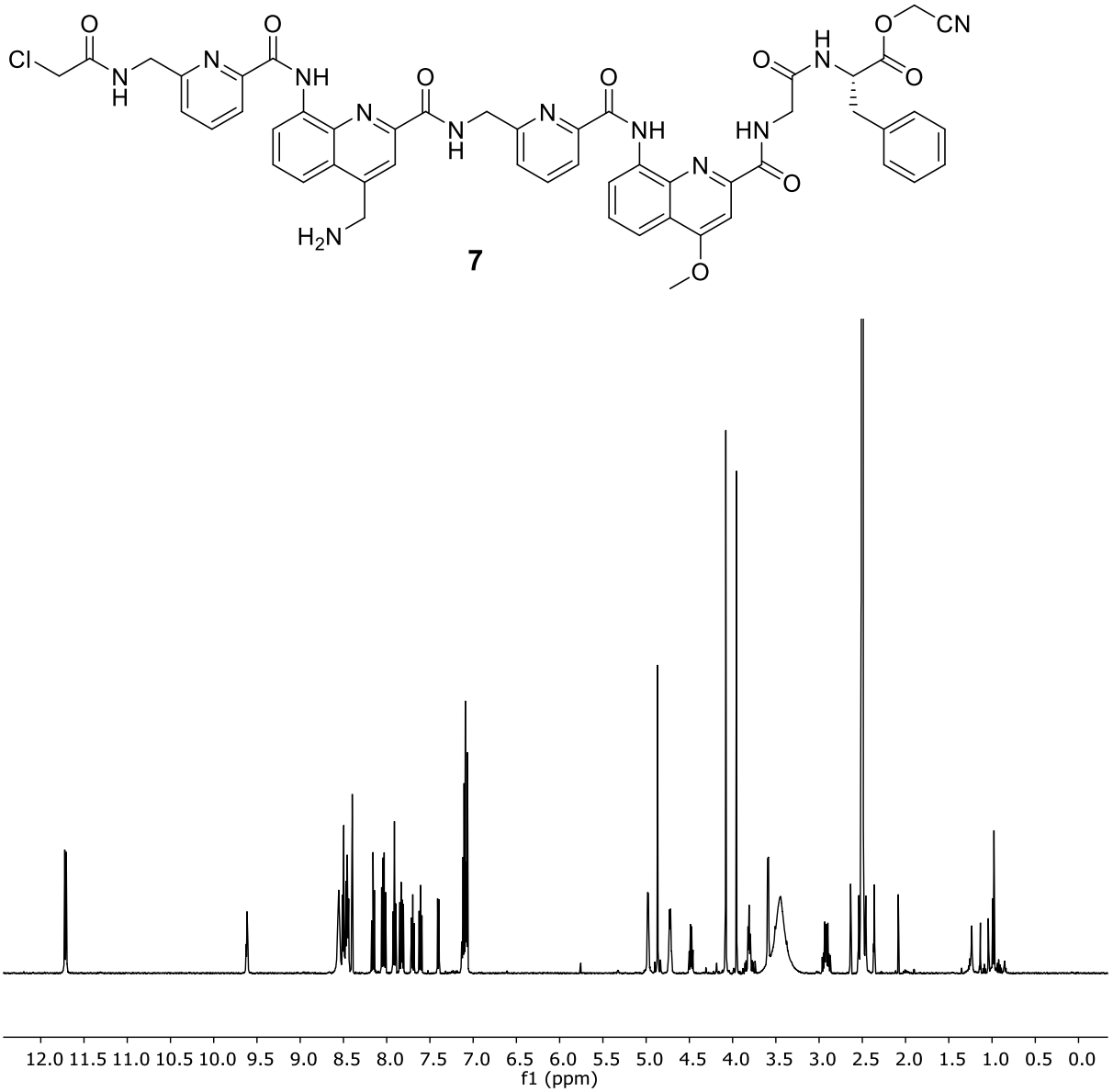

^{1}H NMR spectrum (500 MHz, DMSO-d_6, 25 °C) of **7**.

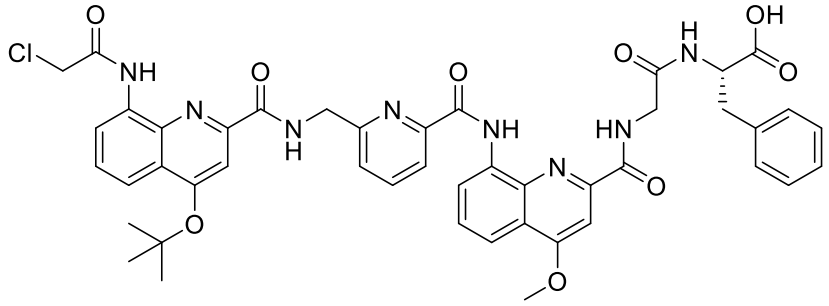

8a

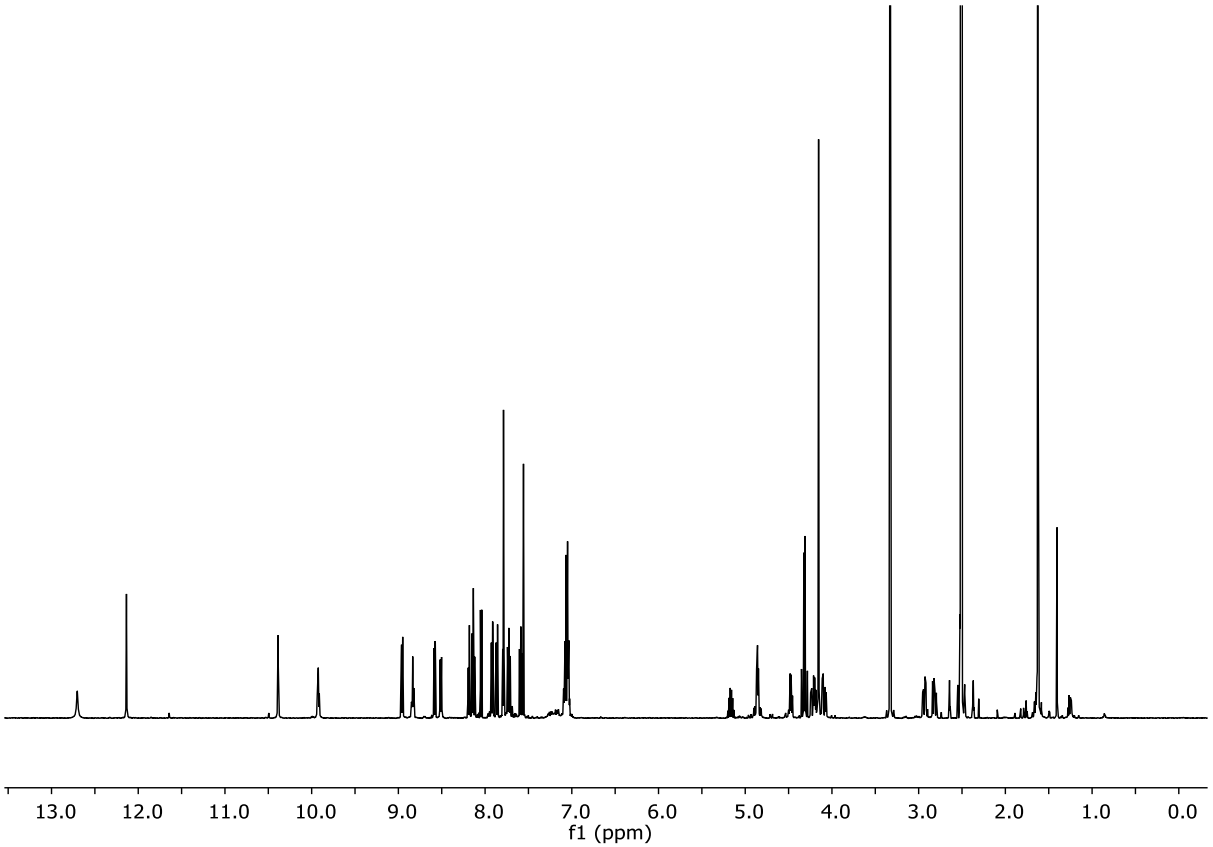

^{1}H NMR spectrum (500 MHz, DMSO-d_6, 25 °C) of **8a**.

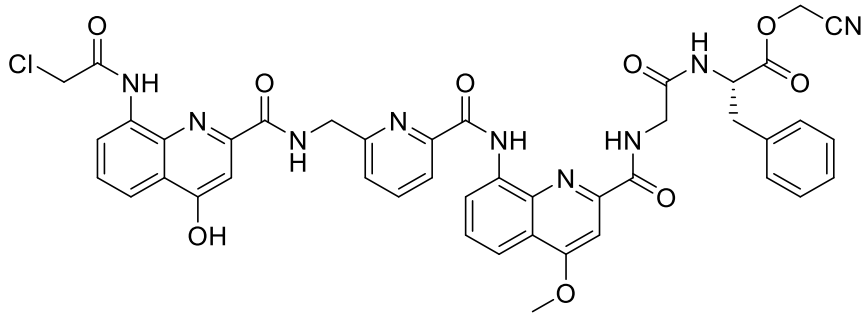

8

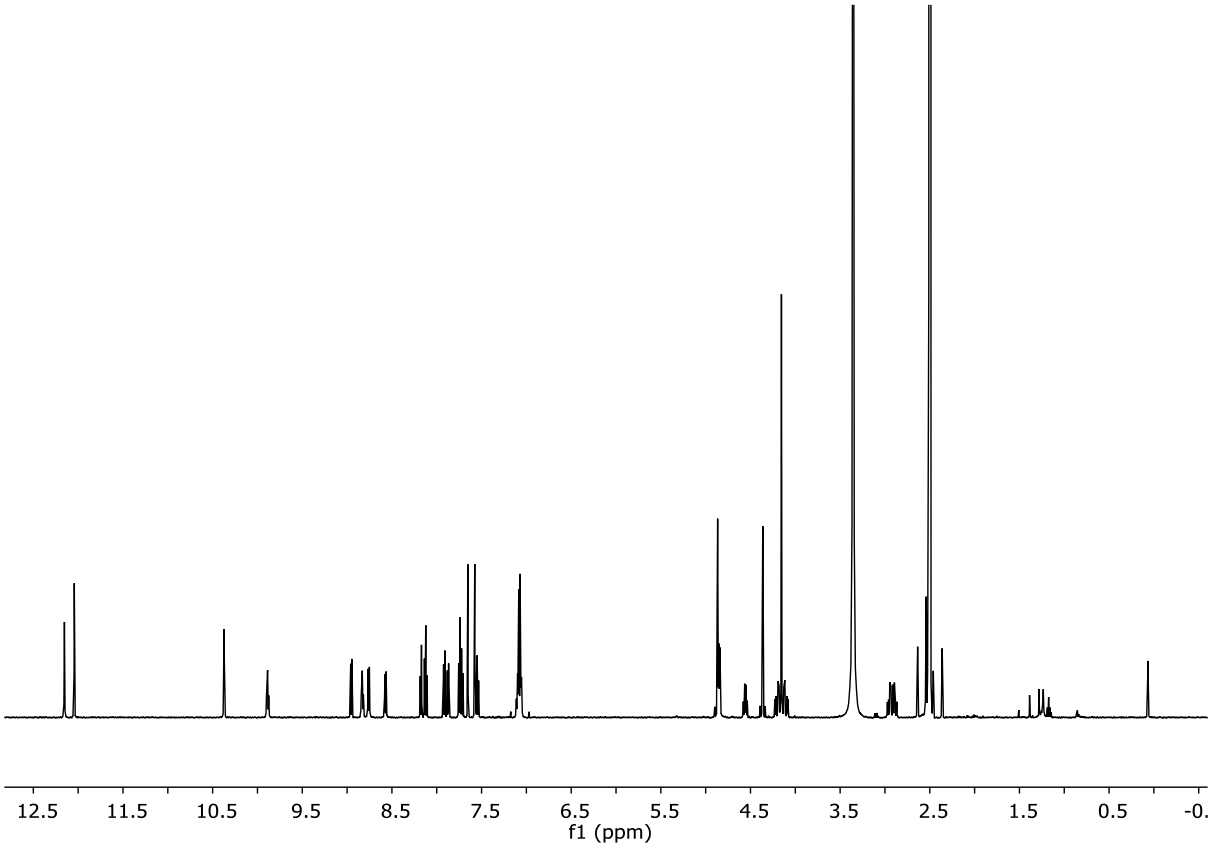

^{1}H NMR spectrum (500 MHz, DMSO-d_6, 25 °C) of **8**.

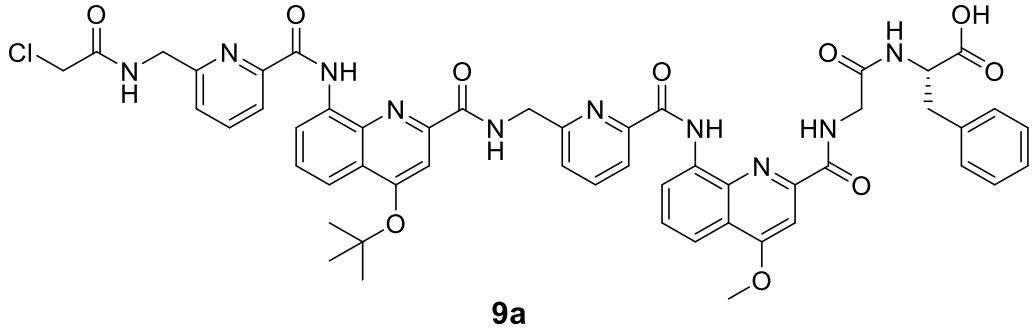

9a

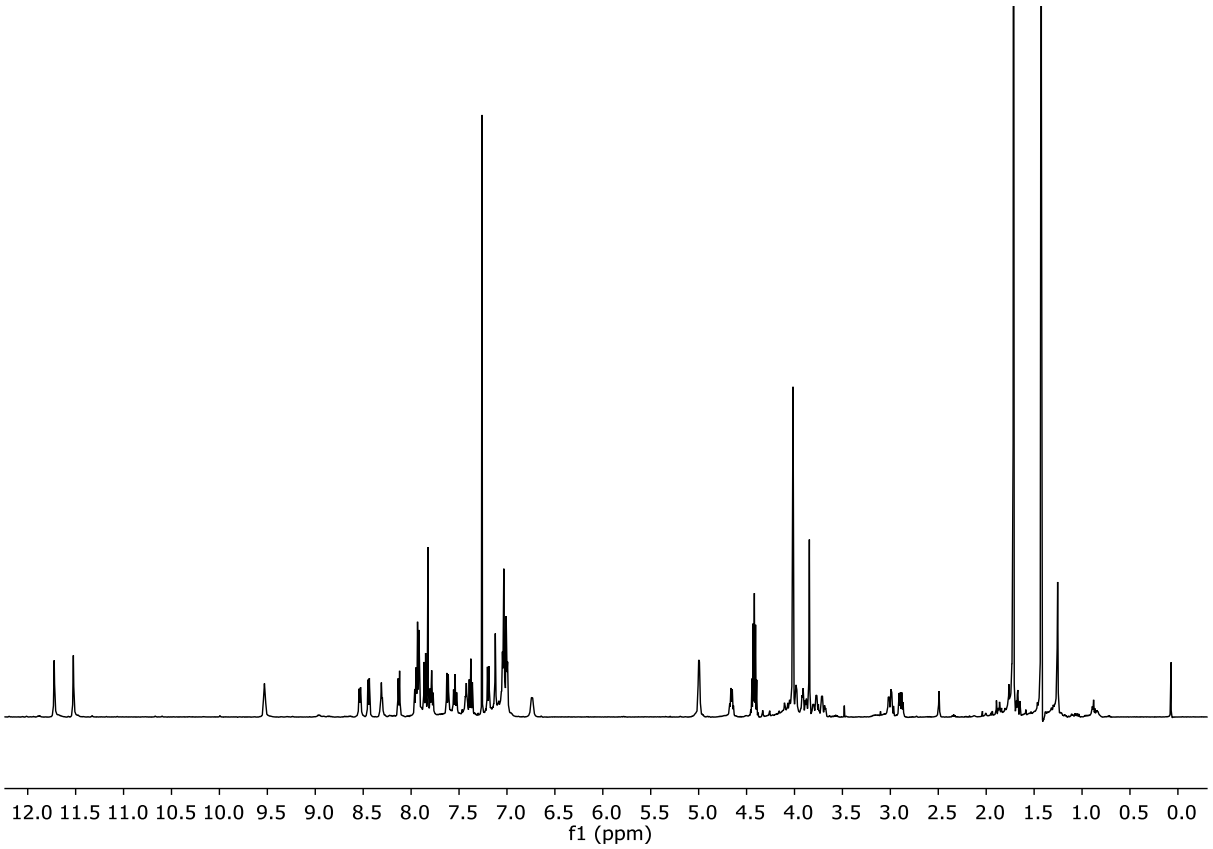

^{1}H NMR spectrum (500 MHz, $CDCl_3$, 25 °C) of **9a.**

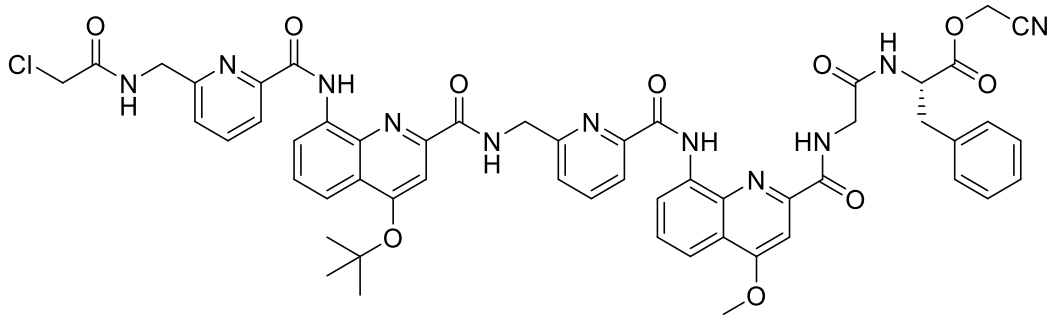

9b

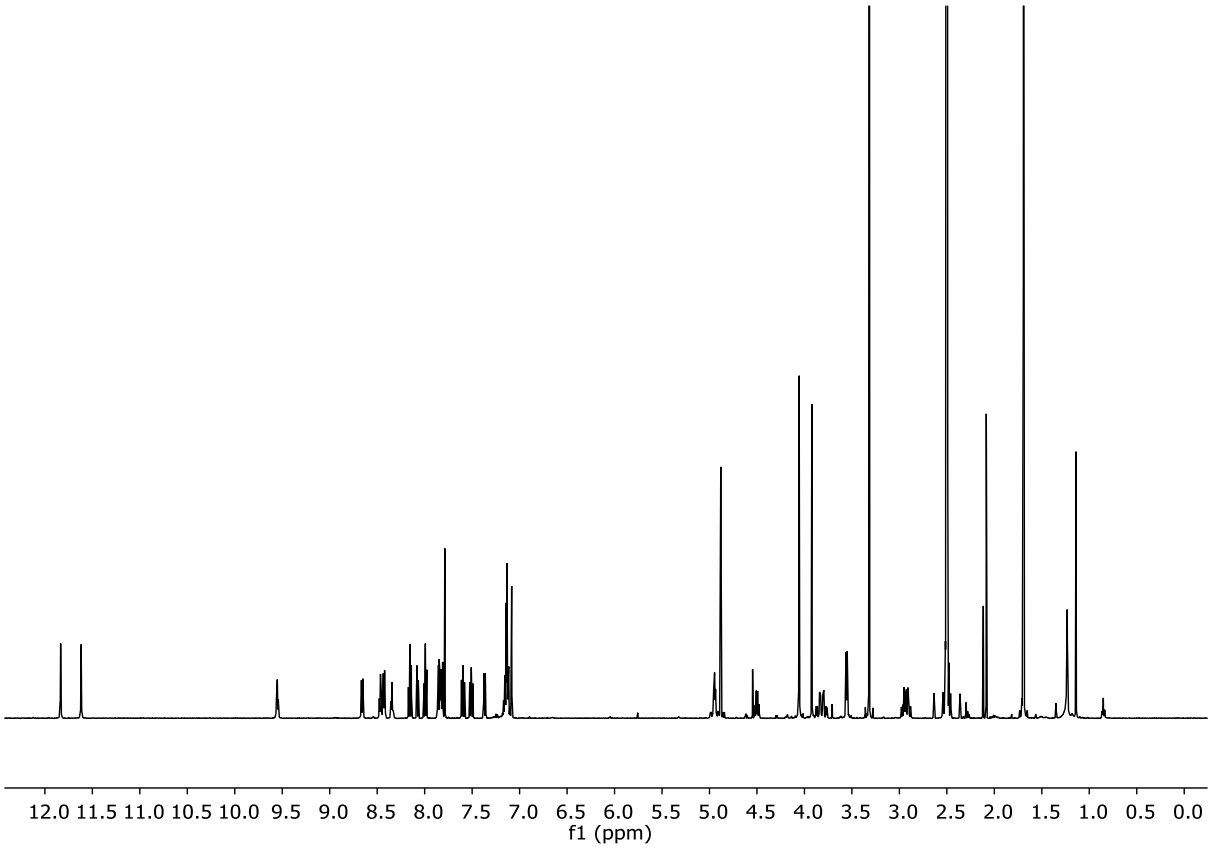

^{1}H NMR spectrum (500 MHz, DMSO-d_6, 25 °C) of **9b**.

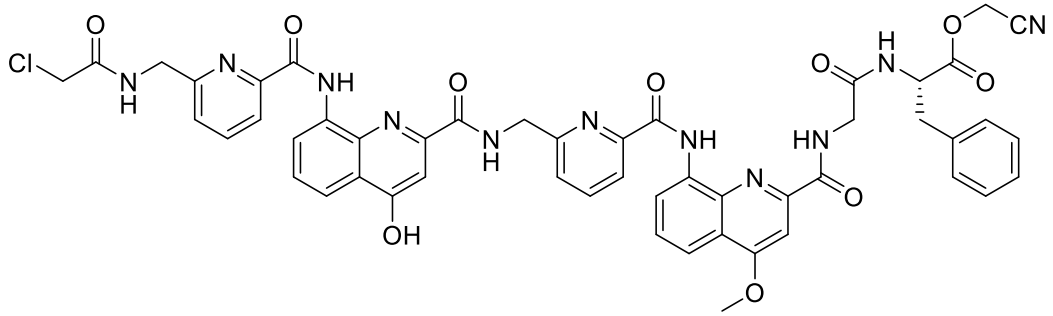

9

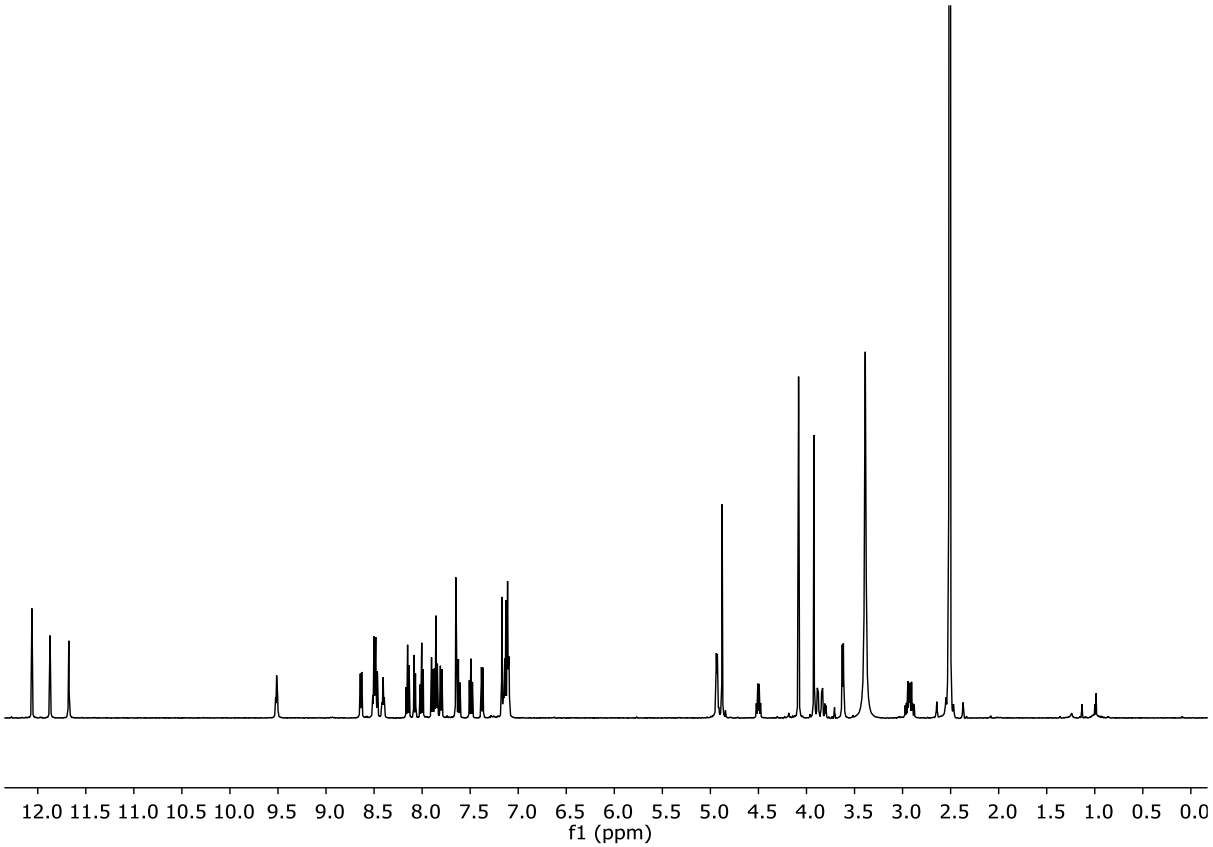

^{1}H NMR spectrum (500 MHz, DMSO-d_6, 25 °C) of **9.**

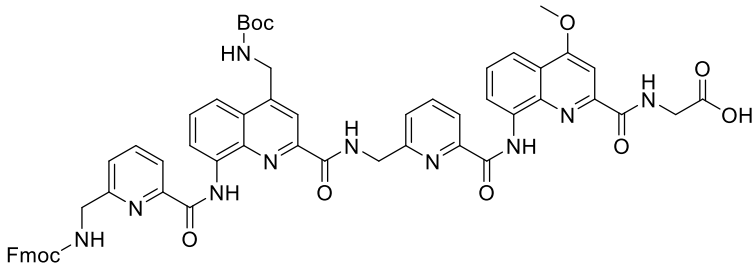

F10

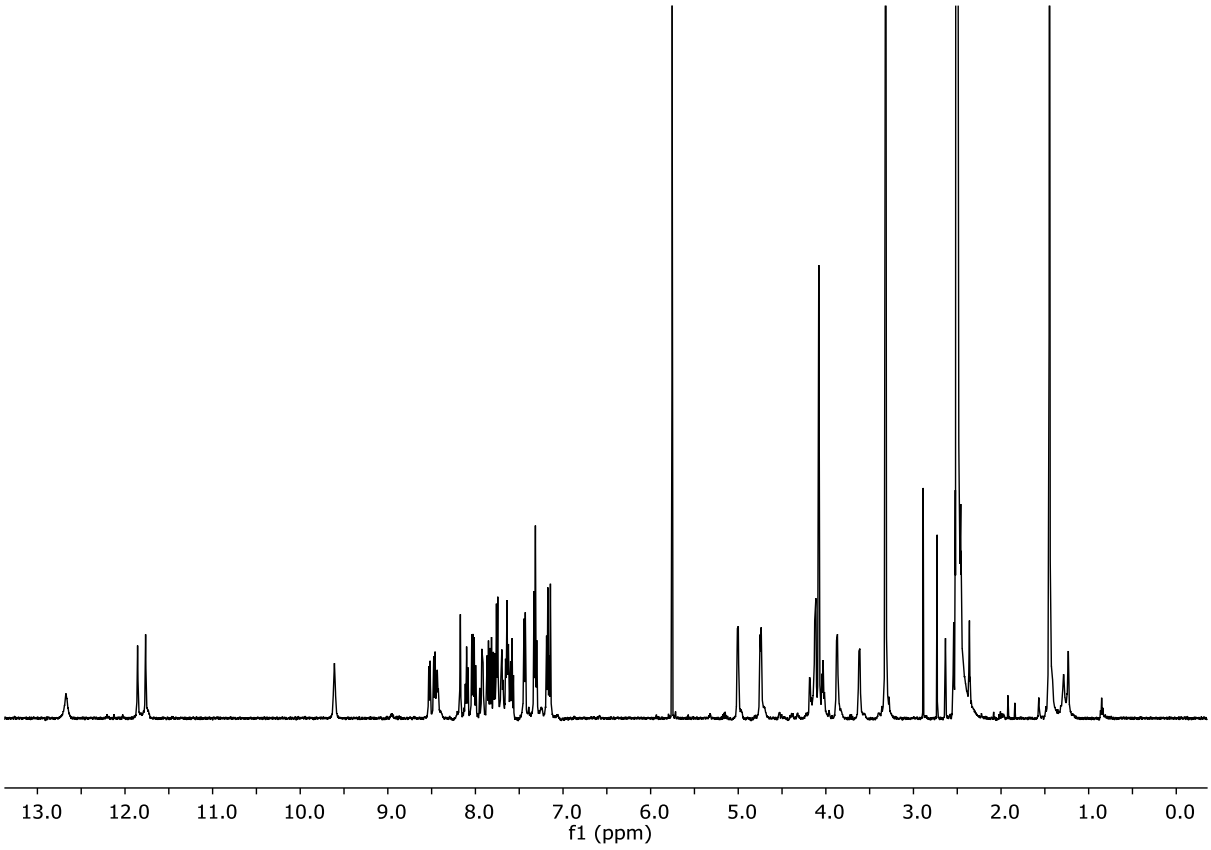

^{1}H NMR spectrum (500 MHz, DMSO-d_6, 25 °C) of **F10**.

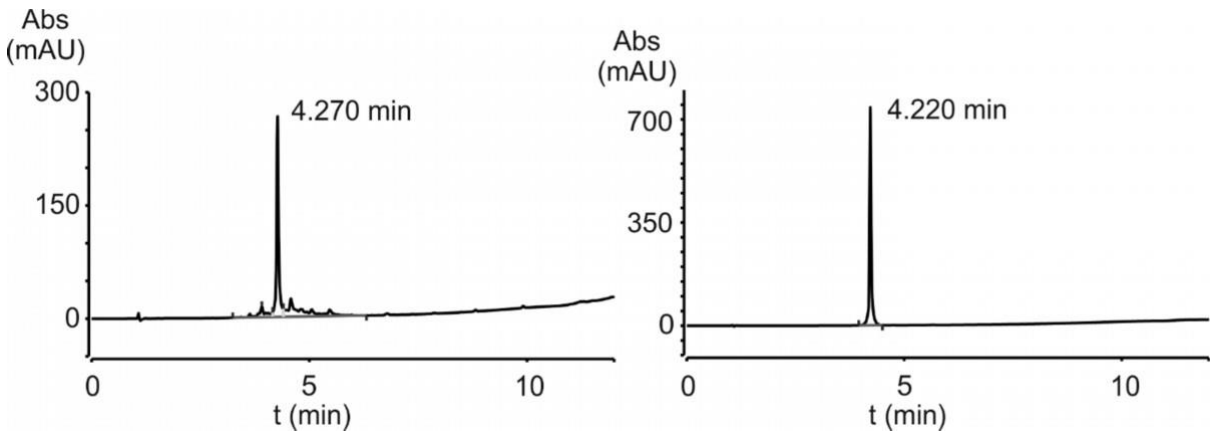

Analytical RP-HPLC profiles of **10** as a crude (left) and purified (right). HPLC gradient: 5-100% of B in 10 min 50 °C, λ = 254 nm).

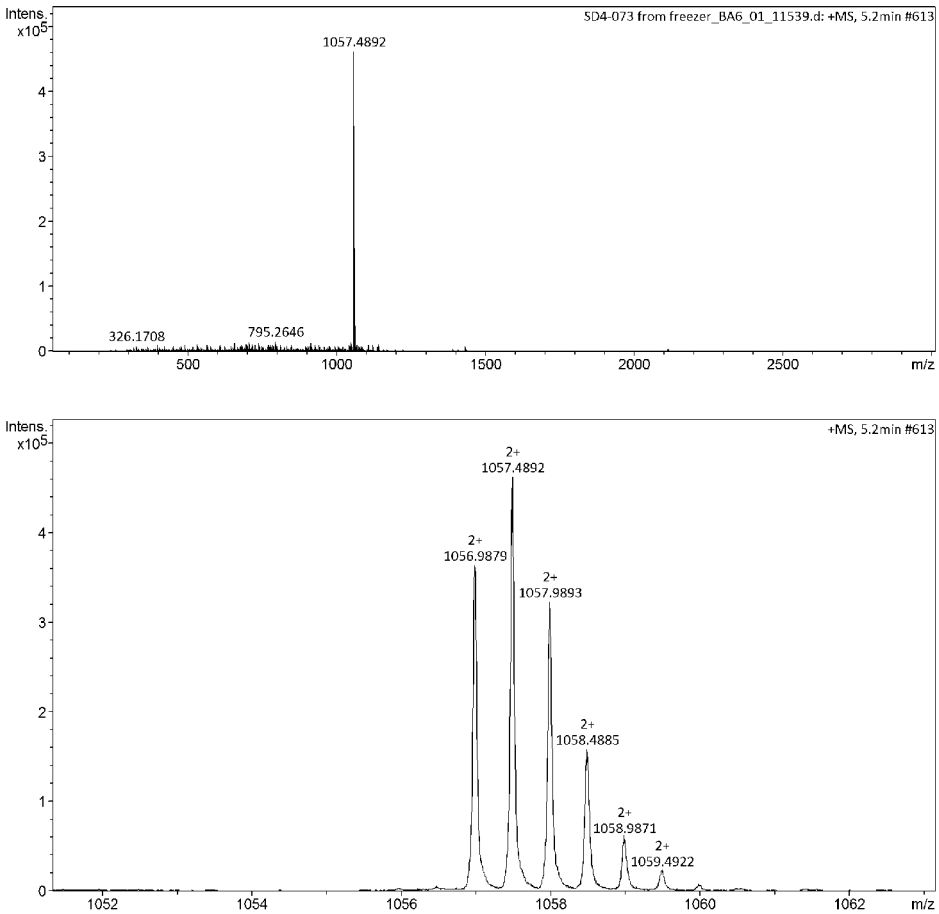

HRMS spectra of compound **10**

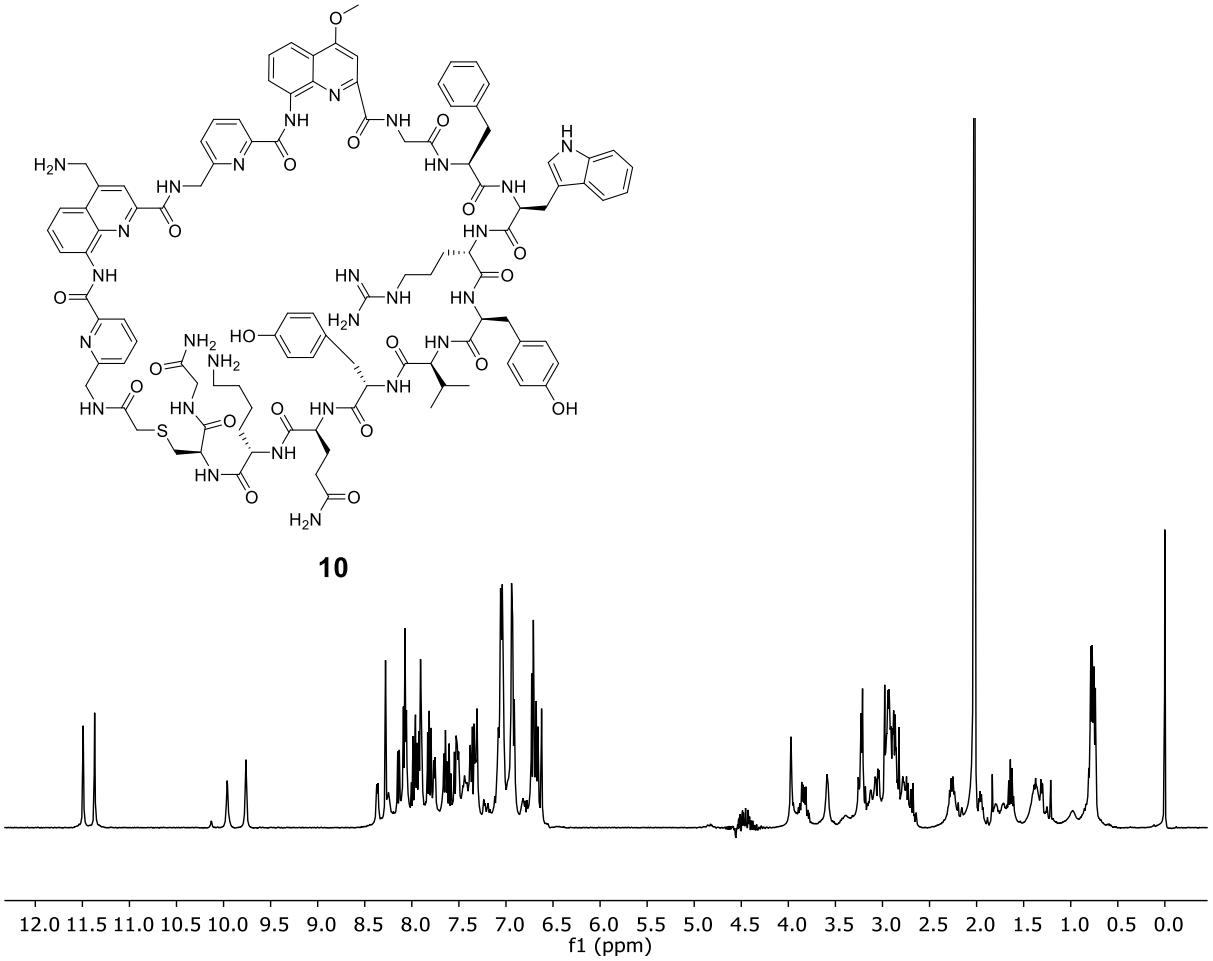

^{1}H NMR spectrum (500 MHz, water with 25% (v/v) acetonitrile-d_3, water supression, 25 °C) of **10**.

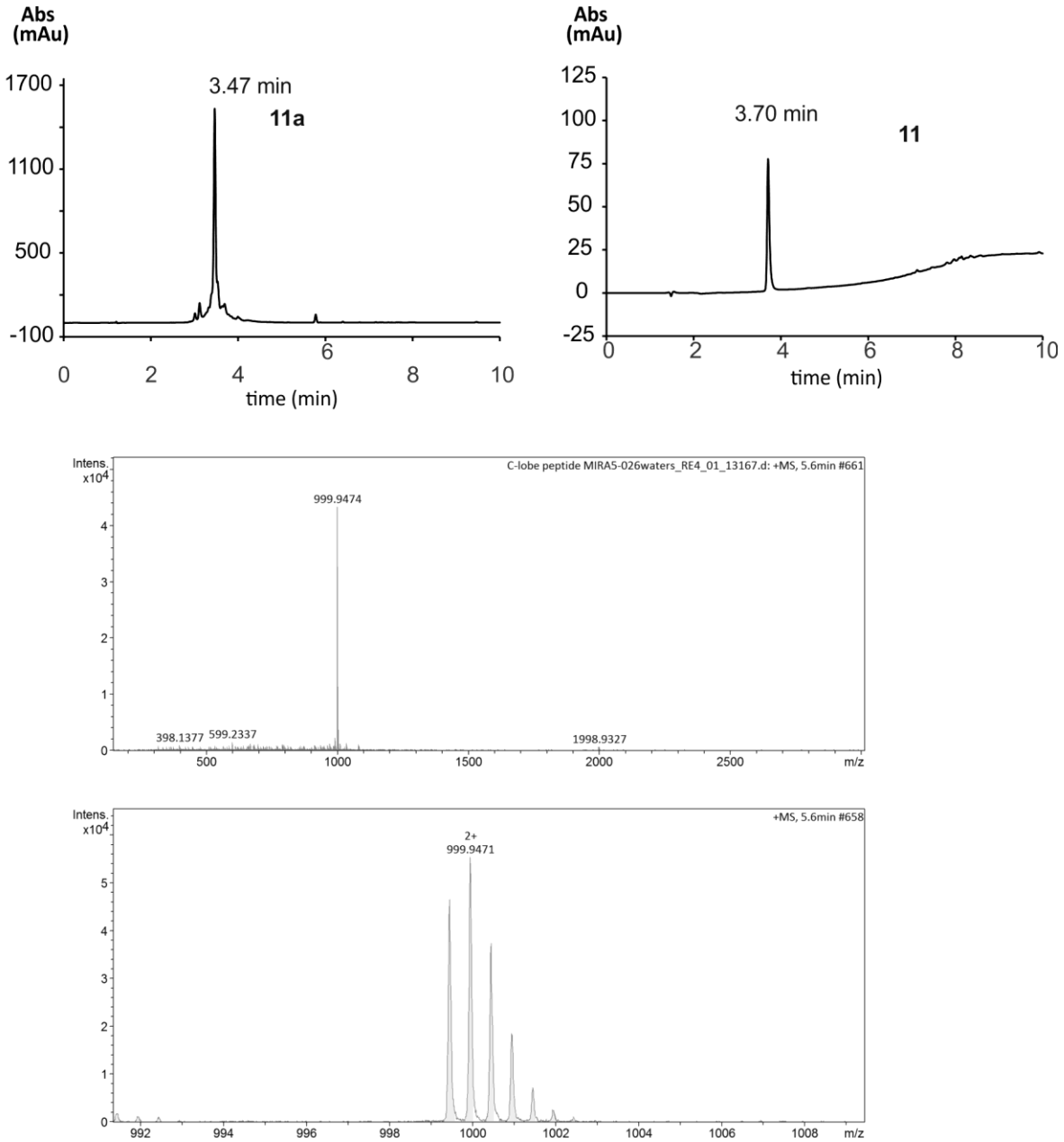

Analytical RP-HPLC profiles of linear foldamer peptide **11a** as a crude (left, HPLC gradient: 5-100% of B in 7 min, 50 °C, λ = 254 nm) and purified macrocycle**11** (right, HPLC gradient: 5-100% of B in 10 min, 50 °C, λ = 254 nm). HRMS spectra of the pure **11** macrocycle.

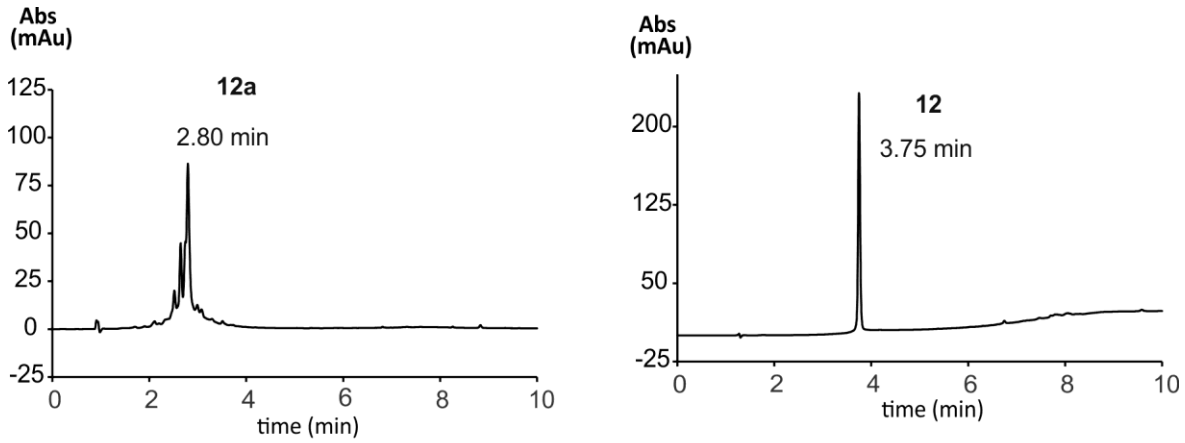

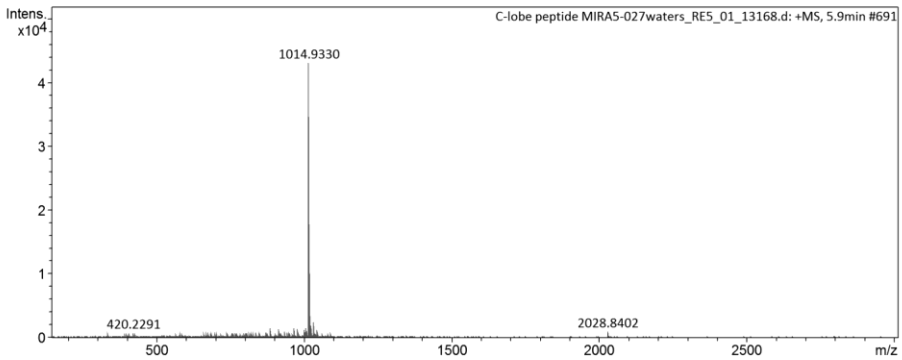

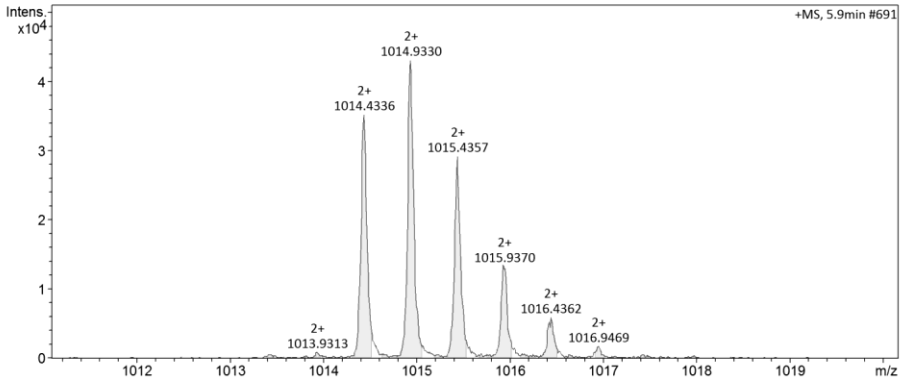

Analytical RP-HPLC profiles of linear foldamer peptide **12a** as a crude (left, HPLC gradient: 5-100% of B in 7 min, 50 °C, λ = 254 nm) and purified macrocycle **12** (right, HPLC gradient: 5-100% of B in 10 min, 50 °C, λ = 254 nm). HRMS spectra of the pure **12** macrocycle.

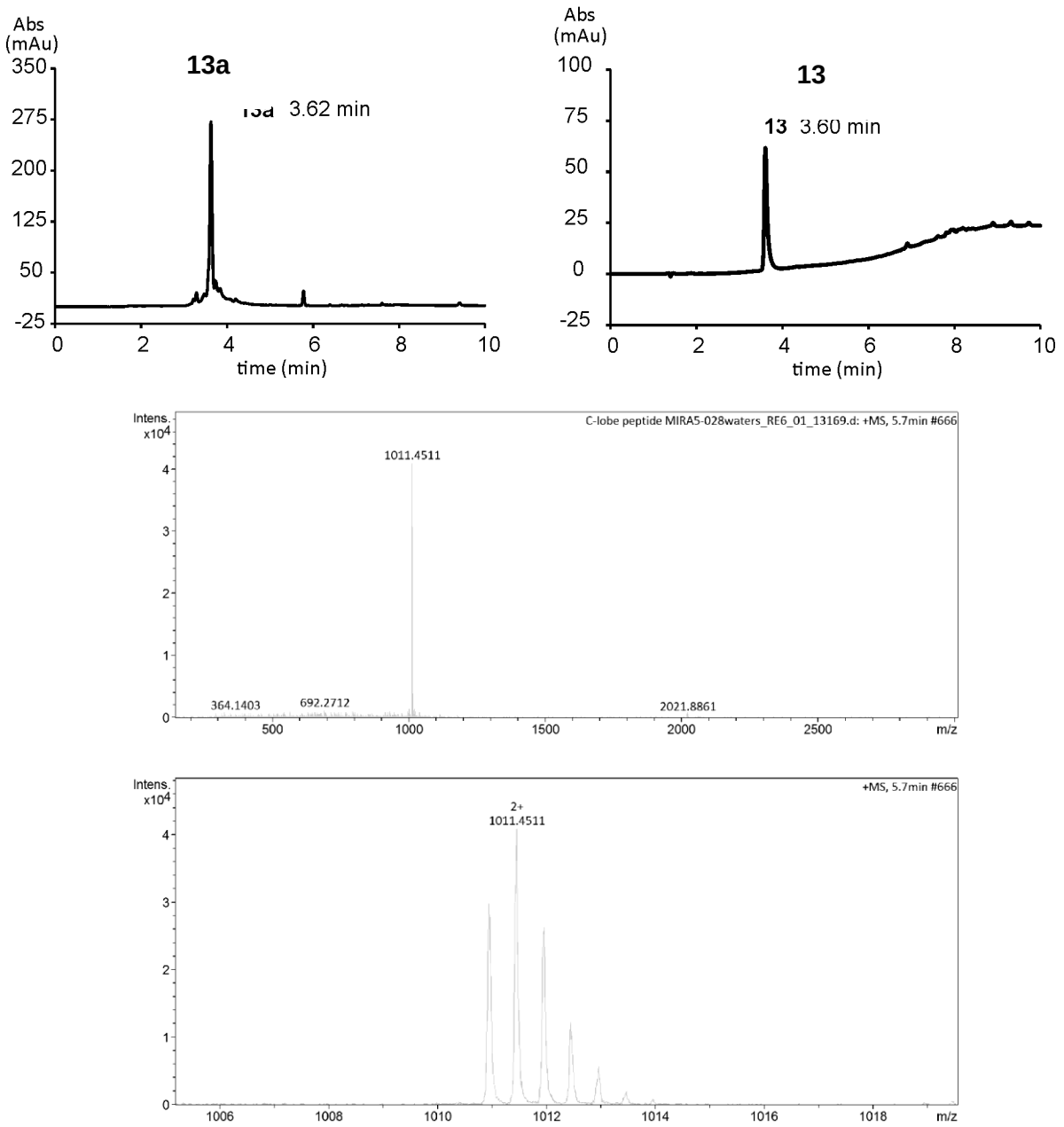

Analytical RP-HPLC profiles of linear foldamer peptide **13a** as a crude (left) and purified macrocycle **13** (right)**.** RP-HPLC gradient: 10–100% (v/v) B over 10 min, 50 °C, λ = 254 nm). HRMS spectra of the pure **13** macrocycle.

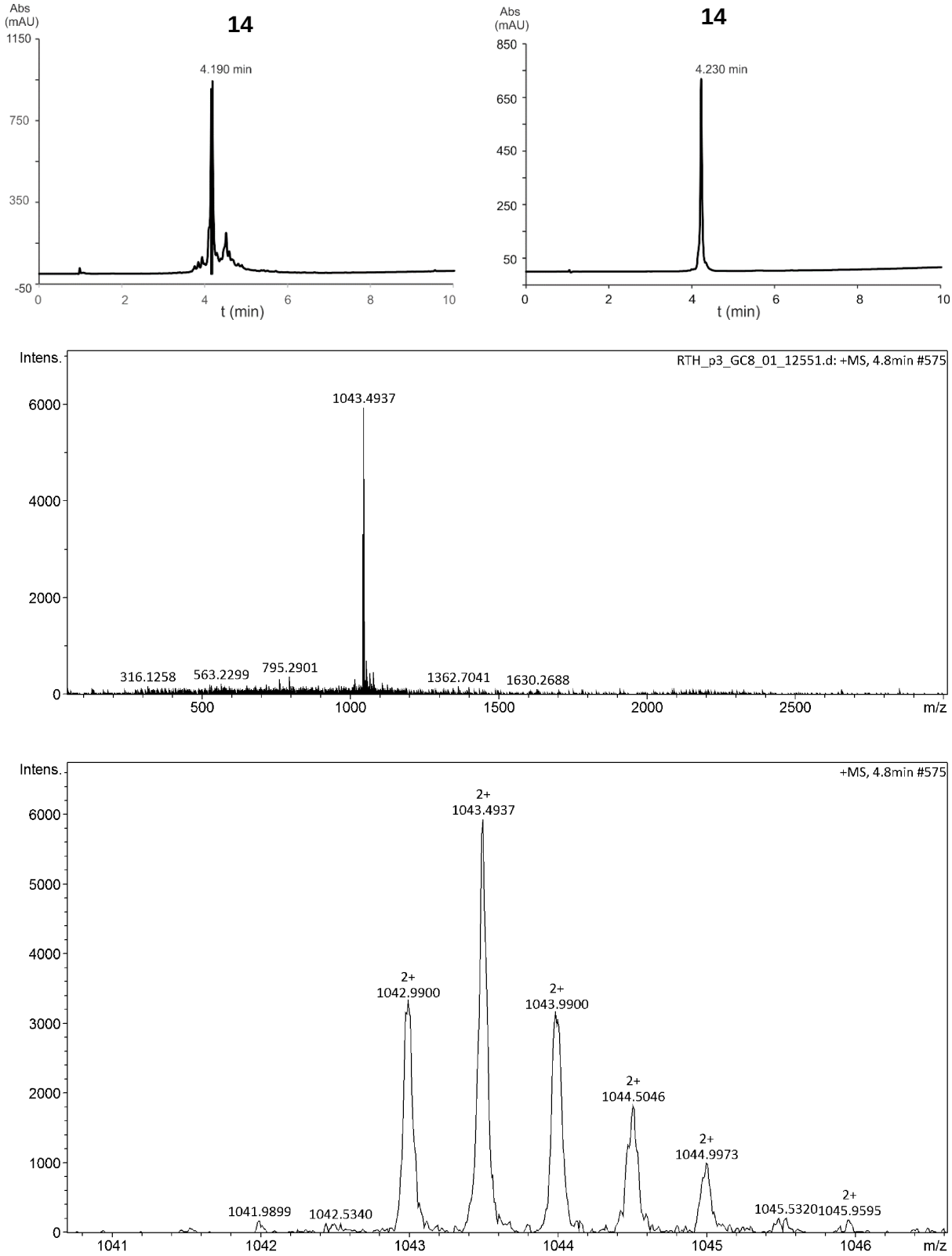

Analytical RP-HPLC profiles of **14** as a crude (left) and purified (right). RP-HPLC gradient: 10–100% (v/v) B over 10 min, 50 °C, λ = 254 nm). HRMS spectra of compound **14**.

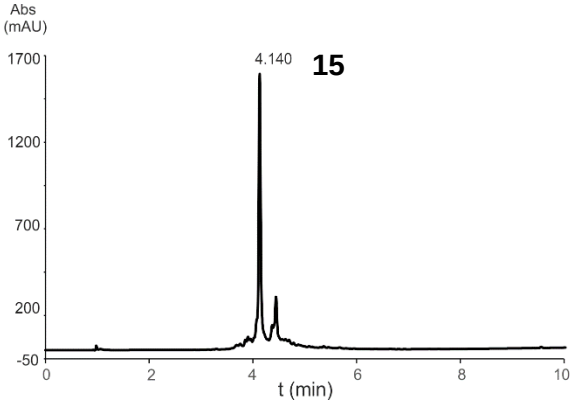

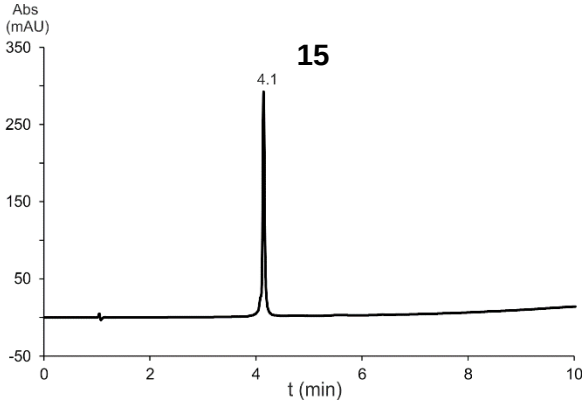

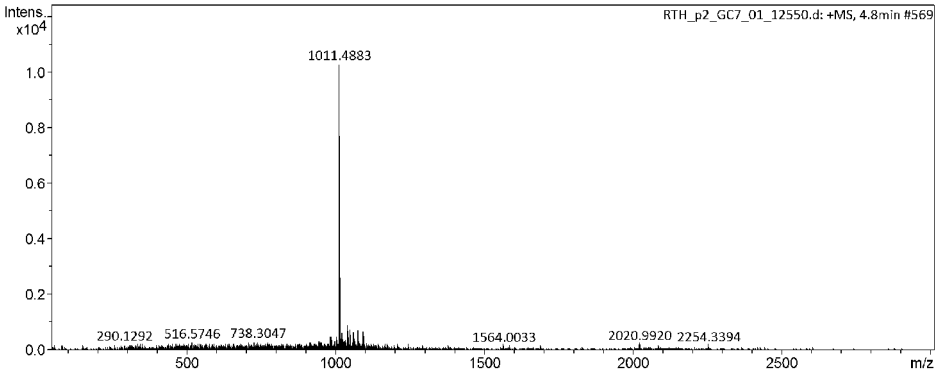

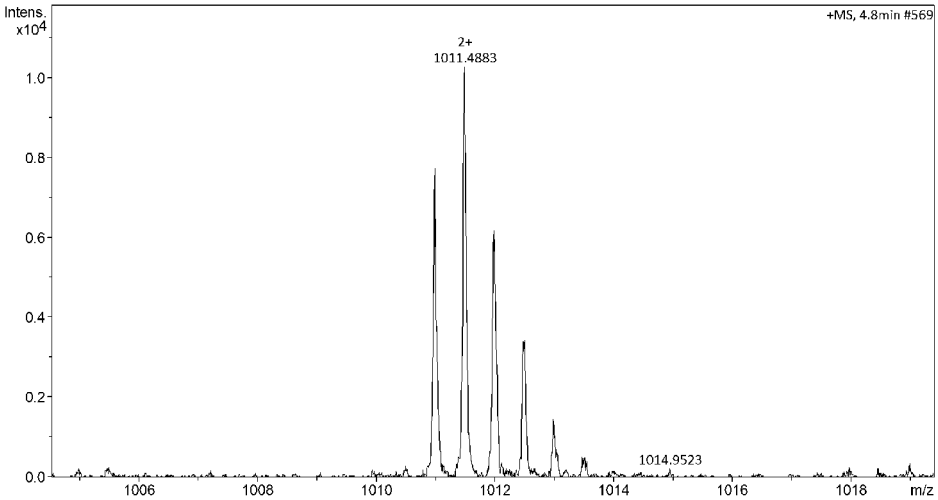

Analytical RP-HPLC profiles of **15** as a crude (left) and purified (right). RP-HPLC gradient: 10–100% (v/v) B over 10min, 50 °C, λ = 254 nm. HRMS spectra of compound **15.**

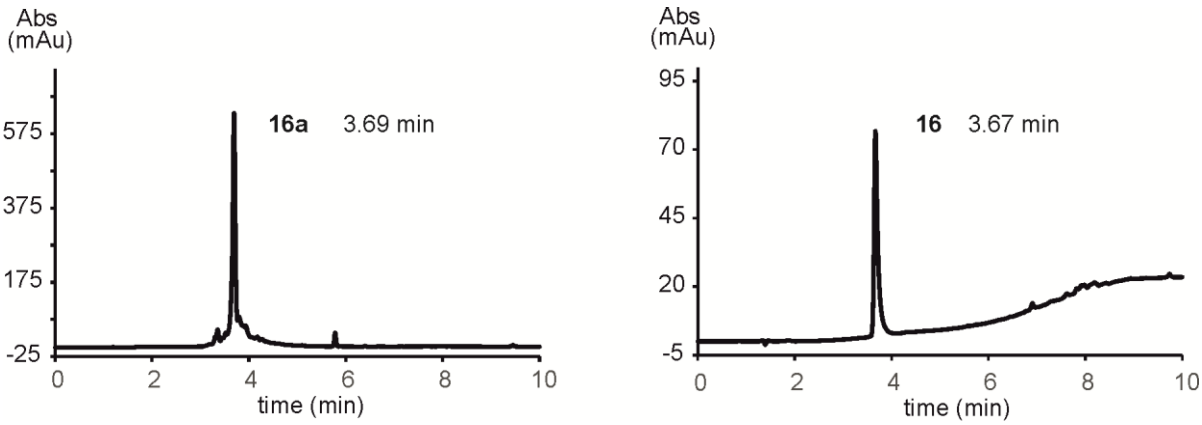

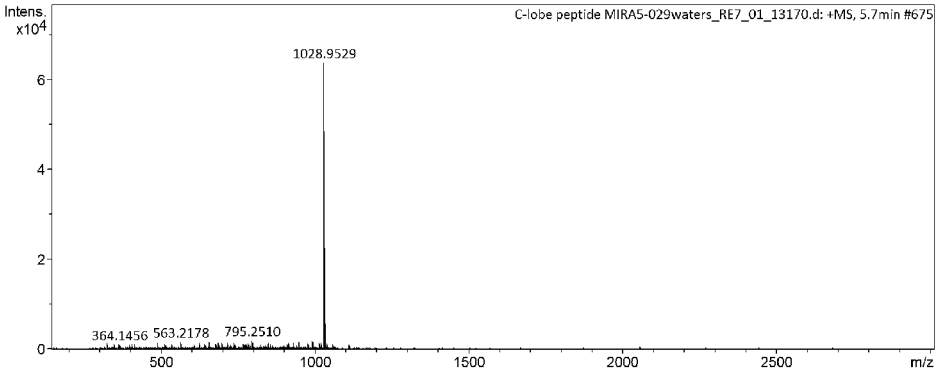

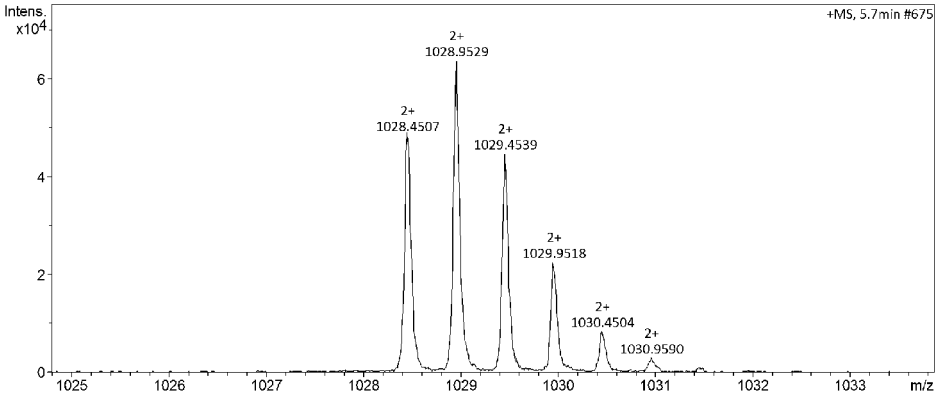

Analytical RP-HPLC profiles of linear foldamer peptide hybrid **16a** as a crude (left) and purified macrocycle **16** (right). RP-HPLC gradient: 5–100% (v/v) B over 7 min, 50 °C, λ = 254 nm. HRMS spectra of compound **16.**

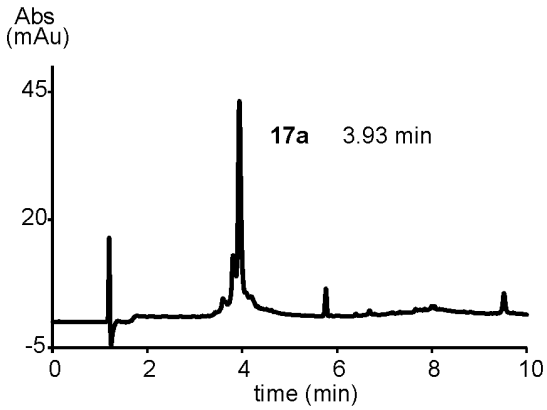

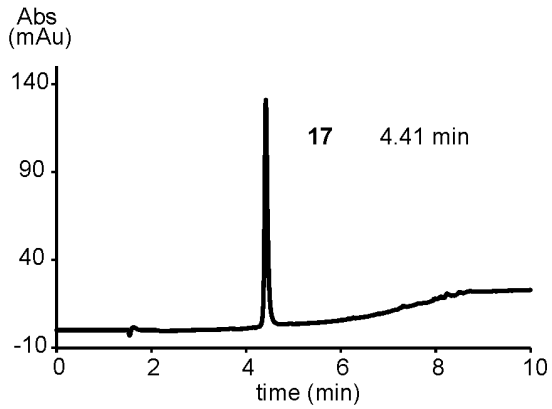

Analytical RP-HPLC profiles of linear foldamer peptide hybrid **17a** as a crude (left, RP-HPLC gradient: 5–100% (v/v) B over 7 min, 50 °C, λ = 254 nm) and purified macrocycle **17** (right, RP-HPLC gradient: 5–100% (v/v) B over 10 min, 50 °C, λ = 254 nm). HRMS spectra of compound **17**.

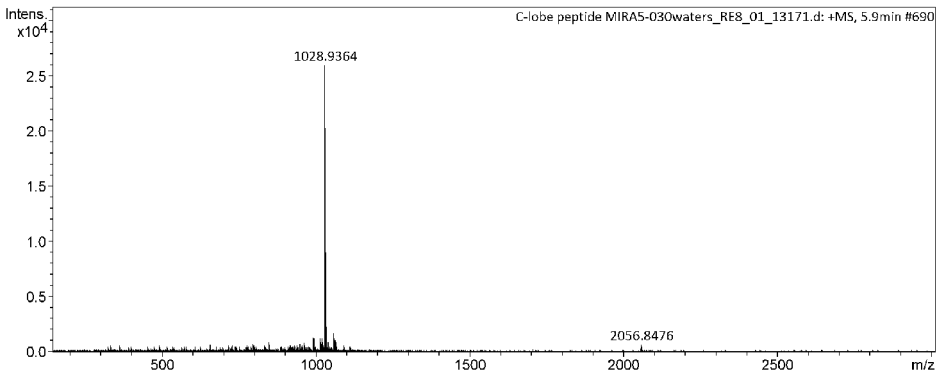

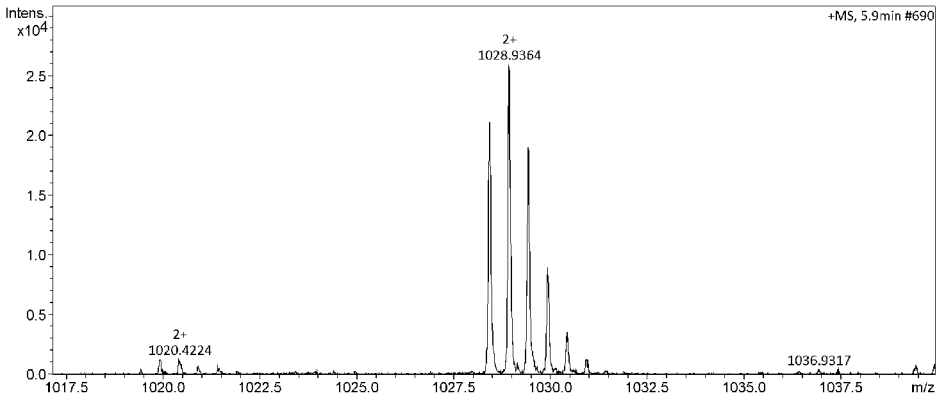

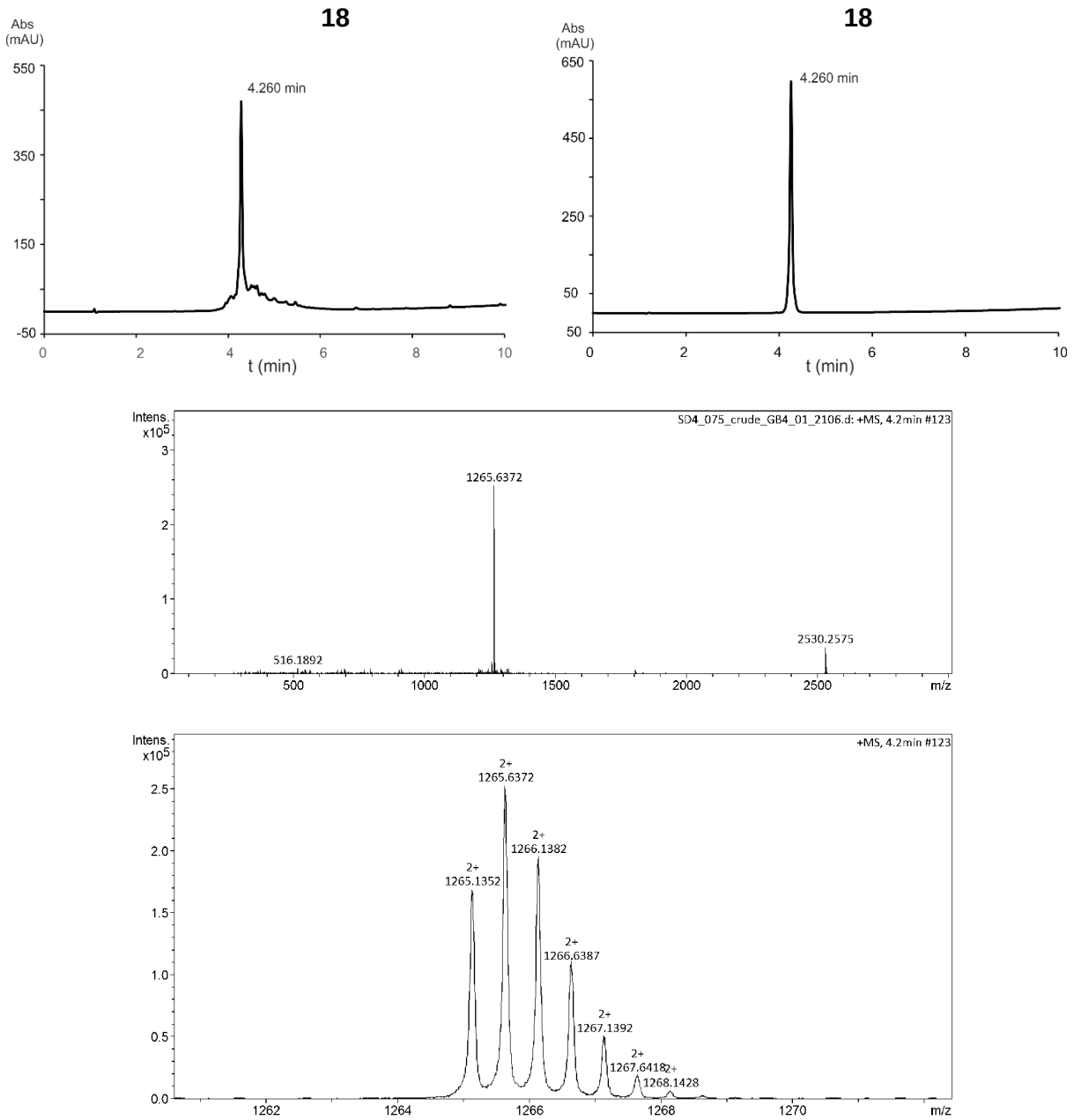

Analytical RP-HPLC profiles of **18** as a crude (left) and purified (right). RP-HPLC gradient: 10–100% (v/v) B over 10 min, 50 °C, λ = 254 nm). HRMS spectra of compound **18**

5. Supporting references

[22] A. C. Wallace, R. A. Laskowski, J. M. Thornton, *Protein Eng.* **1995**, *8*, 127–34.

[23] H. Murakami, A. Ohta, H. Ashigai, H. Suga, *Nat. Methods* **2006**, *3*, 357–359.

[24] Y. Goto, A. Ohta, Y. Sako, Y. Yamagishi, H. Murakami, H. Suga, *ACS Chem. Biol.* **2008**, *3*, 120–129.

[25] T. Katoh, I. Wohlgemuth, M. Nagano, M. V Rodnina, H. Suga, **2016**, DOI 10.1038/ncomms11657.

[26] T. Katoh, Y. Iwane, H. Suga, *Nucleic Acids Res.* **2017**, *45*, 12601–12610.

[27] Y. Hayashi, J. Morimoto, H. Suga, *ACS Chem. Biol.* **2012**, *7*, 607–613.

[28] D. J. Ford, N. M. Duggan, S. E. Fry, J. Ripoll-Rozada, S. M. Agten, W. Liu, L. Corcilius, T. M. Hackeng, R. Van Oerle, H. M. H. Spronk, A. S. Ashhurst, V. Mini Sasi, J. A. Kaczmarski, C. J. Jackson, P. J. B. Pereira, T. Passioura, H. Suga, R. J. Payne, *J. Med. Chem.* **2021**, *64*, 7853–7876.

[29] P. Emsley, B. Lohkamp, W. G. Scott, K. Cowtan, *Acta Crystallogr. Sect. D Biol. Crystallogr.* **2010**, *66*, 486–501.

[30] D. Liebschner, P. V Afonine, M. L. Baker, G. Bunkóczi, V. B. Chen, T. I. Croll, B. Hintze, L.-W. Hung, S. Jain, A. J. McCoy, N. W. Moriarty, R. D. Oeffner, B. K. Poon, M. G. Prisant, R. J. Read, J. S. Richardson, D. C. Richardson, M. D. Sammito, O. V Sobolev, D. H. Stockwell, T. C. Terwilliger, A. G. Urzhumtsev, L. L. Videau, C. J. Williams, P. D. Adams, *Acta Crystallogr. Sect. D Struct. Biol.* **2019**, *75*, 861–877.

[31] E. Potterton, P. Briggs, M. Turkenburg, E. Dodson, *Acta Crystallogr. Sect. D Biol. Crystallogr.* **2003**, *59*, 1131–1137.

[32] I. Jarmoskaite, I. AlSadhan, P. P. Vaidyanathan, D. Herschlag, *Elife* **2020**, *9*, 1–34.

[33] Z. Liu, A. M. Abramyan, V. Pophristic, *New J. Chem.* **2015**, *39*, 3229–3240.

[34] D. A. Case, H. M. Aktulga, K. Belfon, I. Y. Ben-Shalom, S. R. Brozell, D. S. Cerutti, T. E. Cheatham III, V. W. D. Cruzeiro, T. A. Darden, R. E. Duke, G. Giambasu, M. K. Gilson, H. Gohlke, A. W. Goetz, R. Harris, S. Izadi, S. A. Iz-mailov, K. Kasavajhala, A. Kovalenko, R. Kransy, T. Kurtzman, T. S. Lee, S. LeGrand, P. Li, C. Lin, J. Liu, T. Luchko, R. Luo, V. Man, K. M. Merz, Y. Miao, O. Mikhailovskii, G. Monard, H. Nguyen, A. Onufriev, F. Pan, S. Pantano, R. Qi, D. R. Roe, A. Roitberg, C. Sagui, S. Schott-Verdugo, J. Shen, C. L. Simmerling, N. R. Skrynnikov, J. Smith, J. Swails, R. C. Walker, J. Wang, L. Wilson, R. M. Wolf, X. Wu, Y. Xiong, Y. Xue, D. M. York, P. A. Kollman (2020), AMBER 2020, University of California, San Francisco.

[35] J. A. Maier, C. Martinez, K. Kasavajhala, L. Wickstrom, K. E. Hauser, C. Simmerling, *J. Chem. Theory Comput.* **2015**, *11*, 3696–3713.

[36] J. Wang, R. M. Wolf, J. W. Caldwell, P. A. Kollman, D. A. Case, *J. Comput. Chem.* **2004**, *25*, 1157–1174.

[37] J. Wang, P. Cieplak, P. A. Kollman, *J. Comput. Chem.* **2000**, *21*, 1049–1074.

[38] W. Kabsch, C. Sander, *Biopolymers* **1983**, *22*, 2577–2637.

[39] J. Buratto, C. Colombo, M. Stupfel, S. J. Dawson, C. Dolain, B. Langlois d'Estaintot, L. Fischer, T. Granier, M. Laguerre, B. Gallois, I. Huc, *Angew. Chem.* **2014**, *126*, 902–906.

[40] S. De, B. Chi, T. Granier, T. Qi, V. Maurizot, I. Huc, *Nat. Chem.* **2018**, *10*, 51–57.

[41] V. Corvaglia, F. Sanchez, F. S. Menke, C. Douat, I. Huc, *Chem. Eur. J.* **2023**, e202300898